



Diplomarbeit

Untersuchungen des Einflusses von Waferverbiegung und Lithographie Prozessparametern auf Strukturbreitenschwankungen

ausgeführt bei Infineon Technologies in Villach
und dem Institut für Festkörperphysik
an der Technischen Universität Wien

unter der Anleitung von
**Ao.Univ.Prof. Dipl.-Ing. Dr.techn. Christoph
Eisenmenger-Sittner**
Dr. Andreas Behrendt

durch

B.Sc. Thomas Beyreder
Ernst Dohr-Straße 6, 3012 Wolfsgaben

September 7, 2017

Unterschrift Student



TECHNISCHE
UNIVERSITÄT
WIEN
Vienna University of Technology



Diploma thesis

Examination of the influence of wafer bow and lithography process-parameters on critical dimension uniformity

performed at Infineon Technologies in Villach
and the Institute of Solid State Physics
at the Vienna University of Technology

under guidance from
**Ao.Univ.Prof. Dipl.-Ing. Dr.techn. Christoph
Eisenmenger-Sittner
Dr. Andreas Behrendt**

by

B.Sc. Thomas Beyreder
Ernst Dohr-Straße 6, 3012 Wolfsgraben

September 7, 2017

Statement of authorship

Hereby I declare that this diploma thesis is the result of my own original work. Other material and sources used in this work are indicated as such and references to the sources are given in the Bibliography.

Further I assure that this work has not been used for credit elsewhere.

Villach, September 7, 2017

Thomas Beyreder

Abbreviations & Definitions [5]

Definition	Explanation
BARC	bottom-anti-reflective coating
binary mask	reticle made of opaque and transparent regions
Bossungplot	a plot of CD versus focus with dose as a parameter
CAR	chemically amplified resist
CD	critical dimension, lateral dimension of the structure
CD-U	short for critical dimension-uniformity, fluctuations of the CD
COG	Chrome on glass, mask-type
concave bow	also called crying bow \frown
convex bow	also called smiling bow \smile
DOF	depth of focus
Dose-to-clear	minimum exposure dose to clear a large open area of resist
DUV	deep ultra violet, Wavelength $\lambda < 300$ nm
exposure dose	intensity \times exposure time [J/m ²]
exposureplot	a plot of CD vs dose sharpest image point
focus point	focus $< 0 \hat{=}$ inside resist, focus $> 0 \hat{=}$ away from resist this definition fits for the exposure unit from Canon
FEM	focus exposure matrix
foup	front opening unified pod, transport box for a lot of wafers
HMDS	Hexamethyl disilazane, a popular adhesion promoter
line	width of the structure on the wafer
LSL	lower specification limit
NA	numerical aperture
negative resist	exposed parts remain on the wafer
notch	indentation on a wafer used to orientate the wafer
open frame	exposure of the resist without reticle
positive resist	exposed parts are removed from the wafer
PAC	photo active compound
PAG	photo acid generator
PEB	post exposure bake
pellicle	a thin, transparent membrane protecting the mask

pitch	sum of line + space, distance from one line to the same point on the next line
PSM	phase shift mask
	reticle using destructive interference to maximize contrast
process window	dose & focus region in which a stable exposure is possible
reticle	photomask with patterns that are transferred onto the resist during exposure
SEM	Scanning Electron Microscope
shot slot	region in the step & scan exposure
space	distance between two lines
stepper	step and repeat machine for exposure
swing curve	sinusoidal parameter-variation caused by interference effects
trench	lines with narrow width and depth
USL	upper specification limit
wafer	highly pure silicon disc
wafermap	figure showing the progression of a measured variable across the wafer

Abstract

Lithography is the most common method to create structures on microchips as of today. The quality of the lithography process is measured with the critical dimension-uniformity (CD-U). A low CD-U is necessary to ensure a stable lithography process and therefore keep the products yield high.

This thesis examines the influence of wafer bow and lithography parameters - especially development parameters - on the critical dimension-uniformity (also called linewidth uniformity). The research regarding wafer bow shows how given structures on the wafer change on a bowed wafer compared to a flat wafer. It is expected that the wafer bow shows its influence at the PEB (post exposure bake). The variation and the optimization of the development parameters show how CD (critical dimension) and CD-U change with the adjustment of parameters. An efficient process sequence is found as the time of the development process is reduced.

For the wafer bow experiment an oxide layer is grown on 300 mm silicon wafers. Then a part of the oxide layer is removed on one side via wet etch to generate a certain bow. The wafers are distinguished by their bow type: tensile stress from the oxide leads to convex (smiling) bow, compressive stress from the oxide leads to concave (crying) bow and the flat wafers are used to compare bowed to unbowed wafers. After etching the wafers are processed in the lithography steps like a productive wafer. A Scanning Electron Microscope (SEM) measures CD and provides the data for evaluation.

The development parameter experiment uses 300 mm silicon wafers. The wafers are processed in standard coating and exposure steps. The development process runs with altered parameters - e.g. development time - compared to the standard development process as the goal of this experiment is to optimize this process. Finally the CD measurement performed in a SEM provides data for an evaluation of CD-U.

The results of the wafer bow experiments with the resist M170Y show a significantly increased CD-U of smiling bow wafers in comparison to unbowed wafers. This is due to an increase of CD from wafer-centre to wafer-edge. The crying wafers show the reverse trend, an increase of CD from wafer-edge to wafer-centre.

The CD-U of the crying wafers is not as large as the CD-U of the smiling wafers. The centre-edge-CD-trends are a result from the influence of wafer bow at the PEB. Experiments with another resist, M91Y, suggest that the cooling process after the PEB and/or the development step influence the CD.

The experiments regarding development parameter optimization show that the standard process with 50s development time has the best CD-U. A reduction of development time increases CD-U and reduces CD. The average CD decreases with a decrease of development time. Experiment groups with agitation during development (movement of the wafer) show a worse CD-U than the not-moving groups. The double puddle (i.e. subsequent exposure to given amount of developer) groups show worse CD-U, some are even significantly worse.

Kurzfassung

Lithographie ist heutzutage die meist genutzte Methode zur Erzeugung von Strukturen auf Mikrochips. Die Qualität des Lithographie-Prozesses wird mit der Critical Dimension-Uniformität (kurz CD-U) gemessen. Eine niedrige CD-U ist notwendig um einen stabilen Lithographie-Prozess zu gewährleisten und damit die Ausbeute der Produkte hoch zu halten.

Diese Arbeit untersucht den Einfluss von Waerverbiegung und Lithographieparametern - Entwicklungsparametern im Speziellen - auf die Critical Dimension-Uniformität (auch laterale Strukturbreiten-Uniformität genannt). Die Experimente zur Waerverbiegung zeigen wie sich die Strukturen auf dem Wafer ändern, im Vergleich eines gebogenen Wafers zu einem flachen Wafer. Es wird erwartet, dass die Verbiegung ihren Einfluss am PEB (post exposure bake) zeigt. Experimente zur Optimierung der Entwicklungsparameter zeigen wie sich CD und CD-U mit der Variation von Parametern ändern. Der Arbeitsablauf wird effizienter, da die Zeit im Entwicklungsprozess verringert wird.

Im Waerverbiegungsexperiment wird eine Oxidschicht auf 300 mm Siliziumwafern aufgetragen. Dann wird ein Teil dieser Oxidschicht auf einer Seite der Wafer durch Nassätzen entfernt um die gewünschte Verbiegung zu erhalten. Die Wafer werden nach dem Typ der Verbiegung unterschieden: Zugspannung durch das Oxid führt zu konvexem (smiling) "bow", Druckspannung durch das Oxid führt zu konkavem (crying) "bow" und die flachen Wafer dienen zum Vergleich für die gebogenen Wafer. Nach dem Ätzen werden die Wafer mit Lithographie-Schritten wie bei einem produktiven Wafer prozessiert. Ein Rasterelektronenmikroskop (SEM) misst die CD und liefert die Daten für die Auswertung.

Das Entwicklungsparameter-Experiment benutzt fünfundzwanzig 300 mm Siliziumwafer. Diese Proben werden mit Standard Belacker- und Belichtungsschritten prozessiert. Der Entwicklungsprozess findet mit veränderten Parametern statt - z.B. Entwicklungszeit - verglichen mit einem Standardprozess. Das Ziel dieses Experimentes ist es, den Prozess zu optimieren. Schlussendlich liefert die CD-Messung auf einem SEM die Daten für die Evaluierung der CD-U.

Die Ergebnisse zu den Wafer bow Experimenten mit dem Lack M170Y zeigen eine

signifikant erhöhte CD-U für smiling bow Wafer, im Vergleich zu nicht gebogenen Wafern. Dies ist auf eine Vergrößerung der CD von Wafermitte zu Waferrand zurückzuführen. Die crying Wafer zeigen den inversen Trend, eine Vergrößerung der CD von Waferrand zu Wafermitte. Die CD-U der crying Wafer ist nicht so groß wie die CD-U der smiling Wafer. Die Mitte-Rand-CD-Trends sind eine Folge des Einflusses von Waferbow im PEB. Experimente mit einem weiteren Lack, M91Y, deuten an dass der Kühlprozess nach dem PEB und/oder der Entwicklungsschritt die CD beeinflussen.

Die Experimente zur Optimierung der Entwicklerparameter zeigen dass der bisherige Standardprozess mit 50s Entwicklungszeit die beste CD-U hat. Eine Reduzierung der Entwicklungszeit erhöht die CD-U und verringert die CD. Die mittlere CD nimmt mit der Abnahme der Entwicklungszeit ab. Gruppen aus dem Experiment mit Agitation während der Entwicklung (Bewegung des Wafers) zeigen eine schlechtere CD-U als die nicht-bewegenden Gruppen. Die double puddle (d.h. aufeinanderfolgender Auftrag von Entwickler) Gruppen zeigen schlechtere CD-U, manche sind sogar signifikant schlechter.

Contents

1. Introduction	1
2. Theoretical principles	3
2.1. Lithography Processing [5, p.12-25]	3
2.2. Standing Waves and Swing Curves	7
2.2.1. Standing Waves	7
2.2.2. Swing curves	8
2.3. Diffraction, resolution and depth of focus (DOF)	10
2.3.1. Fraunhofer diffraction	10
2.3.2. Resolution and depth of focus [1, p.119-124] [4, p.201-204]	11
2.4. Bow measurement	13
2.5. Film thickness measurement with white light interferometry [1, p.109f]	15
2.6. Scanning electron microscope (SEM) CD measurement	16
3. Impact of wafer bow on CD and CD-U	19
3.1. Preparing wafers with a defined bow	20
3.2. Description of the baking unit/hot plate	23
3.2.1. Operation	24
3.2.2. Bowed wafer on the hot plate	25
3.2.3. Cooling process after the bake	26
3.3. Other examined effects	26
3.3.1. Resist thickness	27
3.3.2. Flatness	28
3.3.3. Development	28
3.3.4. Softbake and hardbake	30
3.3.5. SEM measurement	30
3.4. Experiments with the resist M170Y - 414 nm thickness	31
3.4.1. First experiment	31
3.4.2. Second experiment	35
3.4.3. Third experiment	38
3.4.4. Fourth experiment	48
3.4.5. Fifth experiment	49
3.4.6. Results	51

3.5.	Experiments with the resist M91Y	58
3.5.1.	First experiment - 414 nm thickness	58
3.5.2.	Second experiment - 405 nm thickness	60
3.5.3.	Third experiment - 525 nm thickness	62
3.5.4.	Results	63
3.6.	Discussion	67
3.6.1.	F-Test	67
3.6.2.	Impacts on CD	70
4.	Development process parameters	73
4.1.	Experiments on development time	75
4.1.1.	Open frame wafers	75
4.1.2.	Experiments with a reticle	77
4.2.	Dependency of the development process on position	78
4.3.	Experiments with agitation	81
4.3.1.	First experiment, $\frac{1}{4}$ -rotation vs continuous rotation	83
4.3.2.	Second experiment, no rotation vs continuous rotation	83
4.4.	Experiments with double puddle development	84
4.4.1.	First experiment - different double puddle programs	85
4.4.2.	Second experiment - comparing with single puddle programs	85
4.4.3.	Resist profile cross section for 30s single puddle and centrifuge- 1 double puddle	86
4.5.	Discussion	87
4.5.1.	F-Test	88
5.	Conclusion	91
5.1.	Impact of wafer bow	91
5.2.	Development process parameters	92
	Bibliography	93
A.	Appendix	i
A.1.	Formulas	i
A.2.	Wafermaps of bowed wafers	iii

1. Introduction

The production of integrated circuits includes many chemical and physical processes of highest precision. These operations are executed on a disc made of pure semiconductor material called wafer. Some processes grow thin films onto the substrate, others implant atoms to adjust the properties of the semiconductor. Photolithography or simply lithography is used to generate structures of photoresist on the substrate. The word lithography comes from the greek words “lithos” and “graphia”, meaning “stone” and “write”, respectively. In modern lithography wafers are used instead of stones and the ink is photoresist, a substance which changes its properties with the absorption of light. The wafer is coated with resist during spin-coating, then a part of the resist is exposed to light via mask exposure and the development removes the exposed resist from the wafer and reveals the structures. This binary pattern protects the substrate from subsequent processes like etching or implantation. Ideal lithography results in a pattern which matches the mask (reticle) perfectly and the slopes of the resist are vertical from top to bottom. Precision is the main focus of this technology because of the demands for high quality and small integrated circuit dimensions. [5, p.1]

This work focuses on the influence of wafer bow on the critical dimension (CD), also known as the lateral dimension of the structure. Wafer bow can result from stress in the substrate or in the surface layers. A large bow can make the wafer unprocessable as the machines cannot handle it properly. To counteract bow on wafers a vacuum-chuck holds down the processed wafer in most process steps. There are, however, certain operations where there is no possibility of holding down the wafer by a vacuum-chuck. One of these operations is the post exposure bake where the wafer rests on so called gap pins at atmospheric pressure. The wafer does not touch the hot plate, when it lies on the gap pins. A perfectly flat wafer has a constant distance from heating platform to wafer surface, but a bowed wafer has different distances along the diameter. Therefore the wafer is heated unevenly which affects the CD on the positions and further the CD-U. Wafers with a certain bow are produced and used for experiments on a standard process.

The second topic of this work is the optimization of development parameters in regards of CD-U. One focus is a reduction of development time, which would also lead to a higher throughput. The manufacturer of the resist claims that a devel-

oping time of 15 seconds is sufficient to clear the resist. Experiments regarding development time are performed. Further parameters like nozzle distance and the rotation of wafers during development are varied in another set of experiments.

2. Theoretical principles

2.1. Lithography Processing [5, p.12-25]

In Lithography a light-sensitive material, called photoresist, is applied on a wafer, exposed and developed to form 3D relief images on the substrate. The following section gives an overview over the process steps (fig. 2.1).

Bottom-anti-reflective-coat (BARC) deposition

The goal of the bottom-anti-reflective-coat is to reduce reflectivity and therefore reduce the standing waves effect (see section 2.2 for information about standing waves) and to reduce swing curve effects caused by film thickness and substrate thickness variations. Sidegoals are flattening irregularities of the substrate and providing a clean surface for the resist to ensure good adhesion. The BARC is applied by spin coating, like the photoresist.

Photoresist Coating

Spin coating ensures a thin, uniform coating of photoresist across the whole wafer surface. The dissolved resist is applied by disposing it onto the wafer, which is then spun to create the desired thickness. The thickness is a function of the angular velocity ω (eq. (2.1)) since more resist will drop off the edge with faster rotation. The resist thickness is proportional to the resist viscosity (ν) to the 0.4 – 0.6 power and varies as one over the square root of the angular velocity (ω).

$$d \propto \frac{\nu^{0.4}}{\omega^{0.5}} \quad (2.1)$$

Soft bake

The main reason for this step is to stabilize the resist film by reducing the amount of solvent in the resist. Usually the resist contains about 20% to 40% solvent by weight and after soft bake this value is between 3% and 10%. The side effects of this process are reduction of film thickness, change of PEB and development properties, improved adhesion and higher resistance against contamination.

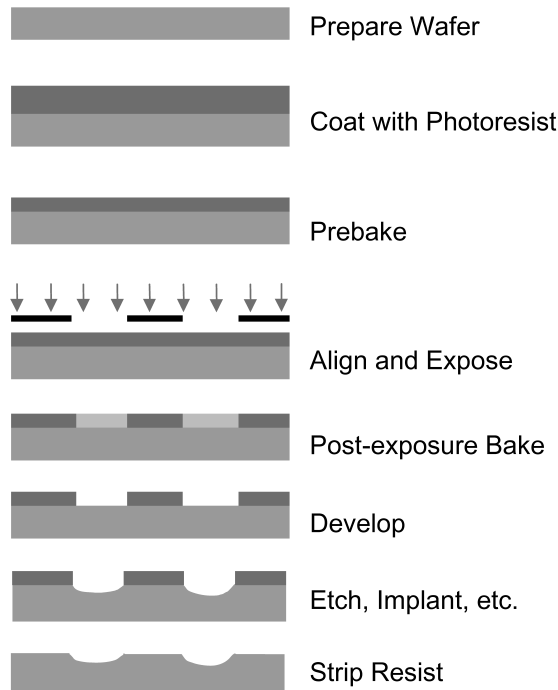


Figure 2.1.: Lithography process steps [5, p.13]

Negative effects at high temperatures include decomposition of PAC and oxidation or cross-linking of resin. Therefore a temperature which maximizes the benefits and minimizes the detriments is chosen.

Bake is usually done on so called hot plates. The wafer is brought into close proximity to a hot metal plate. The distance between wafer backside and hot plate is crucial to reduce the possibility of contamination. The follow up step is a controlled cooling after the bake, since exposure and development need a cold (room temperature) wafer.

Exposure

The preferred method in lithography nowadays is projection printing, since contact lithography has high defect densities and proximity lithography has poor resolution (see fig. 2.2). As the name suggests a lens-system projects the structures on the wafer. The production of high-quality lens systems improved so much that the defects only play a minor role in the quality of the image. These optical systems are diffraction-limited, meaning that diffraction effects like Fraunhofer-diffraction determine the quality of the image.

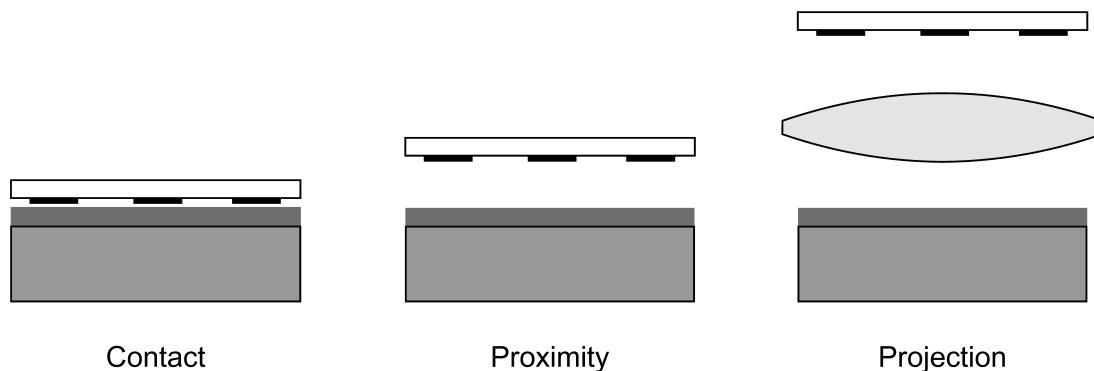


Figure 2.2.: Exposure methods [5, p.19]

There are two methods to expose a wafer with a small image field: scanning and step-and-repeat (see fig. 2.3). Scanning projection lithography projects a slit of light from the reticle, also called photomask, onto the wafer. In order to expose the whole wafer, both wafer and mask are moved simultaneously. The slit width, intensity and scan speed determine the exposure dose. The other method is step-and-repeat (also called stepper) which exposes a whole rectangle area at once. The reticle to image proportion can be 1:1 or a reduction in order to achieve maximum resolution.

Nowadays step-and-repeat and scanning are united in the step-and-scan method (see fig. 2.4). In this method an exposure field (for example $30\text{ mm} \times 20\text{ mm}$) is scanned, then wafer and reticle are moved to scan the following exposure fields. The scan direction changes from field to field because of the position of the slit on the scan map. Scanning and moving is repeated until all fields are exposed.

Post exposure bake (PEB)

This step is crucial for chemically amplified resists (CARs) to become soluble enough to be removed during development. The acid in the resist generated by exposure and the functional groups within the resist have a thermally induced reaction. Another effect at this bake stage is to smoothen out standing wave formations (see fig. 2.6) and make the resist thermally stable.

Development

In the development an aqueous base - the developer - is applied onto the wafer. The dispense is done by a moving robot arm with valves on its bottom side. The valves pour the developer on the wafer. The wafer is resting on a vacuum-chuck

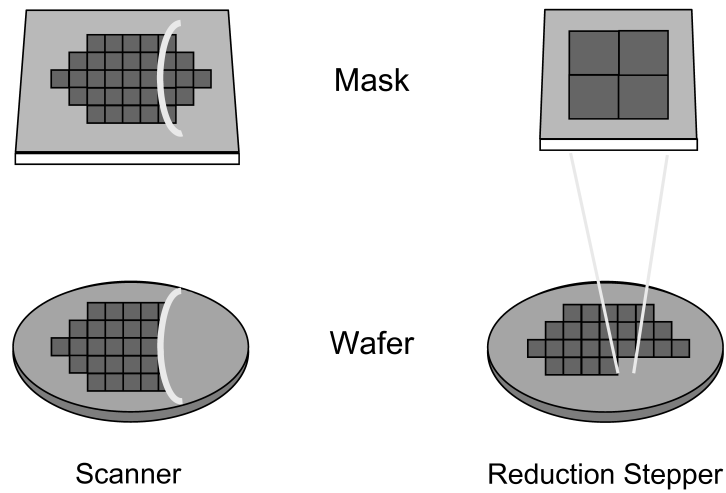


Figure 2.3.: Scanners and steppers [5, p.20]

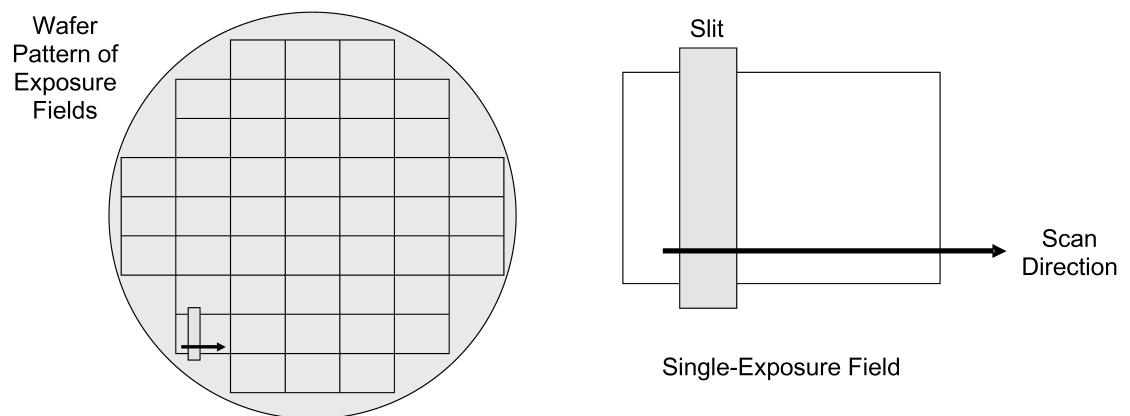


Figure 2.4.: Step-and-scan [5, p.21]

during this process. After the application the developer rests on the wafer for a given time, e.g. 50 s. The developer removes the exposed resist during this time. Afterwards the wafer is spin rinsed and dried.

Hard bake

The goal of the hard bake - also called post bake - is to harden the resist image to endure the upcoming processes like etching or implantation and to remove the water from the resist from the development. During the bake cross-links in the resin polymer are created within the resist, making the image more thermally stable. Selecting the right temperature is an important part, since a too high temperature will cause the resist to flow, this is indicated by the glass transition temperature of the resist. A bake above the glass transition temperature leads to a significant change of the profiles with rounded top contours. Usually the temperature for the hard bake is less than the temperature for the soft bake or PEB.

Side-effects of the hard bake are the removal of solvent, water etc. and the improvement of adhesion of the resist to the substrate. Alternatives to the hard bake are deep-UV-hardening, plasma and electron beam treatments.

Process handling

The lithography processes can either be handled by multiple tools focusing on one of the topics explained above or by a single cluster with many chambers (also called units). One unit is able to do a certain process (spin coating, development, PEB, ...), but there are multiple units per process available in order to gain throughput. The wafer has to go through one chamber per process step. The flow of wafers through the units is regulated by the so called wafer-flow. If the wafer-flow sends the wafers in such a way that all available chambers are used, the throughput is at the maximum. But this wafer-flow makes it hard to compare the results from the measurements after the processes. For statistical reasons a wafer-flow through a single unit per process step is used. The advantage of the cluster tool is that the wafers are sealed from the environment. All the experiments in this thesis are performed in a cluster tool. [5, p.12-25]

2.2. Standing Waves and Swing Curves

2.2.1. Standing Waves

The drawback resulting from the use of monochromatic light for exposure is the occurrence of swing curves and standing waves. Swing curves describe the sinu-

soidal variation of some parameters with resist thickness, while standing waves form on the slope of the resist. Those standing wave formations are formed when monochromatic light reflects at the border between resist and substrate. Reflected light waves and light waves coming from the lens interfere with each other, therefore influence the exposure dose absorbed by the resist and form this wave-like structure after development. The intensity-maxima are located every $\frac{\lambda}{2n}$, with λ being the wavelength of the incoming light and n being a natural number greater than zero. Figure 2.6 shows the cross section of a resist with standing waves on the walls of the structures. [4, p.204-206]

The incident light wave I_0 splits into a reflected part I_R and a passing part I_1 at the boundary between air and resist. The latter part I_1 is reflected a second time at the boundary between resist and wafer-substrate. I_1 is split into another reflected part I_{1R} and a part I_S going into the wafer. Standing waves are a result of the interference of I_1 and I_{1R} . The interference of light waves in this system with and without BARC is shown in fig. 2.5. The usage of a BARC reduces the effect of standing waves and swing curves. The BARC is positioned between resist and substrate. A part of the light, I_2 , can leave the resist. The BARC absorbs a lot of light and the reflected part passing through the resist I_B interferes destructively with the light waves in the resist I_{1R} . The disadvantage of using a BARC is that it is an additional layer to be removed, because it is a non-photosensitive compound which does not dissolve during development.

2.2.2. Swing curves

There are several parameters varying with resist thickness in a sinusoidal way. The term used for such variations is swing curves. This effect is a result from the same interference interaction described in the last paragraph about standing waves. Less light makes its way into the resist which results in an underexposed resist. The most important parameters changing this way are CD and dose-to-clear.

Both the dose-to-clear and the CD change in the same sinusoidal way because less light for exposure means that either an increased dose is needed to achieve the desired linewidth or if the dose is not changed, the CD increases. Figure 2.7 shows the dose-to-clear versus resist thickness with and without the standing waves effect. [5, p.129ff.]

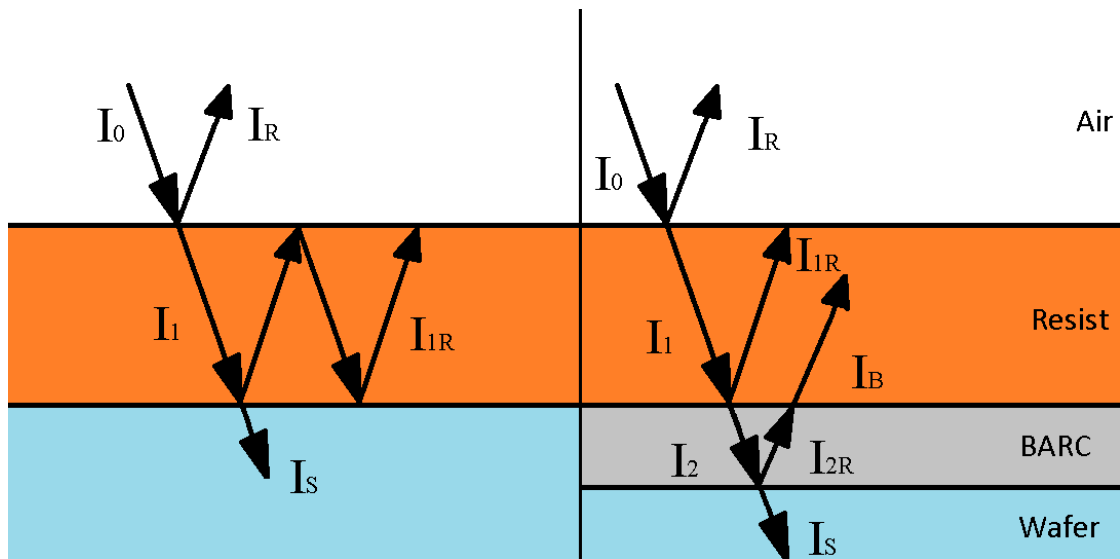


Figure 2.5.: Interference of light waves with (right) and without (left) BARC (not drawn to scale)

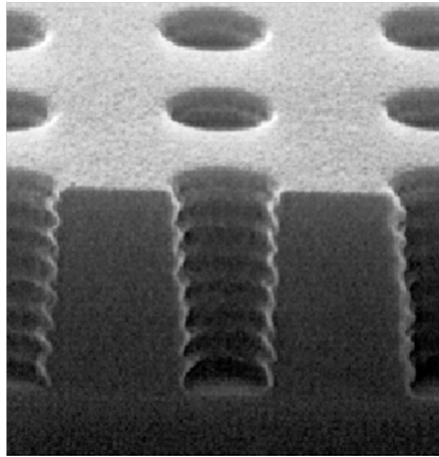


Figure 2.6.: Standing waves on circular structures [6, p.109]

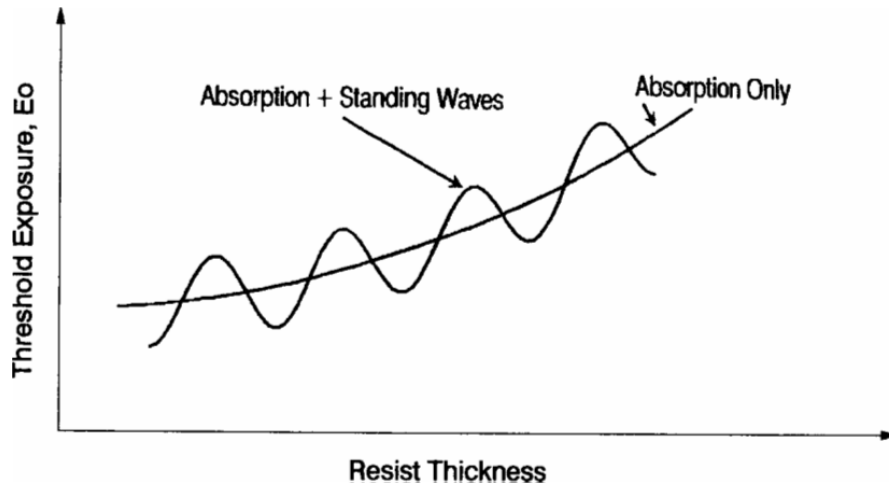


Figure 2.7.: Swing curve of the dose-to-clear [6, p.91]

2.3. Diffraction, resolution and depth of focus (DOF)

2.3.1. Fraunhofer diffraction

Diffraction occurs when light passes through a slit. The effects depend on the wavelength of the light, the broadness and form of the slit and the observation distance. The basic principle leading to diffraction theory is the wavefunction of the photon. The wavefunction describes the path the photon takes from the emitting source through obstacles - e.g. a slit - until it is absorbed. Analytical models simplify the calculation of light propagation immensely. Kirchhoff's diffraction formula is derived from the wave equation and works well near the slit. Fresnel diffraction is a simplified case applying to the near field. Fraunhofer diffraction is the far field approximation. In the optical systems of scanners and steppers the distance between slit and wafer is big enough to describe the light intensity by Fraunhofer diffraction. Figure 2.8 shows a Fraunhofer diffraction pattern. [4, p.198ff]

The Fraunhofer diffraction integral (eq. (2.2)) is used to calculate the electric field of the diffraction pattern. E_i is the electric field incident on the reticle. The spatial frequencies $f_x = \frac{nx'}{z\lambda}$ and $f_y = \frac{ny'}{z\lambda}$ are scaled coordinates in the x'-y' image plane. t_m is the electrical field transmittance and is binary in the case of a slit or binary mask (COG), but can have a more complex behaviour in the case of a PSM. The equation resembles the Fourier transformation in 2 dimensions. [5,

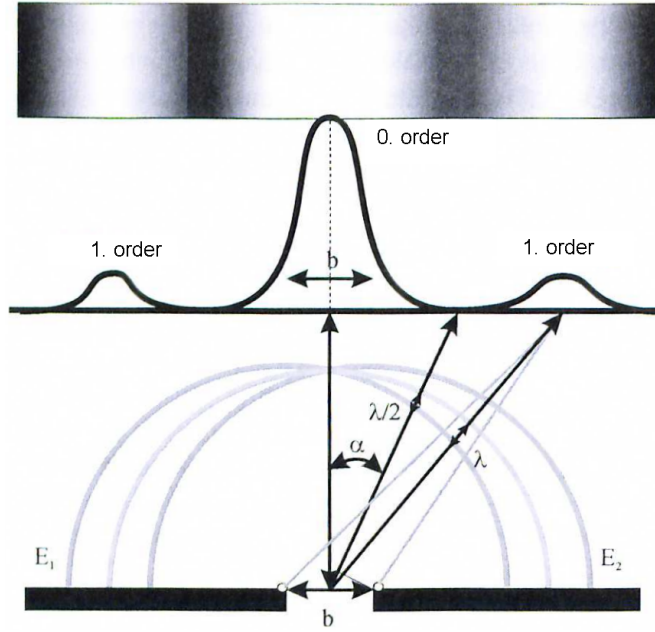


Figure 2.8.: Diffraction on a single slit [1, p.120]
(altered into English language)

p.41]

$$T_m(f_x, f_y) = \int_{-\infty}^{\infty} \int_{-\infty}^{\infty} E_i(x, y) t_m(x, y) e^{-2\pi i(f_x x + f_y y)} dx dy \quad (2.2)$$

2.3.2. Resolution and depth of focus [1, p.119-124] [4, p.201-204]

The Rayleigh criterium (eq. (2.3)) describes the minimal distance between 2 objects to be able to distinguish them. The definition of Lord Rayleigh states that 2 objects count as separated, when the central diffraction maximum is located at the first minimum of the other object. A lower distance results in a single observable object. The Rayleigh criterium is used in lithography to calculate the smallest possible lateral dimension of structures on the wafer.

$$R = CD_{min} = k_1 \frac{\lambda}{NA} \quad (2.3)$$

$$NA = n \sin(\alpha) \quad (2.4)$$

NA is the numerical aperture and is calculated by the product of refractive index and sine of the half-angle of the focused light by the projection lens (eq. (2.4)).

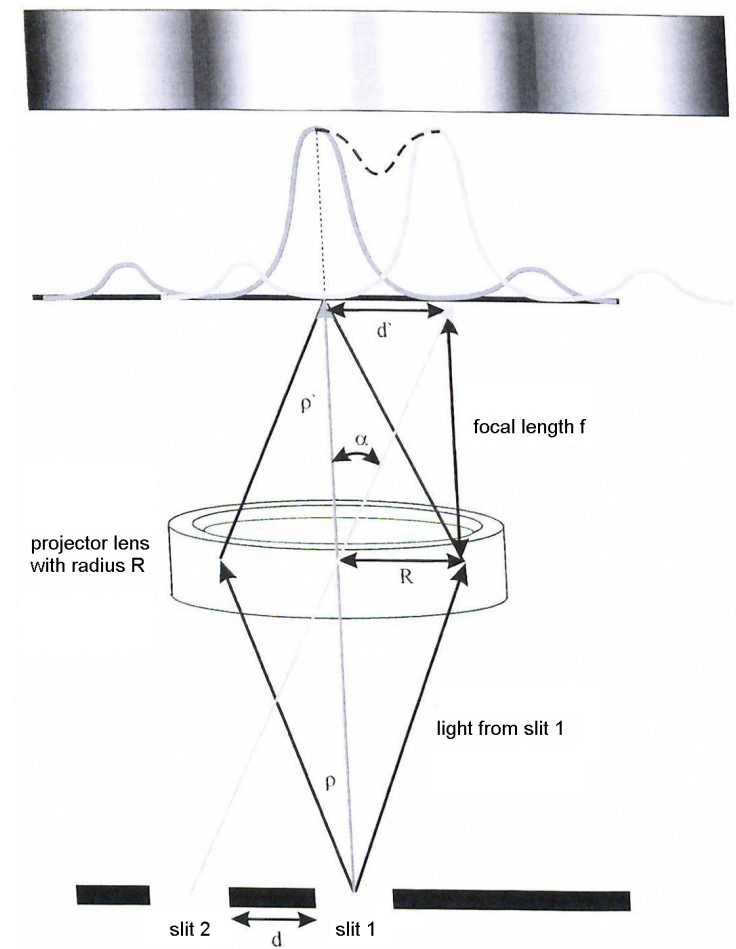


Figure 2.9.: Diffraction with light going through 2 slits and a projection system [1, p.123]
(altered into English language)

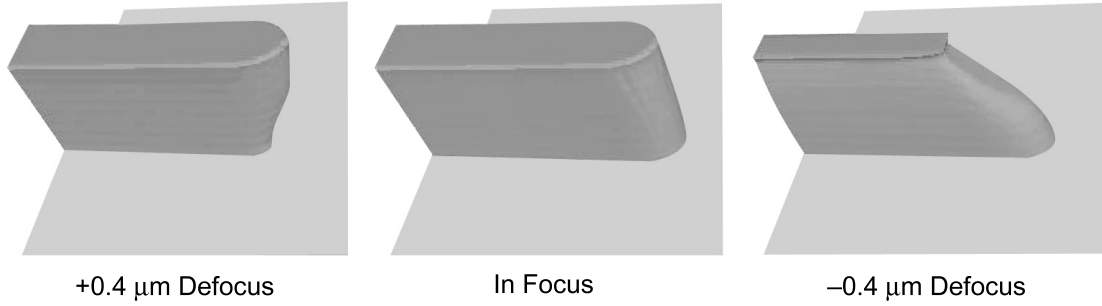


Figure 2.10.: Impact of focus on the shape of the end of an isolated line [5, p.359]

k_1 is a factor from the exposure tool. λ is the wavelength of the laser, which is $\lambda = 248 \text{ nm}$ in our case.

The depth of focus (eq. (2.5)) describes how close objects must lie in respect to the z-axis to be projected onto the screen sharply (or in our case the wafer). Objects farther away are not projected as sharp features and may be deformed (fig. 2.10).

$$DOF = k_2 \frac{\lambda}{NA^2} \quad (2.5)$$

k_2 is associated with the exposure tool. It is important to balance out CD_{min} and DOF in such a way, that a small CD is reached with a sufficient depth of focus.

2.4. Bow measurement

Bow is a measure of convex ($\hat{=}$ smiling bow) or concave ($\hat{=}$ crying bow) deformation of the median surface at the centre of the wafer (see fig. 2.11). The bow measurement works by calculating the distance between the centre point of the median surface and a median reference plane, which is calculated by a least squares fit. [3, p.2043]

The experiments in chapter 3 require to know the bow of the wafers. For productive wafers it is important that the value of the bow is low enough to ensure a safe handling and processing of the wafer in the production line. The MX2012 from the company “Eichhorn und Hausmann Metrology” is used for the measurements. This tool uses a capacitive, dual-channel method to calculate thickness, total thickness variation (TTV), bow, warp and some other parameters of the wafers. For the purpose of the experiments the bow is the important parameter. The MX2012 brings the wafer into a vertical position before the measurement

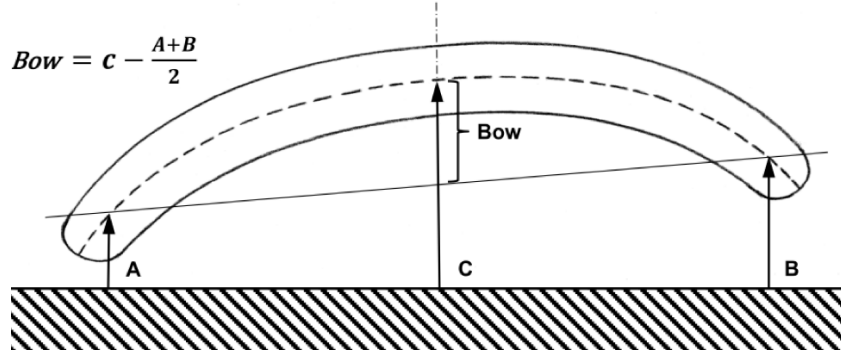


Figure 2.11.: Definition of bow on a curving wafer [3, p.2043]

starts to eliminate the gravitational bow.

Figure 2.12 shows the measurement principle. The evaluation of the parameters is based upon distance measurements performed by multiple capacitive sensors embedded in 2 probe plates facing each other. The sample wafer is positioned between the plates. The top probe and the upper silicon surface form the capacitor C_1 and the bottom probe and the lower silicon surface form the capacitor C_2 . The thickness is calculated with the relations given in equations 2.6 & 2.7. A is the area of the capacitor, d is the thickness of the capacitor and ϵ_0 is the electric constant or also called vacuum permittivity. A least squares fit calculates the median reference plane, which is used to evaluate the local bow at every measurement point. The centrebow is the difference between the centre point warp value and the average of the warp values on the border of the wafer.

$$C = \epsilon_0 \frac{A}{d} \quad (2.6)$$

$$\frac{1}{C_{tot}} = \frac{1}{C_1} + \frac{1}{C_2} \quad (2.7)$$

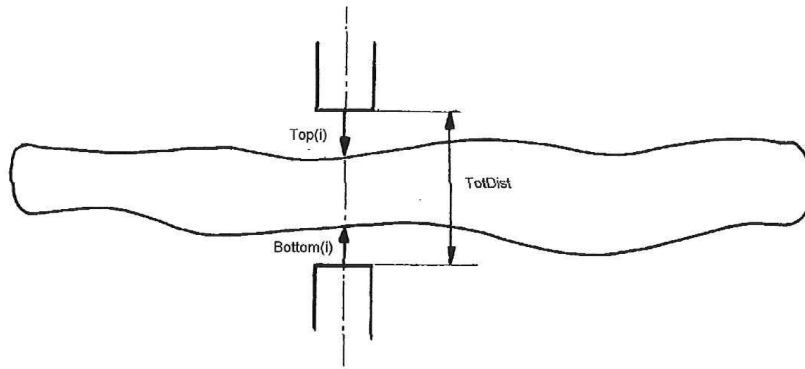


Figure 2.12.: Measurement principle [10, p.3]

2.5. Film thickness measurement with white light interferometry [1, p.109f]

The thickness of a resist or oxide film can be measured by spectroscopy with white light. White light consists of a range of wavelengths, usually from 380 nm up to 780 nm. When the white light rays hit the border between air and film a part of the rays are reflected while the other part is refracted. The grade of refraction depends on the refractive index which is a function of the wavelength of the light. The Cauchy coefficients are used to calculate the refractive index in dependence of the wavelength.

When the light rays hit the border between film and substrate, the rays are reflected towards the surface (similar like in the case in fig. 2.5 left part). Then the rays travel back towards the border between film and air and are refracted again. The part of the ray which went through the film and the part that reflected on the surface interfere with each other. Some wavelengths interfere constructively - increasing the amplitude of the light wave - while others interfere destructively - decreasing the amplitude of the light wave. The thickness of the film d and the refractive index n influence which wavelengths experience constructive or destructive interference. If the refractive index of the film is known, one only needs to measure the intensity versus wavelength (see fig. 2.13). Then the film thickness can be calculated from the maxima and minima of the spectrum.

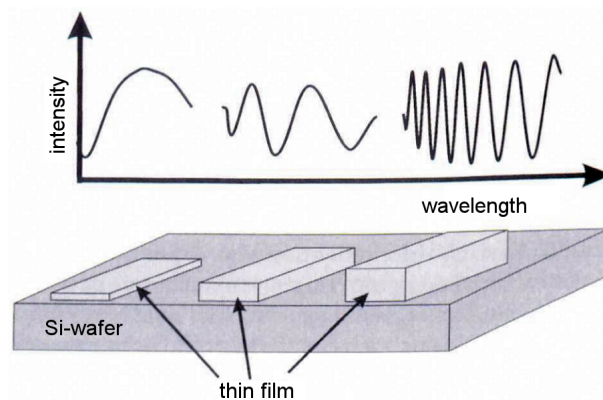


Figure 2.13.: Thin film optical measurement [1, p.110] (altered into English language)

2.6. Scanning electron microscope (SEM) CD measurement

The scanning electron microscope (SEM) uses an electron beam instead of a photon beam in conventional microscopy to create an image. The resolution is a function of wavelength (see eq. (2.3)), that means that the electron beam needs a small wavelength. The generation of electrons with a small wavelength is done with so called electron-guns. A voltage of a few kV is applied on the heated cathode to pull out electrons. A magnetic lens system filters out the slow electrons and focuses the electrons to a thin beam. This beam is directed onto the sample. Backscattered electrons and secondary electrons are detected by a scintillator and form the image as e.g. in fig. 2.15.

The CD measurement of the resist structures on the wafers is measured at a SEM. The wafer cannot be fixed with a vacuum chuck, because the SEM is evacuated and therefore the chuck would not be able to mount a wafer. Instead the wafer is fixed with three mounts that press the wafer down against a plate. The SEM uses image recognition to locate the position of the structures on the wafer. Figure 2.15 shows three spaces between 4 lines in a large area. The structures run vertically. Figure 2.16 shows the measurement of one space between two lines. The CD is measured between the dashed lines. On the bottom of the picture is a line that shows the brightness of the last measurement point. The brightness line corresponds to the transition from darker regions to brighter regions in the picture. The two peaks of the line show the position of the resist-slope and correspond to the light-grey lines in the picture. 32 measurement points are averaged to calculate the final CD-value, which is shown at the upper right of the picture. The cross section of

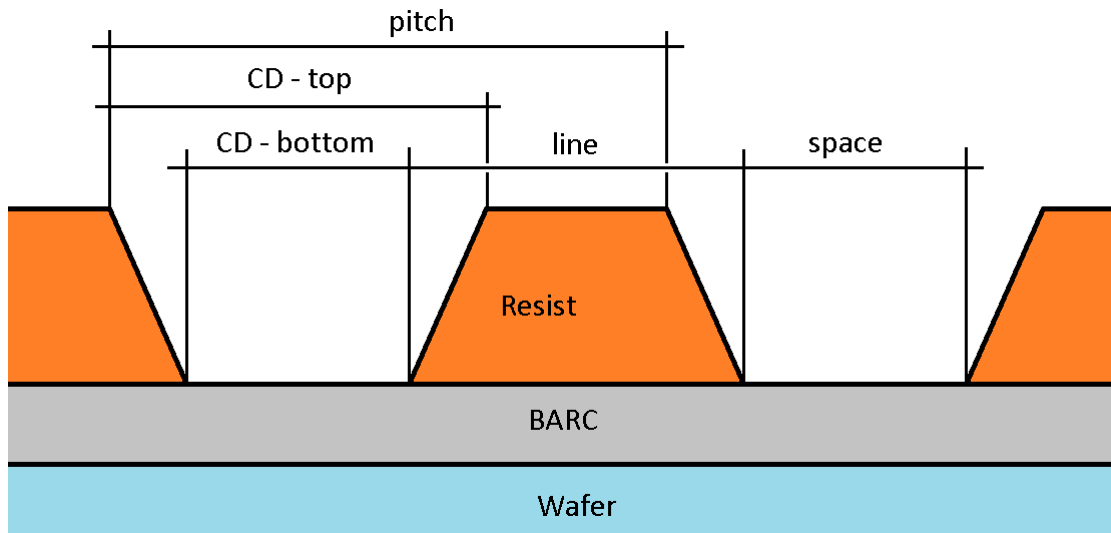


Figure 2.14.: Definitions of space, line, pitch, CD - top & CD - bottom (not drawn to scale)

the structures on the wafer is shown in fig. 2.14. The measurement recipe is set to measure the so-called space. The shape of the resist profile, as seen in fig. 2.14, is a trapeze which allows us to measure two dimensions for the space. The SEM measures the CD-bottom.

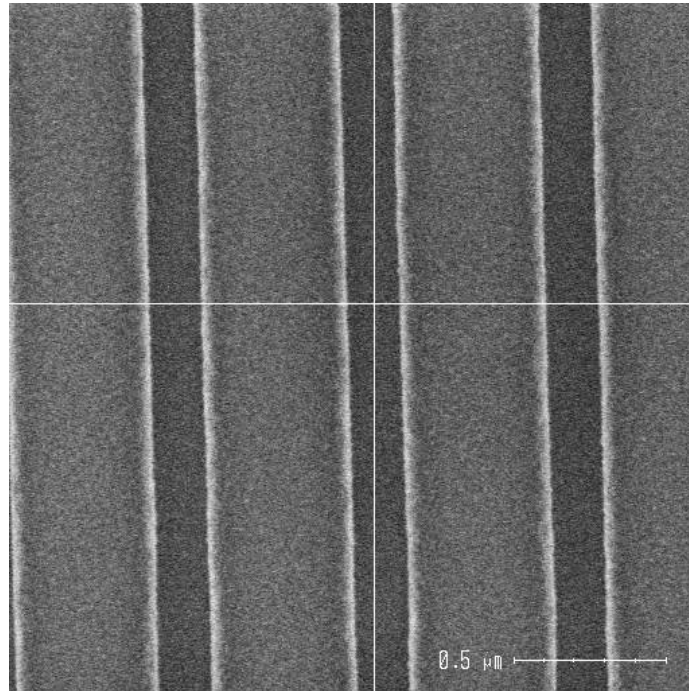


Figure 2.15.: Overview of the structures on the substrate

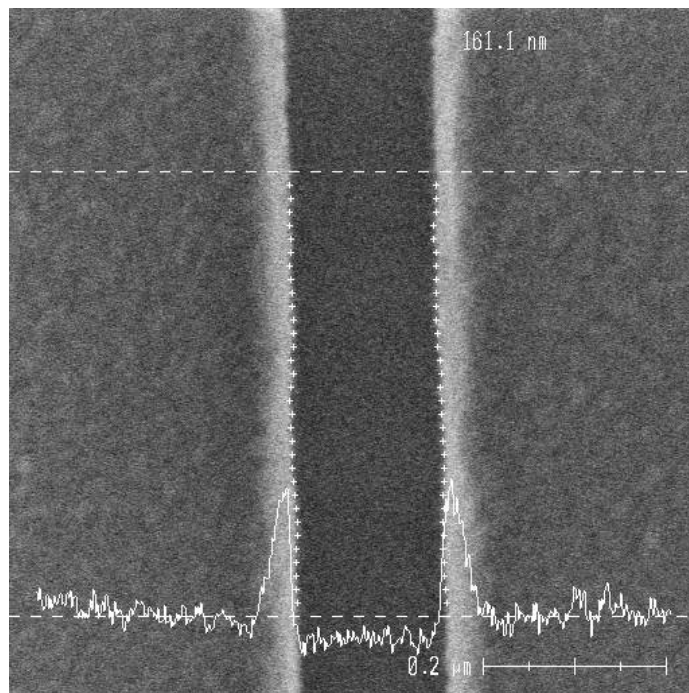


Figure 2.16.: SEM CD measurement with the measured CD, the punctured line follows the CD-bottom

3. Impact of wafer bow on CD and CD-U

Wafer bow causes handling and processing problems in manufacturing processes and induces defects during various packaging assembly processes. Therefore the reliability of devices built by bowed wafers is endangered. [3, p.2042]

At the bakes - softbake, PEB and hardbake - the wafer is heated from below with proximity heating. Because the distance between hot plate and wafer is depending on the value and type of bow, the assumption is that the wafer experiences a different heat budget compared to a not bowed wafer. The DUV resists are sensitive to the PEB temperature and change the CD of the structures on the wafer as shown in fig. 3.1. The slope of the curve is dependent on the chemical properties of the resist and may increase or decrease with higher temperature. This example shows a decreasing slope.

We expect the CD to vary with the radius from the centre, because the bow increases in the same way. The resists (M170Y and M91Y) show different temperature behaviour in the PEB, which is the reason for the experiments with both resists. The resist M170Y has a negative temperature coefficient of $-2.2 \text{ nm}/^{\circ}\text{C}$ at 130°C . That means the larger the temperature in the PEB, the smaller the structures on the substrate. M91Y has a positive temperature coefficient of $0.7 \text{ nm}/^{\circ}\text{C}$ at 130°C , which means a larger CD with larger temperature. [7, p.73-82]

The split-groups for the experiments have different type of bow (crying, smiling) and different values. The goal of having different groups is to show whether we can see the influence of bow on the CD/CD-U and see how much bow the machines are able to handle. The following experiments show the evaluated results from CD-measurements from a SEM.

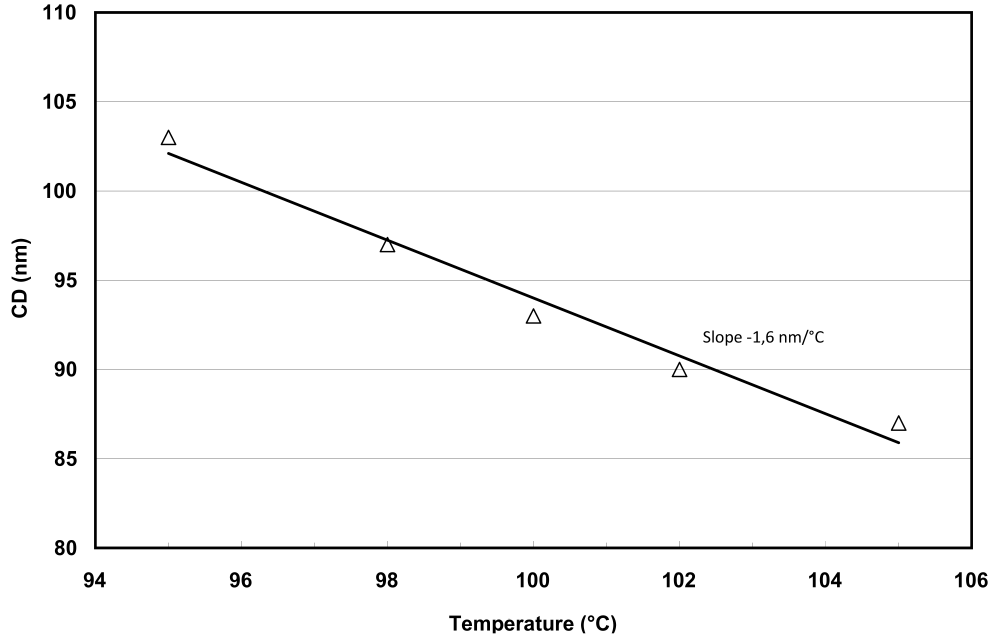


Figure 3.1.: PEB sensitivity curve for a positive DUV resist with a negative temperature dependency [8, p.284]

3.1. Preparing wafers with a defined bow

Bow is a measure of convex or concave deformation of the median surface at the centre of the wafer. The preferred method for bowing a wafer is by inducing tensile or compressive stress on the wafer. This is accomplished by oxide layers with different thickness on the top and bottom side of the wafer. With this method the bow can be set convex ($\hat{=}$ smiling $\hat{=}$ \smile) or concave ($\hat{=}$ crying $\hat{=}$ \frown) depending on the difference of the oxide-thickness of the top and bottom layers. In this work the terms crying and smiling are used because it is easier to imagine. The oxide layer induces the stress on the wafer. By thinning one oxide layer and keeping the other one at a constant thickness, the stress increases in value and therefore the bow is increased as well. [1, p.88]

The path of the wafers for the first experiment from entering the production line until the SEM CD measurement is given in fig. 3.2 and fig. 3.3. A layer of silicon oxide with a thickness of e.g. $1\text{ }\mu\text{m}$ is produced by thermal oxidation in the oven at 1100°C . Because we want to examine smiling and crying bow, some wafers are turned on the backside for the next steps. A protective layer of resist is applied on the substrate in order to protect the surface from the etch. During wet-etching the whole wafer dives into a bath of concentrated hydrogen fluoride, which removes

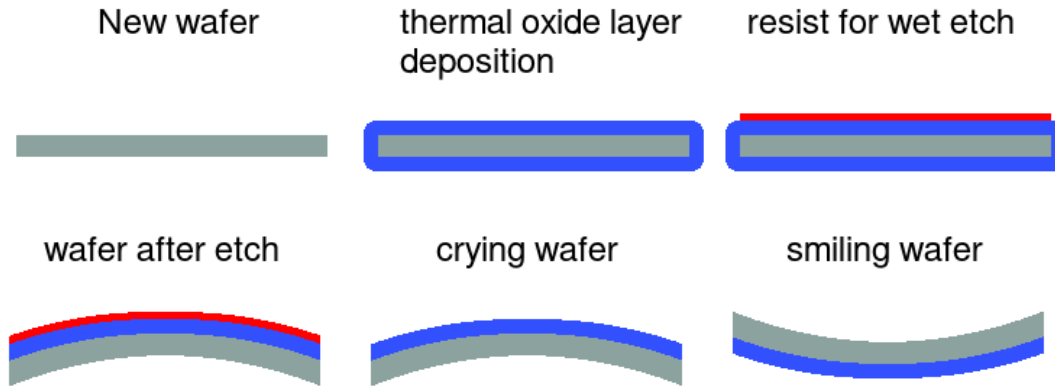


Figure 3.2.: Preparation of the bowed wafers

oxide from the unprotected areas. The longer the wafer stays in the bath, the more oxide is removed. Depending on the targeted bow the wafers are etched with various process times. The wafers are taken out of the etch-bath when the time for the corresponding etch-thickness is reached. The etched wafers have a thinner oxide on one side, while the other side has the thickness from before (e.g. $1\text{ }\mu\text{m}$), as it was protected by the resist. Therefore the tensile stress on the wafer is bigger on the side with the thicker oxide layer and the wafer bows. Afterwards the resist is removed and the bow is measured (e.g. table 3.3). The expected bow is not reached for some wafers. After an oxide thickness measurement it is clear that the etch-time was too short for some groups.

Figure 3.4 illustrates the bow of a wafer in a contour plot, after the wet-etch. The values for fig. 3.4 result from a measurement on a machine with multiple capacitive sensors measuring the distance between them while the wafer is between them. For more information on this topic see section 2.4.

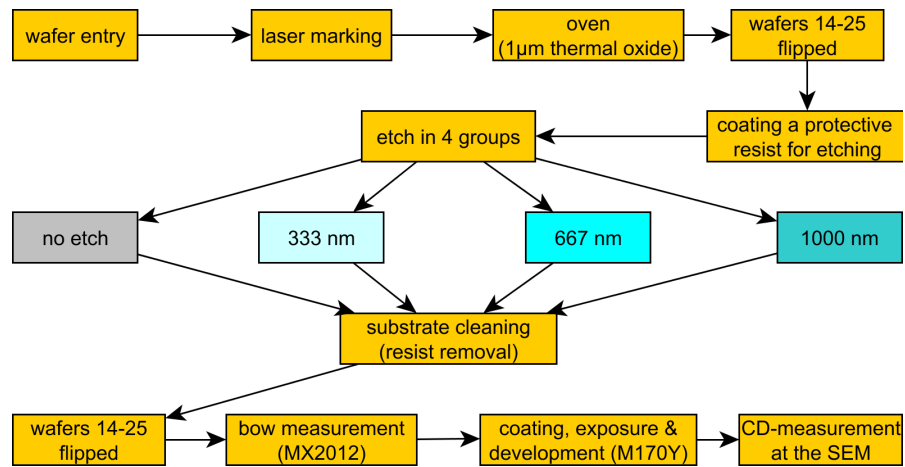


Figure 3.3.: Process steps to generate a bow on the wafers for the first experiment

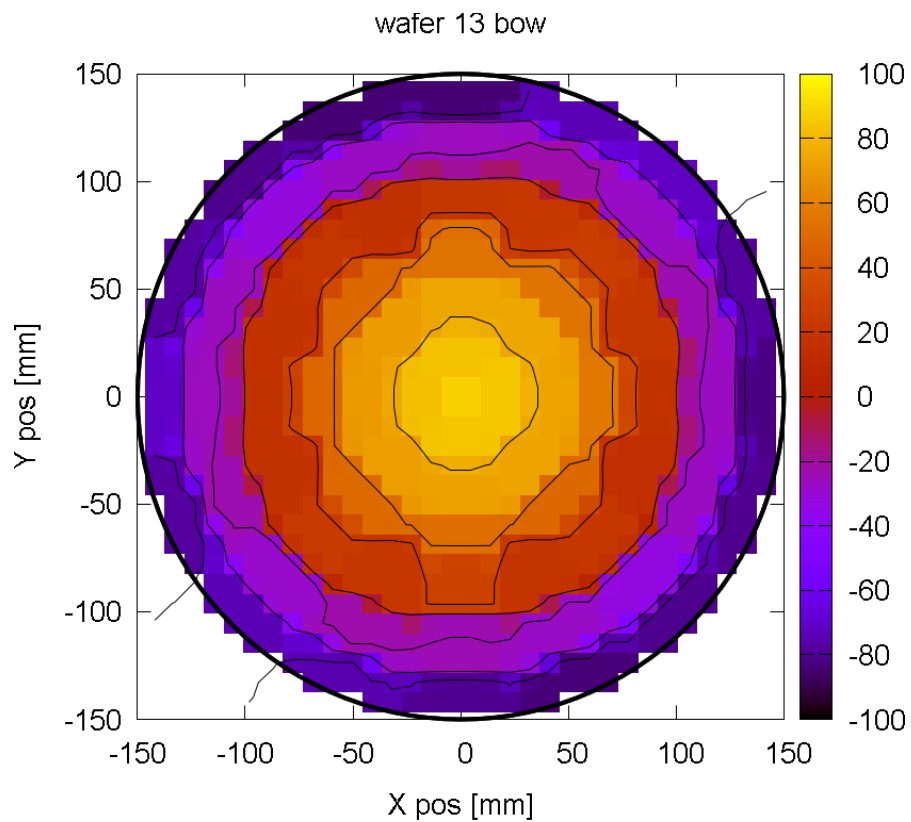


Figure 3.4.: Wafer bow measurement on the MX2012 for a wafer from the 160 µm bow crying group

3.2. Description of the baking unit/hot plate

It is necessary to describe the layout of the baking unit on account of the assumption that the PEB of a bowed wafer has the largest influence on CD of the resist-structures. The baking unit is a chamber with two wafer gates. If the gates are closed, the chamber is sealed from the environment. However, in the interior ambient atmosphere at normal pressure is present. Figure 3.5 shows the positions of the cool arm, hot plate, gap pins, wafer placement guides and the wafer-gates. The robot arm places the wafer on 3 support pins, which lower the wafer onto the cool arm. Then the cool arm moves above the hot plate. A second set of 3 support pins lifts the wafer from the cool arm and lowers the wafer onto the hot plate when the cool arm has withdrawn. The cool arm is not a fully circular disk, since there are openings for the support pins and a flat end to fit the arm in. The circular hot plate consists of a solid plate with 7 heating zones inside, which provide precise temperature control of the whole plate. There are in total 13 gap pins on the hot plate, 1 central pin, 4 radial distributed at 200 mm-wafer positions (located at 75 mm radius) and 8 radial distributed at 300 mm-wafer positions (located at 125 mm radius). The gap pins create a distance of 100 μm between wafer and hot plate. The heating method is called proximity heating, because the wafer is not allowed to touch the hot plate directly to avoid contamination on the wafer bottom side. The heat transfer methods are radiation and convection. The chambers inside the cluster tool are not evacuated, which means that they work under air pressure. Wafer placement guides slide the wafer into the correct position if the placement from the robot arm is offset. Located above the hot plate is the exhaust ventilation, which is heated to prevent condensation of water. After the bake is completed, the support pins lift the wafer, the cool arm comes forward, the pins lower the wafer on the cool arm, the cool arm moves toward the gates, the wafer is cooled for a given time before the support pins on the gate side lift the wafer

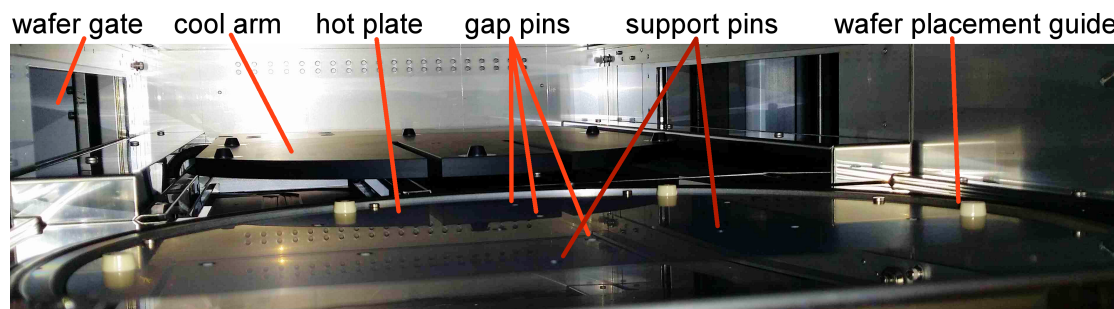


Figure 3.5.: hot plate inside the cluster machine (the exhaust ventilation was removed for this photo)

and robot arm takes the wafer. The following section describes the operations in more detail. [9, p.118ff]

3.2.1. Operation

The following describes operation of the bake unit receiving a wafer and sending it out after heat treatment and a cooling process. [9, p.120f]

- Standby in the following status:
 - Gate shutter: Closed
 - Cool arm: Out
 - Wafer support pins on the cool arm: Down
 - Chamber: Closed
 - Wafer support pins on the hot plate: Down
- Preparation to receive a wafer
 - The gate shutter opens. The wafer support pins on the cool arm move up.
- Receiving a wafer
 1. The robotic arm places a wafer on the wafer support pins on the cool arm.
 2. The wafer support pins on the cool arm move down to place the wafer on the gap pins on the cool arm. The chamber opens. The gate shutter closes.
 3. The cool arm moves to a position over the hot plate.
 4. The wafer support pins on the hot plate move up to receive the wafer from the cool arm.
 5. The cool arm returns to the original position.
 6. The chamber closes. The wafer support pins on the hot plate move down to place the wafer on the gap pins on the hot plate.
- Performing heat treatment
 - The hot plate heats the wafer.
- Moving the wafer
 1. The chamber opens. The wafer support pins on the hot plate move up.
 2. The cool arm moves to a position between the hot plate and the wafer.
 3. the wafer support pins on the hot plate move down to place the wafer on the gap pins on the cool arm.

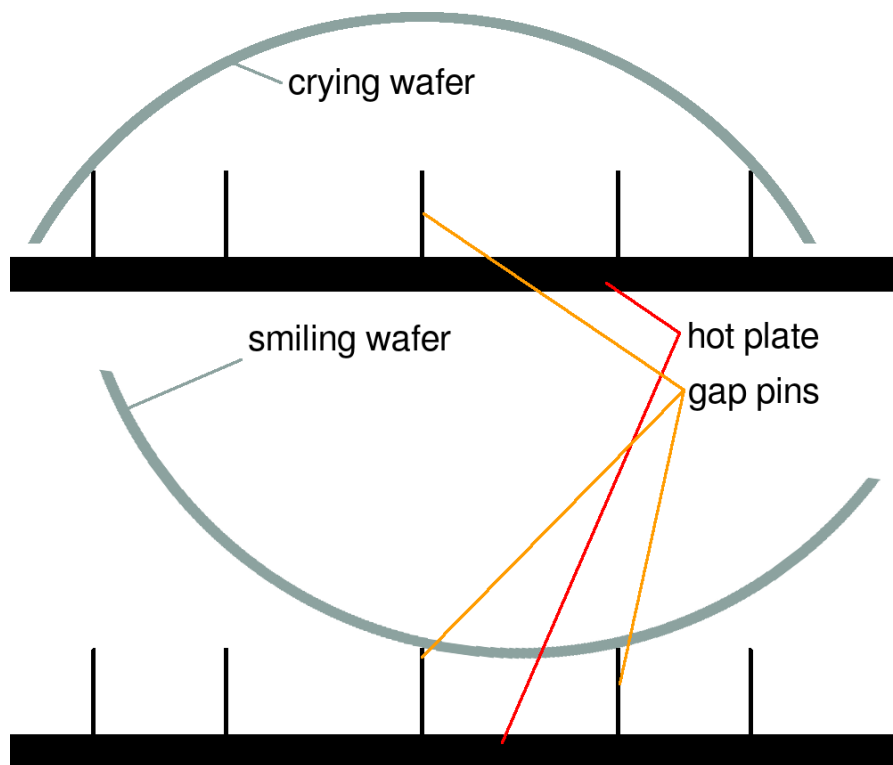


Figure 3.6.: Positioning of the bowed wafers on the hot plate (not drawn to scale)

4. The cool arm returns to the original position.
 - Performing a cooling process
The cool arm cools the wafer. The chamber closes.
 - Preparation to send the wafer
The wafer support pins on the cool arm move up. The gate shutter opens.
 - Sending the wafer
The robotic arm receives the wafer from the wafer support pins on the cool arm.

3.2.2. Bowed wafer on the hot plate

We know how the baking unit handles the wafer. Now we want to take a look at how a bowed wafer is positioned on the hot plate. Figure 3.6 shows a crying and a smiling wafer on top of the gap pins of a hot plate. The crying wafer touches the outer gap pins and the inner gap pins have no contact to the wafer because of the bow. The position is stable because the crying wafer rests on 8

gap pins. The smiling wafer touches the central gap pin and 2 gap pins at the 200 mm-wafer-positions. The reason for this is that the wafer tilts to the side because it cannot lie just on the central gap pin. The smiling wafers position is unstable and we do not know in what direction the wafer tilts when it is positioned. The position defines the distance between wafer and hot plate. When the wafer is near to the hot plate it experiences more heat than when the wafer is farther away. For the crying wafers we have a higher temperature at the wafer-edge and a lower temperature at the wafer-centre. For the smiling wafers we have a higher temperature at the wafer-centre and a lower temperature at the wafer-edge.

The wafermaps for the smiling wafers in appendix A.2 indicate that the direction of the tilt changes from wafer to wafer. The tilt causes the wafer to lie asymmetrical. The distance from wafer to hot plate for the left wafer-edge is more than for the right wafer-edge of the smiling wafer in fig. 3.6.

3.2.3. Cooling process after the bake

A cooling process after the PEB brings the wafer back to 20 °C. The cooling is done on the cooling arm of the PEB-unit as described above. The manual for the machine mentions that the cool arm has gap pins similar to the ones of the hot plate, but when we took a look into the unit we saw no gap pins for the cool arm (see fig. 3.5). This means that the position of the wafer is even less determined than at the bake. We assume that the wafers lie similar like in fig. 3.6 with the difference that there are no gap pins and the wafer touches the surface of the cool arm.

The distance of the bowed wafers in the cooling process influences how fast the wafer is cooled. The closer the wafer is to the cooling arm, the faster it cools. That means that the crying wafers cool faster at the wafer-edge and slower at the wafer-centre. The smiling wafers cool faster near the CD-centre and slower at the wafer-edge.

3.3. Other examined effects

The biggest effect of wafer bow at processing is expected in the PEB, but there are other steps where the bow may influence the CD of the structures. Every step described in Lithography Processing [5, p.12-25] has the potential to influence CD if a bowed wafer is processed. During those operations the wafer is held by a vacuum-chuck which sucks the wafer bottom close to the chuck surface. Therefore the wafer bow is counteracted. This vacuum-chuck has a radius of 60 mm which makes it smaller than the 300 mm wafers. That means that the wafer is sucked

wafer no.	type of bow	average d	maximum d	minimum d	σ
1	smiling	412.4 nm	413.7 nm	412.0 nm	0.35 nm
2	smiling	412.1 nm	413.3 nm	411.8 nm	0.26 nm
3	smiling	412.3 nm	413.5 nm	411.9 nm	0.33 nm
4	smiling	412.6 nm	413.6 nm	412.3 nm	0.21 nm
5	smiling	412.4 nm	413.4 nm	412 nm	0.31 nm
6	smiling	412.6 nm	413.5 nm	412.2 nm	0.23 nm
7	smiling	412.5 nm	413.4 nm	412.1 nm	0.22 nm
8	no bow	412.9 nm	413.6 nm	412.5 nm	0.26 nm
9	no bow	412.8 nm	413.6 nm	412.5 nm	0.23 nm
10	no bow	412.9 nm	413.6 nm	412.6 nm	0.23 nm
11	no bow	413.0 nm	413.6 nm	412.6 nm	0.26 nm

Table 3.1.: Resist thickness d on bowed wafers

flat inside the vacuum-chuck-radius, but outside of it the wafer is deformed.

3.3.1. Resist thickness

Spin coating of BARC and resist depends on parameters like rotation speed, substrate topography, humidity, resist viscosity, etc. Bow may be able to influence the properties and cause a non-uniform distribution of resist (and BARC) thickness. A thin film thickness measurement is performed on the smiling wafers to show if the bow affects the resist thickness. The crying wafers were not used because they show a smaller change in CD-U as the experiments below show. The preparation steps before the measurement are coating the wafer with the resist M170Y and the softbake. The results are shown in table 3.1. The graph in fig. 3.7 shows the comparison between a not bowed wafer and two smiling wafers. The smiling wafers in fig. 3.7 were chosen for the comparison because they show the largest and smallest standard deviations σ of the smiling wafers. The graph shows the almost symmetrical resist thickness of the not bowed wafer across the wafer radius, the form is similar to a sombrero. Multiple measurements of not bowed wafers showed similar results, meaning that the shape is stable. On the contrary the smiling wafers are slightly unstable with symmetrical or asymmetrical form. It is not yet clear why the shape varies from wafer to wafer. The standard deviation of the smiling wafers is similar to the not bowed wafers. From the results of the thickness measurement it can be concluded that the influence of wafer bow on resist thickness is minor.

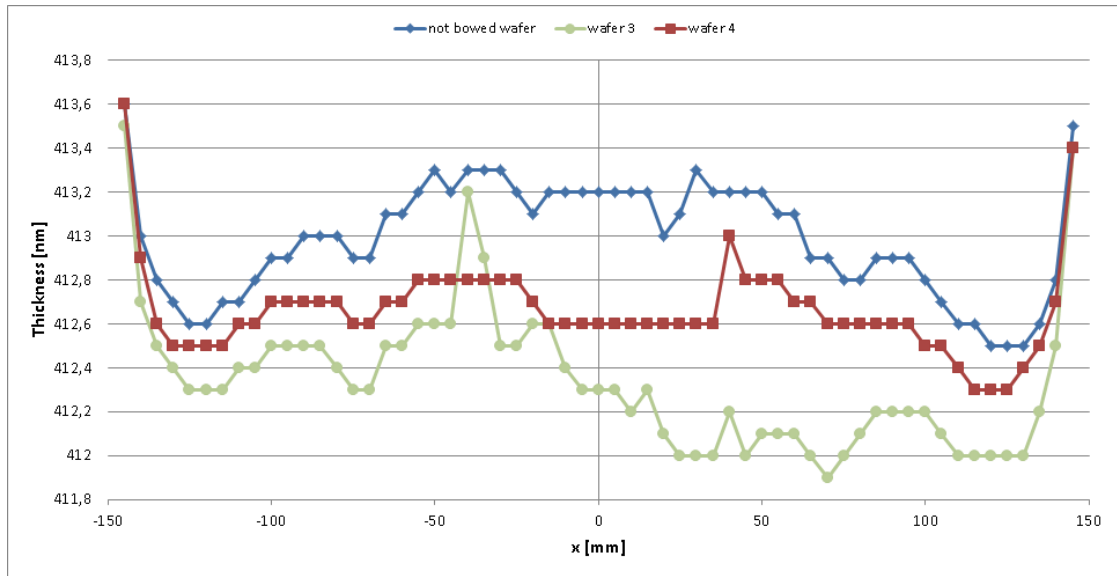


Figure 3.7.: Resist thickness measurement on a not bowed (16) and two smiling wafers (3 & 4)

3.3.2. Flatness

The scanner has a larger vacuum-chuck that can suck the whole wafer on the surface. It adjusts the focus onto the surface of the wafer for a single point for every shot region before the exposure. During exposure the focus is not readjusted to the changing topography of the wafer. In case of an uneven surface - which could be the case for the bowed wafers - the scanner may come in defocus and this causes a change in CD. This change depends on the process window of the resist. A flatness measurement on the wafers determines the not corrigible focus. The process window can be seen in fig. 3.8, the maximum is $0.25\text{ }\mu\text{m}$, but most of the values are smaller than $0.1\text{ }\mu\text{m}$. The process window for the M170Y and for the dose 220 J/m^2 can be extracted from fig. 3.9. A specification limit of $\pm 10\text{ nm}$ for the CD and the CD-target 160 nm result in a process window of $0.8\text{ }\mu\text{m}$ on a planar wafer. The focus between $-0.3\text{ }\mu\text{m}$ and $0.5\text{ }\mu\text{m}$ fulfils the set specification limit. This process window is enough for the necessary value of around $0.25\text{ }\mu\text{m}$ from the flatness measurement. We conclude that the influence of wafer bow on the exposure process is small.

3.3.3. Development

The bow and topography of the wafer causes the developer to flow from higher regions to lower regions. E.g. a smiling wafer accumulates developer in the centre,

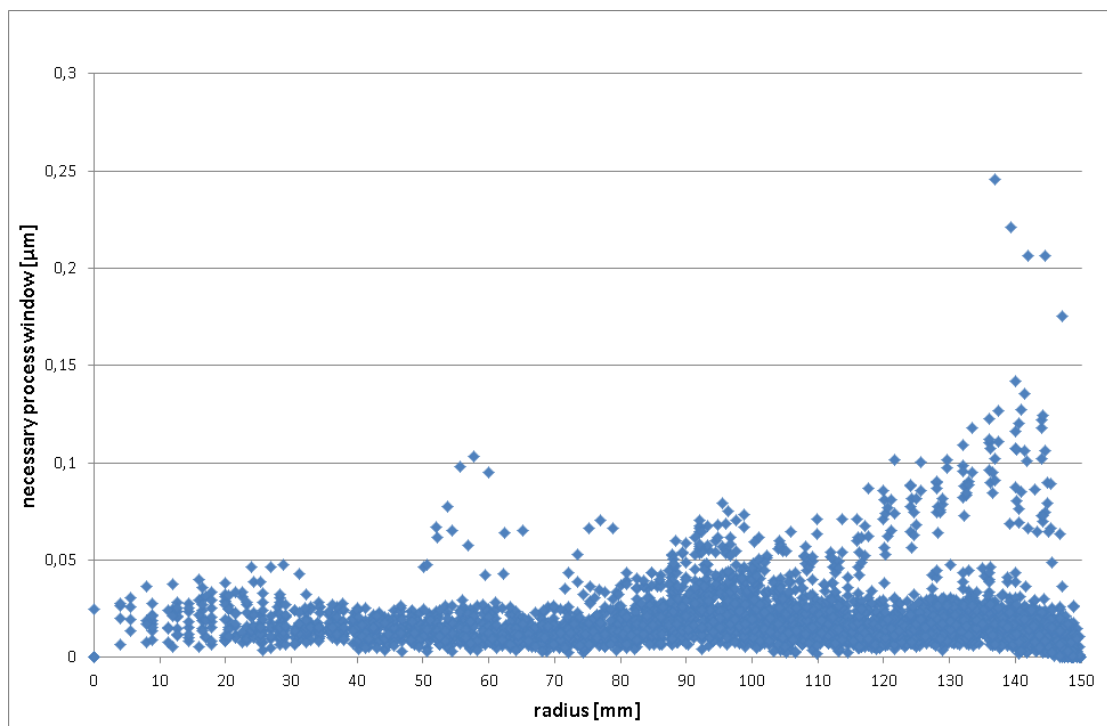


Figure 3.8.: Necessary process window over radius

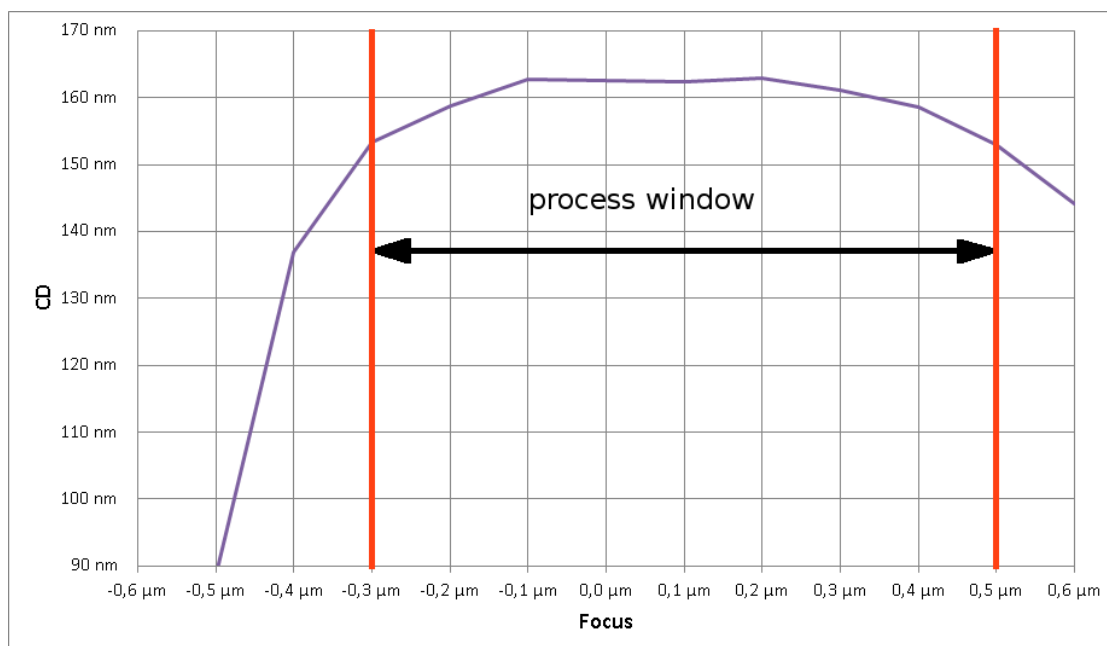


Figure 3.9.: CD over focus to determine the process window of the resist M170Y - borders of the chosen process window in orange

while the developer accumulates at the edge or even flows off the edge of a crying wafer. It is hard to estimate the impact of bow on the development process and the resulting CD. A contact angle measurement shows that the average contact angle of water on the resist M170Y after exposure and PEB is $65.33^\circ(\pm 0.34^\circ)$. This contact angle is considered to be hydrophobic.

The flow of developer - caused by the height difference - may increase the removal of resist. The accumulation of developer to a deeper puddle (like on a smiling wafer) may increase the removal of resist because of stronger internal currents. We suspect that this influence is stronger than the other ones in this section and comparable or even stronger than the influence in the PEB depending on the resist. This subject needs further investigation.

3.3.4. Softbake and hardbake

The hot plates for soft bake and hard bake have a similar structure like the hot plate for the PEB. The softbake reduces the amount of solvent in the resist. A bowed wafer may experience a different temperature budget in this bake and therefore the reduction of solvent may differ in comparison to a unbowed wafer. The experiments in the section Resist thickness include the soft bake, but we don't see a large increase of the standard deviation and conclude that the influence of the bow on the soft bake is small.

The hard bake removes solvent from the resist and water from the previous development. It does not influence the CD.

3.3.5. SEM measurement

The SEM measurement holds the wafer without a vacuum chuck, so the wafer is not flattened. That means that the machine has to focus onto different heights on the wafer surface. The focus is adjusted by a magnetic field. This magnetic field causes the electron beam to rotate slightly, which changes the resulting image. This results in tilted lines on the SEM-picture instead of vertical ones in the normal case. The CD-evaluation program uses horizontal sum lines to determine the CD. The tilted lines change the route of the sum lines slightly and therefore influence the result of the CD measurement. The change of CD resulting from this geometrical situation can be estimated with the cosine of the tilt-angle. The tilt-angle is roughly 3° for most of the SEM-pictures and results in a change of 0.137%. For the CD-target of 160 nm this implies an error of 0.22 nm. This error considers only the geometrical effect by measuring with a tilt. Other focus effects are not taken into account.

running Nr.	Nr. of wafers	resist	exposure dose	focus	resist thickness
1	25	M170Y	220 J/m ²	0 µm	414 nm
2	19	M170Y	220 J/m ²	0 µm	414 nm
3	25	M170Y	220 J/m ²	0 µm	414 nm
4	25	M170Y	220 J/m ²	0 µm	414 nm
5	10	M170Y	220 J/m ²	0 µm	414 nm
6	11	M170Y	220 J/m ²	0 µm	414 nm

Table 3.2.: Parameters of the M170Y wafer bow experiments

3.4. Experiments with the resist M170Y - 414 nm thickness

3.4.1. First experiment

All wafer bow experiments are performed on a cluster machine, which combines a coating track, a scanner and a development track. The experimental parameters are shown in table 3.2 with the running number 1. The recipes for the lithography processing are almost the same as for productive lots, only a single unit wafer-flow is used. The reticle for exposure is a test-reticle with 180 nm space and 650 nm pitch, but the CD-target is 160 nm which is achieved by the dose of 220 J/m². The centrebow after oxide etching is shown in table 3.3. The negative centrebow-values indicate that the bow type is crying, while the positive values indicate smiling bow. There are in total 7 split-groups (rounded to the next 5 nm): no bow, 55 µm crying, 110 µm crying, 160 µm crying, 50 µm smiling, 110 µm smiling and 155 µm smiling. Centrebow measurements are performed after each lithography processing iteration, because the bake processes can change the stress of the oxide layer on the substrate. The differences between the displayed centrebow measurements in table 3.3 is negligible and further measurements before and after the later experiments showed similar results.

The scanner displayed a few focus control errors during the processing of the wafers, showing some of the possible problems with the handling of highly bowed wafers (namely the 155 µm smiling group). The errors have minor impact on the results as it was expected to have some errors. The evaluation shows a few outliers which may be the result of the mentioned errors. The outliers are defined by the SEM-pictures which show no structures, massively deformed structures or a value without a picture.

wafer	etched side	bow type	centrebow	centrebow after experiment
1	-	no bow	-0.26 μm	-0.41 μm
2	-	no bow	-0.42 μm	-0.30 μm
3	-	no bow	-0.88 μm	-0.73 μm
4	-	no bow	-1.15 μm	-1.23 μm
5	backside	crying	-54.85 μm	-54.43 μm
6	backside	crying	-53.14 μm	-53.24 μm
7	backside	crying	-53.82 μm	-53.77 μm
8	backside	crying	-110.66 μm	-110.45 μm
9	backside	crying	-111.20 μm	-111.33 μm
10	backside	crying	-111.34 μm	-111.33 μm
11	backside	crying	-156.94 μm	-156.87 μm
12	backside	crying	-157.30 μm	-157.25 μm
13	backside	crying	-166.71 μm	-166.51 μm
14	-	no bow	-1.06 μm	-1.16 μm
15	-	no bow	-1.59 μm	-1.44 μm
16	-	no bow	-1.75 μm	-1.80 μm
17	frontside	smiling	51.07 μm	50.99 μm
18	frontside	smiling	51.69 μm	52.10 μm
19	frontside	smiling	51.41 μm	51.44 μm
20	frontside	smiling	109.05 μm	108.78 μm
21	frontside	smiling	107.77 μm	107.65 μm
22	frontside	smiling	107.78 μm	107.53 μm
23	frontside	smiling	153.61 μm	153.24 μm
24	frontside	smiling	154.66 μm	154.20 μm
25	frontside	smiling	154.13 μm	154.28 μm

Table 3.3.: Properties of the bowed wafers for the first experiment

bow group	bow type	avg CD [nm]	CD-centre [nm]	CD-edge [nm]	3σ [nm]
no bow	no bow	158.7	158.7	158.6	5.3
55 μm	crying	158.2	158.2	157.9	6.2
110 μm	crying	160.2	160.8	159.9	6.2
160 μm	crying	160.2	159.5	161.9	6.1
50 μm	smiling	160.6	161.1	160.3	5.6
110 μm	smiling	163.0	160.5	164.2	10.2
155 μm	smiling	163.9	161.6	166.7	11.0

Table 3.4.: CD-U values of the first M170Y experiment

After processing the wafers in the cluster, the CD-bottom of the space structures is measured in a SEM according to the procedure described in section 2.6. The structures from the resist M170Y are removed after the experiment. This rework is done by a $\text{H}_2\text{O}_2/\text{H}_2\text{SO}_4$ mixture. Following this, a second bow measurement is performed (see centrebow after M170Y in table 3.3). The wafers experienced several heating (and cooling) processes during the coating, exposure and development steps with the resist M170Y. The heating stimulates diffusion processes between the oxide and silicon. The bow can change as a result of diffusion. However, only a small change of maximal 0.45 μm is observed. The change of bow is negligible and there is no significant change caused by the lithography steps.

The results of this experiment with the resist M170Y are shown in table 3.4. The average CD (shortened to avg CD), CD-centre, CD-edge and 3σ are average values of the groups. The 110 μm crying bow group, 160 μm crying bow group and 155 μm smiling bow group have some outliers with the definition from above. The outliers are a sign of a bad handling or processing in the machines. The corresponding values are removed from further analysis.

The average CD increases slightly for an increasing crying bow, from 158.7 nm at no bow, to 160.2 nm at 160 μm bow. The 3σ increases noticeable from 5.3 nm at no bow, to 6.1 nm at 160 μm bow. The difference between the CD of the centre and the CD of the edge is negligible.

The smiling bow groups have a bigger increase of average CD as well as CD-U (indicated by 3σ) than the crying groups. Average CD increases from 158.7 nm at no bow, to 163.9 nm at 155 μm bow. The 3σ increases steadily from 5.3 nm at no bow, to 11.0 nm at 155 μm bow. The CD-U is a lot worse for smiling wafers

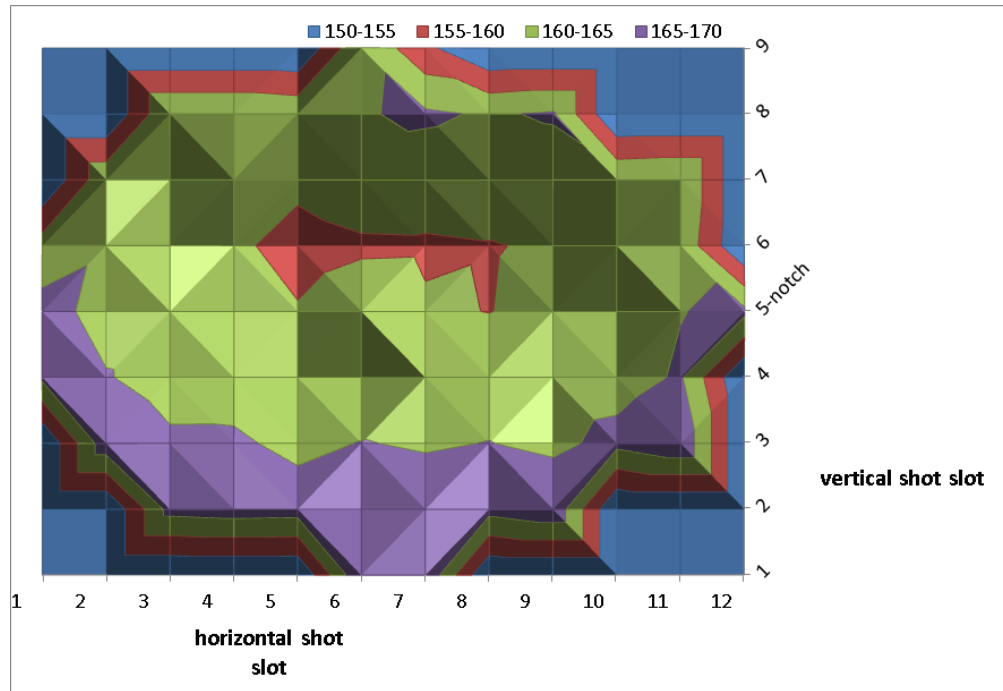


Figure 3.10.: Wafermap of the 155 μm smiling group with M170Y

than for crying wafers for the bigger bow groups. The CD in the centre is slightly increased for all smiling bow groups (e.g. 161.6 nm) compared to not bowed wafers (158.7 nm). The CD at the edge is strongly increasing with the increase of the bow value. It increases from 160.3 nm for 50 μm bow up to 166.7 nm for 155 μm bow. The difference between CD-centre and CD-edge is increasing with the same rate.

A graph showing the wafermap of the 155 μm smiling group is shown in fig. 3.10. In this plot the average CD in respect to the shot position is shown in a contour plot. The shot position is the position of the exposure region for a single exposure shot on the wafer. The position can be calculated to a radius from the centre or given in row/column coordinates as seen in the wafermaps. The average CD of a certain shot results from all wafers' CD in the respective group on that position. The colors indicate a certain CD-value-range given in the legend. The x and y coordinates are the exposure shot regions. The notch position is at 3 o'clock. The previous mentioned difference between CD at the centre and CD at the edge of the wafer can easily be seen in the wafermap. The wafermap of the 110 μm groups looks similar, but all the other groups have a mostly constant CD across the wafer. The wafermaps of the crying groups do not show a distinct pattern like the smiling groups.

bow group	average	minimum	maximum
no bow	996.87 nm	991.89 nm	1001.82 nm
crying	997.29 nm	992.85 nm	1001.35 nm
smiling-50 μm	690.35 nm	680.34 nm	703.19 nm
smiling-110 μm	357.18 nm	339.11 nm	371.03 nm
smiling-155 μm	86.27 nm	60.08 nm	106.39 nm

Table 3.5.: Results of the oxide thickness measurement

The smiling wafers have an oxide top layer. In order to investigate whether the oxide layer influences the measured CD by swing curves effects an oxide thickness measurement is performed. The standing waves (discussed in section 2.2) are wave formations on the sidewall of the resist. The waves change the contrast in the SEM-image and may therefore influence the CD. The average, minimal and maximal oxide thickness of each group is shown in table 3.5. The crying wafers were etched on the backside, so the frontside has the same thickness as the no bow group. The range of oxide thickness for the no bow and crying groups is 10 nm, while the smiling groups have a range of up to 50 nm. The contour plot of the measurement of a 155 μm smiling wafer is shown in fig. 3.11. This range is enough to go from a minimum on the swing curve to a maximum. Therefore we conclude that the oxide thickness variation influences the CD on the wafer and may be the cause of bad uniformity too. The later experiment with the resist M91Y with 405 nm resist thickness has inconsistencies in the evaluation of CD-U and the wafermaps show no patterns like in the most experiments with wafer bow. We think that the oxide thickness variation plays a role for the M91Y experiment in particular.

3.4.2. Second experiment

The wafers from the last section are etched again to remove the oxide completely on one side. The oxide thickness is measured for all the wafers in the following experiments to ensure that only a thin native oxide layer remains. The absence of the oxide variation eliminates the effect of the standing waves for the smiling wafers because the surface is bare silicon. A side-effect is an increase of the centrebow, see table 3.6 for the new values. There are 3 split-groups: no bow, 175 nm crying and 170 nm smiling. Six wafers could not be used for this experiment because the bow turned out to be smaller than expected. The number of wafers in the split-groups have increased, because we reduced the number of split-groups. The parameters for the experiments are shown in table 3.2 with the running number 2.

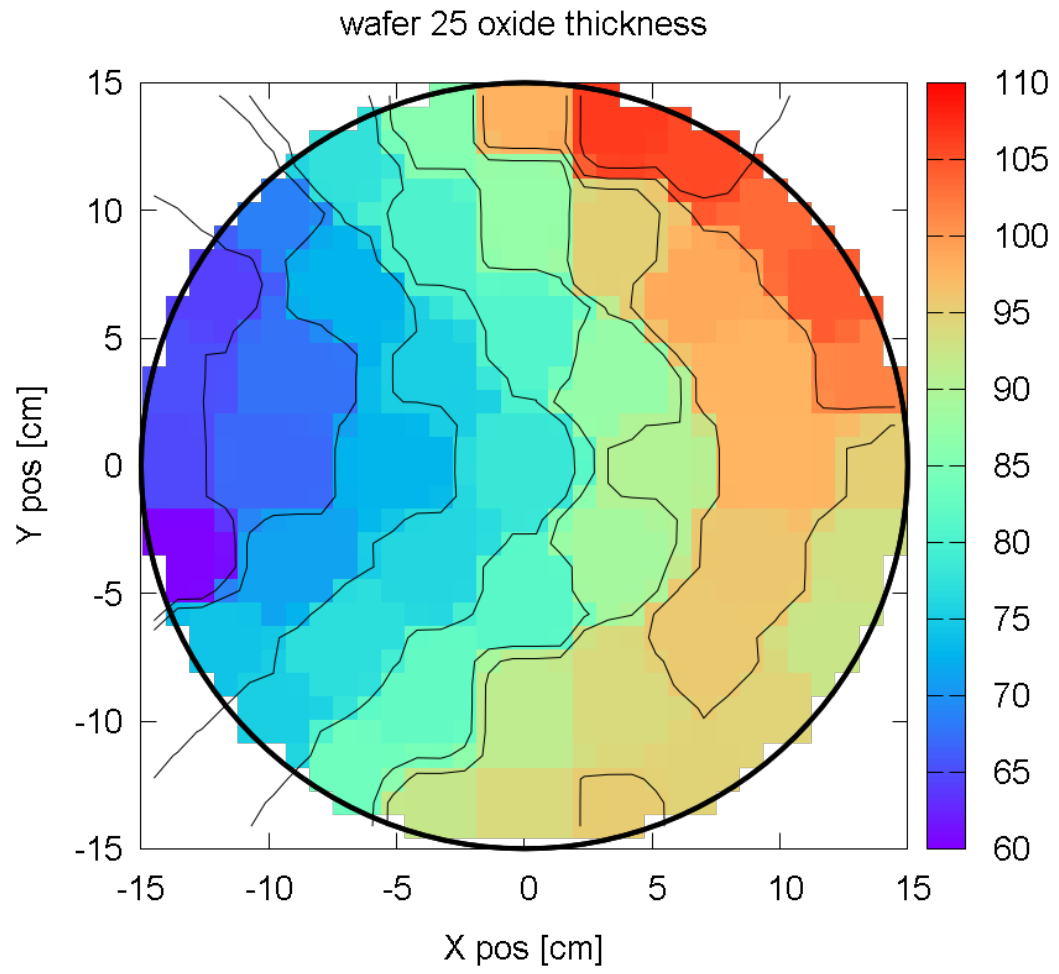


Figure 3.11.: Oxide thickness measurement of a 155 μm smiling wafer (wafer no.25)

wafer	etched side	oxide thickness range	bow type	centrebowl
1	frontside	0-1 nm	smiling	168.36 μm
2	frontside	0-1 nm	smiling	170.27 μm
3	frontside	0-1 nm	smiling	168.36 μm
4	frontside	0-1 nm	smiling	168.57 μm
5	frontside	0-1 nm	smiling	169.81 μm
6	frontside	0-1 nm	smiling	169.81 μm
7	frontside	0-1 nm	smiling	168.50 μm
8	backside	990-1000 nm	crying	-174.84 μm
9	backside	990-1000 nm	crying	-174.48 μm
10	backside	990-1000 nm	crying	-175.16 μm
11	backside	990-1000 nm	crying	-174.88 μm
12	backside	990-1000 nm	crying	-174.36 μm
13	backside	990-1000 nm	crying	-174.33 μm
14	backside	990-1000 nm	crying	-174.59 μm
15	backside	990-1000 nm	crying	-175.04 μm
16	-	990-1000 nm	no bow	-1.51 μm
17	-	990-1000 nm	no bow	-1.61 μm
18	-	990-1000 nm	no bow	-1.96 μm
19	-	990-1000 nm	no bow	-2.35 μm

Table 3.6.: Properties of the bowed wafers for the second experiment

bow group	bow type	avg CD [nm]	CD-centre [nm]	CD-edge [nm]	3σ [nm]
no bow	no bow	162.7	162.8	162.7	4.7
175 μm	crying	163.2	164.2	162.6	5.3
170 μm	smiling	170.3	166.0	172.7	12.2

Table 3.7.: CD-U values of the second M170Y experiment

The results from the experiment are shown in table 3.7. From the crying bow group we can see a slightly increased average CD of 163.2 nm in comparison to the no bow group with 162.7 nm. This results from a larger average CD at the centre, the value is 164.2 nm there. The 3σ of the crying group is 5.3 nm and is also slightly increased in comparison to the no bow group with 4.7 nm, because of the increase of CD at the centre, while the edge is at smaller values. This is shown in fig. 3.12.

The smiling bow group has a large average CD of 170.3 nm compared to the no bow group with 162.7 nm and the crying group with 163.2 nm. The CD at the centre is increased with 166.0 nm, but the CD at the edge is even larger with 172.7 nm. The wafermap in fig. 3.13 shows this behaviour, but also that the smallest CD is not in the wafer centre but roughly 30 mm away from the centre at the horizontal shot 5 and vertical shot 4 to 5. The 3σ of the smiling group is 12.2 nm and therefore larger than the 3σ from the no bow group 4.7 nm, the crying group 5.3 nm and the first experiment with 11.0 nm.

3.4.3. Third experiment

A new lot of wafers with a bow of up to 385 μm was prepared. The centrebow and the oxide thickness is shown in table 3.8. The parameters of the experiment are shown in table 3.2 with the running number 3. There are 4 split-groups: 255 μm smiling, 370 μm smiling, 275 μm crying and 385 μm crying.

We expect the observed trends of the CD to continue, especially the centre-edge-CD-trend. We are interested to see if the 3σ is going to increase significantly for the crying bow groups. For the smiling bow groups it is most interesting to see how far the CD is increasing and if there is an end for it or if it continues to rise.

The results of the M170Y experiment are shown in table 3.9. We can see that the average CD is increased for all groups in comparison with the no bow group from the second experiment with 162.7 nm (see table 3.7). The crying bow groups show an increase of the average CD from 166.6 nm of the 275 μm group to 167.8 nm of

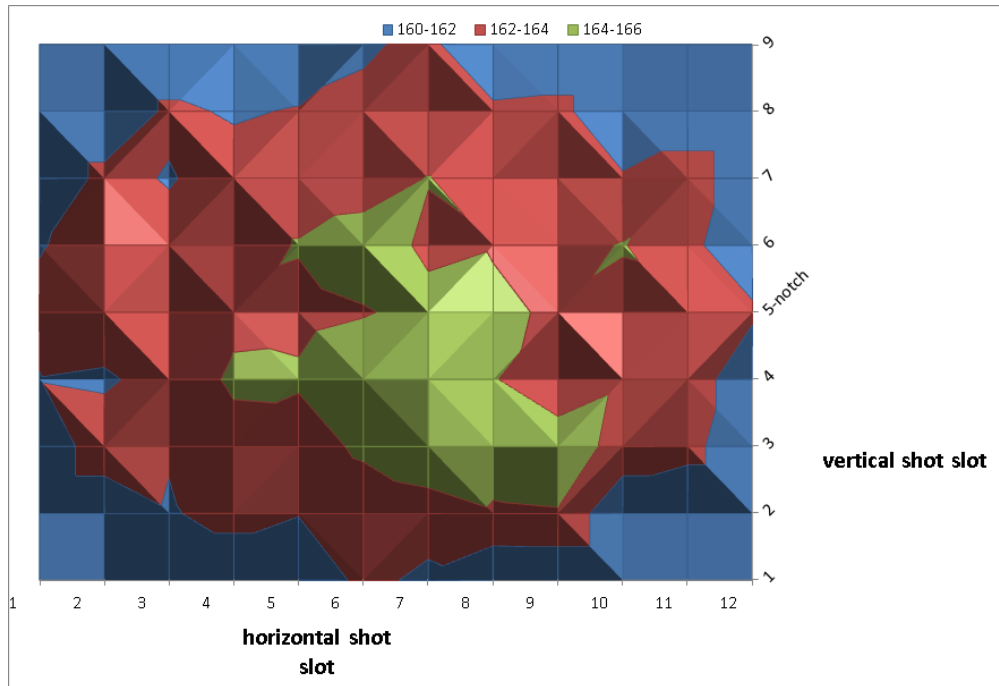


Figure 3.12.: Wafermap of the 175 μm crying group with M170Y

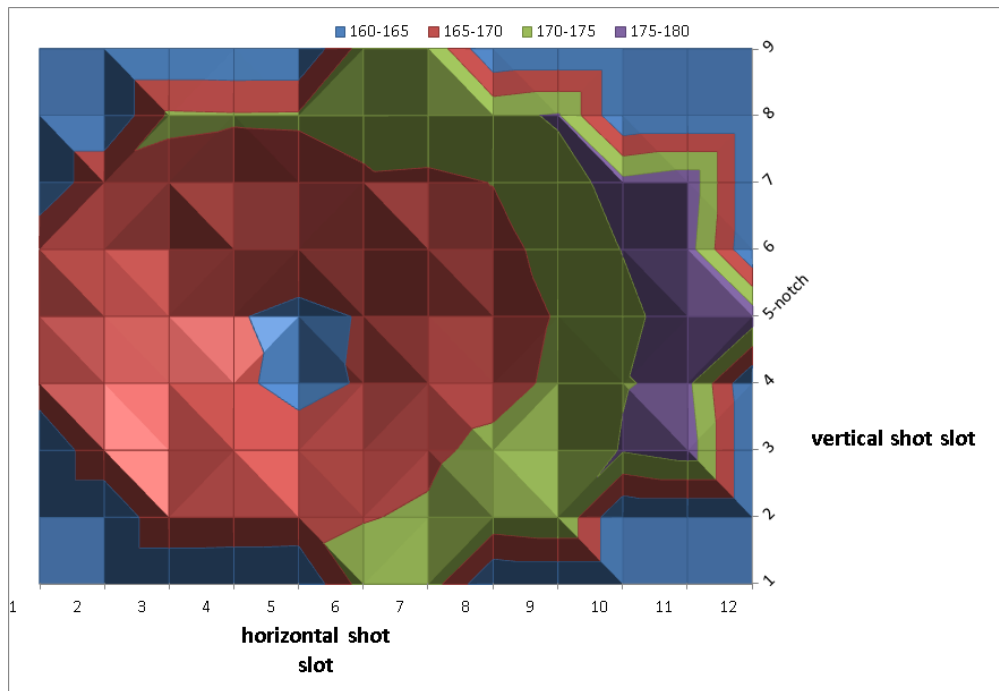


Figure 3.13.: Wafermap of the 170 μm smiling group with M170Y

wafer	etched side	oxide thickness range	bow type	centrebow
1	frontside	0-11 nm	smiling	267.13 μm
2	frontside	0-11 nm	smiling	255.58 μm
3	frontside	0-11 nm	smiling	255.10 μm
4	frontside	0-11 nm	smiling	254.97 μm
5	frontside	0-11 nm	smiling	254.50 μm
6	frontside	0-11 nm	smiling	254.64 μm
7	backside	1.625-1.635 μm	crying	-272.91 μm
8	backside	1.625-1.635 μm	crying	-273.13 μm
9	backside	1.625-1.635 μm	crying	-273.20 μm
10	backside	1.625-1.635 μm	crying	-273.63 μm
11	backside	1.625-1.635 μm	crying	-274.01 μm
12	backside	1.625-1.635 μm	crying	-285.27 μm
13	frontside	0-5 nm	smiling	370.82 μm
14	frontside	0-5 nm	smiling	369.82 μm
15	frontside	0-5 nm	smiling	370.03 μm
16	frontside	0-5 nm	smiling	369.44 μm
17	frontside	0-5 nm	smiling	369.51 μm
18	frontside	0-5 nm	smiling	369.47 μm
19	backside	2.354-2.361 μm	crying	-385.40 μm
20	backside	2.354-2.361 μm	crying	-385.27 μm
21	backside	2.354-2.361 μm	crying	-385.69 μm
22	backside	2.354-2.361 μm	crying	-385.66 μm
23	backside	2.354-2.361 μm	crying	-385.81 μm
24	backside	2.354-2.361 μm	crying	-386.62 μm
25	backside	2.354-2.361 μm	crying	-385.84 μm

Table 3.8.: Properties of the bowed wafers for the third experiment

bow group	bow type	avg CD [nm]	CD-centre [nm]	CD-edge [nm]	3σ [nm]
275 μm	crying	166.6	168.7	165.4	5.8
385 μm	crying	167.8	170.2	165.9	6.9
255 μm	smiling	171.6	169.4	172.6	9.1
370 μm	smiling	171.4	169.5	171.8	10.0

Table 3.9.: CD-U values of the third M170Y experiment

bow group	bow type	avg CD [nm]	CD-centre [nm]	CD-edge [nm]	3σ [nm]
275 μm	crying	167.9	169.6	166.4	6.4
385 μm	crying	169.2	171.0	167.4	7.3
255 μm	smiling	172.9	170.7	174.1	9.4
370 μm	smiling	173.0	172.3	173.0	8.7

Table 3.10.: CD-U values of the repetition of the third M170Y experiment

the 385 μm group. The CD-edge is roughly the same for both crying groups, but the CD-centre goes from 168.7 nm from the 275 μm crying group up to 170.2 nm from the 385 μm crying group. The 3σ increases in the same way from 5.8 nm from the 275 μm crying group up to 6.9 nm from the 385 μm crying group. The wafermaps of the 275 μm crying bow group and of the 385 μm crying bow group are shown in fig. 3.14 and fig. 3.15 respectively. We can see same the centre-edge-CD-trend from the previous experiments on crying bow wafers.

The average CD is almost the same for both smiling bow groups, 171.6 nm versus 171.4 nm. Both smiling groups also have almost the same CD-centre, 169.4 nm versus 169.5 nm. The CD-edge is slightly different between the groups, 172.6 nm for the 255 μm smiling bow group and 171.8 nm for the 370 μm smiling bow group. The average CD and CD-centre from the smiling groups are larger than those of the 170 μm smiling bow group from the second experiment. The CD-edge from the smiling bow groups is slightly smaller than the one of the 170 μm smiling bow group from the second experiment. The 3σ increases from 9.1 nm of the 255 μm smiling bow group to 10.0 nm of the 370 μm smiling bow group, but the 170 μm smiling bow group from the previous experiment has a larger 3σ of 12.2 nm. It is not clear why the smaller bow has a worse CD-U than the larger bow groups.

The wafermaps of the smiling groups look similar and are shown in fig. 3.16 for the 255 μm smiling bow group and in fig. 3.17 for the 370 μm smiling bow group. The wafermaps (see appendix A.2) of the single wafers show that the orientation of the largest spots varies from wafer to wafer. This may be due to a tilt of the wafers in the PEB, either caused by bad handling of the robot arm or by small variations in the thickness of the oxide.

Repetition of the third experiment

The third experiment with bow up to 385 μm is repeated to show that we are able to reproduce the observations. The parameters are the same (see table 3.2, running number 4), the experiment happened 3 weeks after the initial one. We

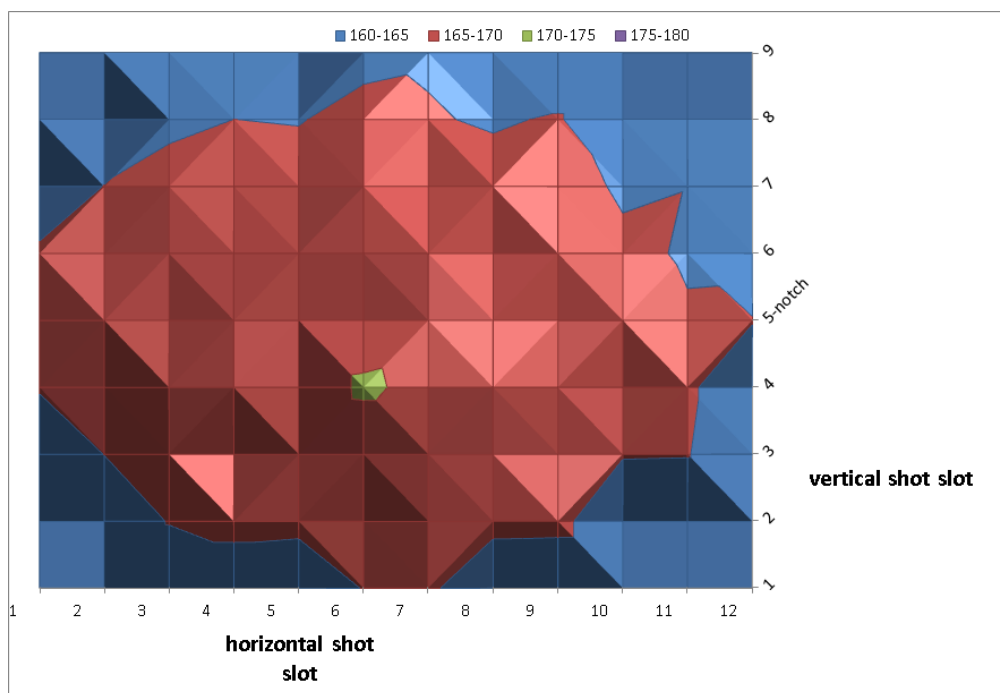


Figure 3.14.: Wafermap of the 275 μm crying group with M170Y

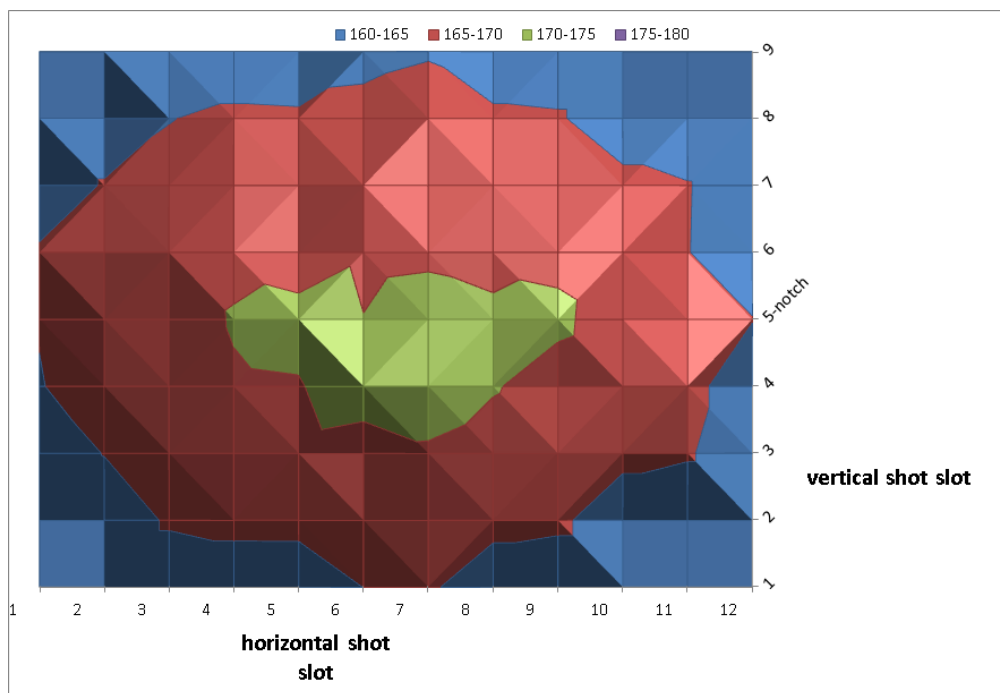


Figure 3.15.: Wafermap of the 385 μm crying group with M170Y

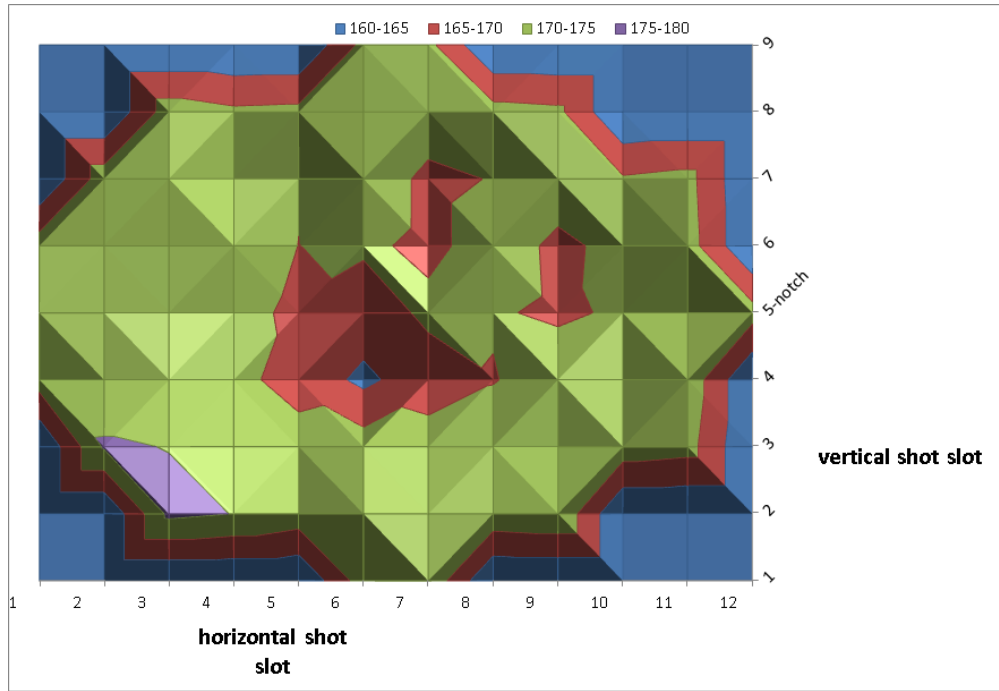


Figure 3.16.: Wafermap of the 255 μm smiling group with M170Y

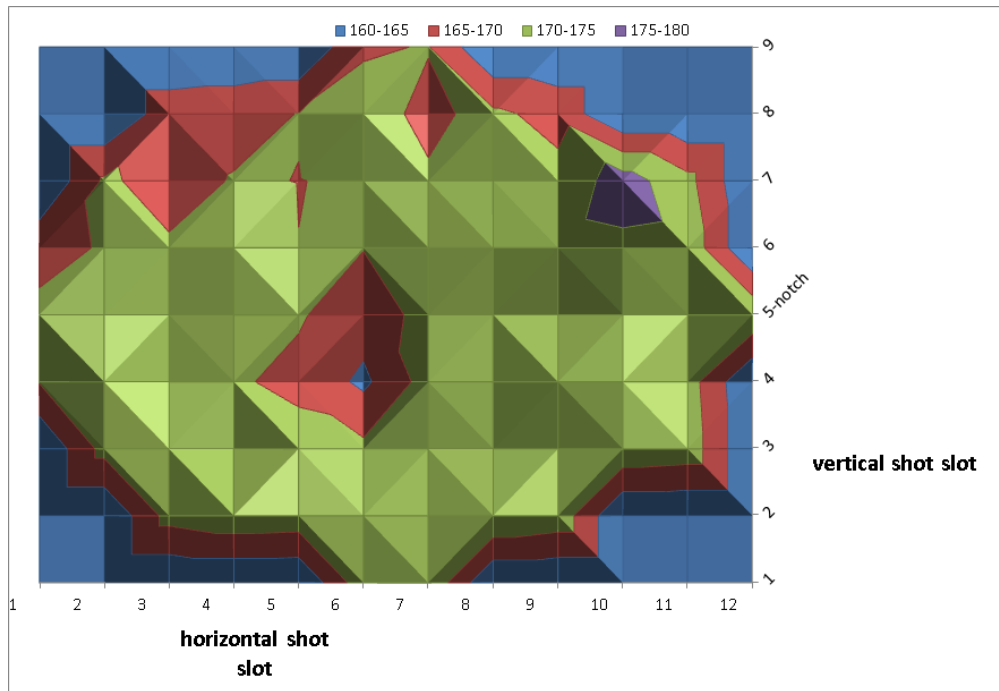


Figure 3.17.: Wafermap of the 370 μm smiling group with M170Y

expect to see similar results like in the third experiment.

The results of this experiment are shown in table 3.10. The crying bow groups show an increase of the average CD from 167.9 nm of the 275 μm group to 167.9 nm of the 385 μm group. The CD-centre increases from 169.6 nm of the 275 μm crying group to 171.0 nm of the 385 μm crying group. The CD-edge of the 275 μm crying group is 166.4 nm, the CD-edge of the 385 μm is 1 nm larger. The 3σ increases from 6.4 nm of the 275 μm crying group to 7.3 nm of the 385 μm crying group.

The wafermap of the 275 μm crying group is shown in fig. 3.18, the wafermap of the 385 μm crying group is shown in fig. 3.19. The wafermaps of the crying groups look similar to the ones of the third experiment, except that the golden spot in the wafer-centre is larger, which means that the CD is larger than in the previous experiment.

The average CD for the smiling groups is almost the same, 172.9 nm versus 173.0 nm. In this experiment the CD-centre is larger for the 370 μm smiling group with 172.3 nm compared to the 170.7 nm of the 255 μm smiling group. In the previous experiment the average CD in the centre was almost the same. The CD-edge decreases with increasing bow value, 174.1 nm for the 255 μm smiling group decreases to 173.0 nm for the 370 μm smiling group. This behaviour is similar to the previous experiment. The 3σ of the 255 μm smiling group is 9.4 nm and the 3σ of the 370 μm smiling group is 8.7 nm. The 3σ for the 255 μm smiling group went up while it went down for the 370 μm smiling group, in comparison with the previous experiment.

The wafermaps of the 255 μm and 370 μm smiling groups are shown in fig. 3.20 and fig. 3.21 respectively. The largest part of the wafermaps has a large CD, indicated by the golden color, and near the centre are a few spots with the minimal CD, indicated by the red color. The largest CD values are near the notch for both groups. The location of the largest CD values for this experiment is different than in the third experiment, probably because the wafer position on the hot plate differs from wafer to wafer. The wafermaps of the single wafers indicate that, because the smallest and largest CD-spots are in different positions from wafer to wafer (see Wafermaps of bowed wafers in the appendix).

Comparison 3rd experiment with the repetition

The average CD is about 1.4 nm larger for all the groups than at the initial experiment (see fig. 3.22). We consider the increase of the average CD between the experiments as a minor change. The 3σ of the crying groups from the repetition

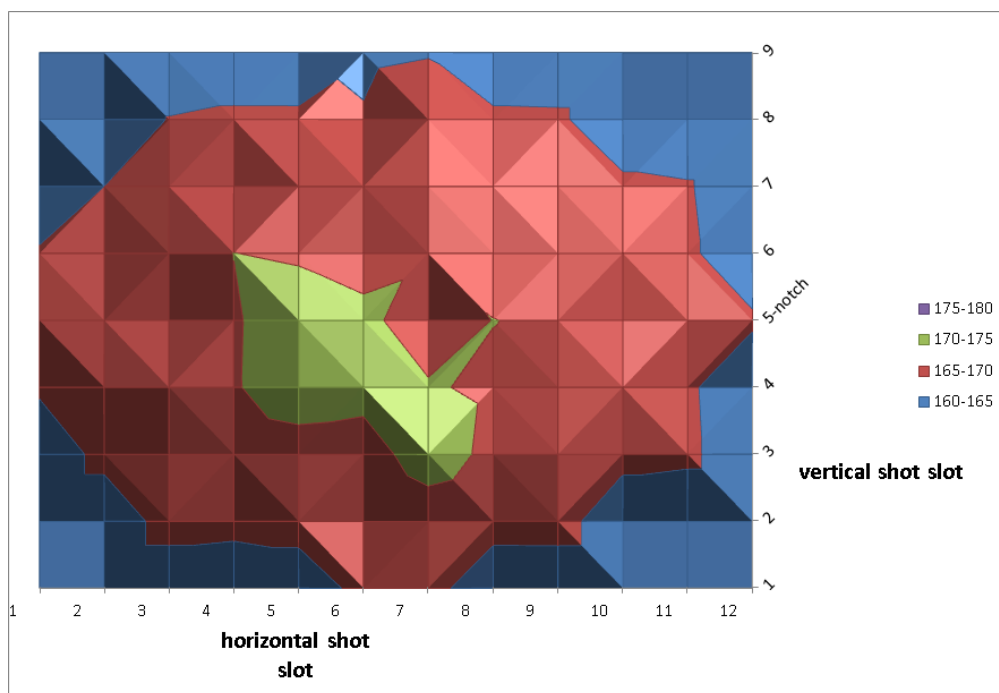


Figure 3.18.: Wafermap of the 275 μm crying group with M170Y

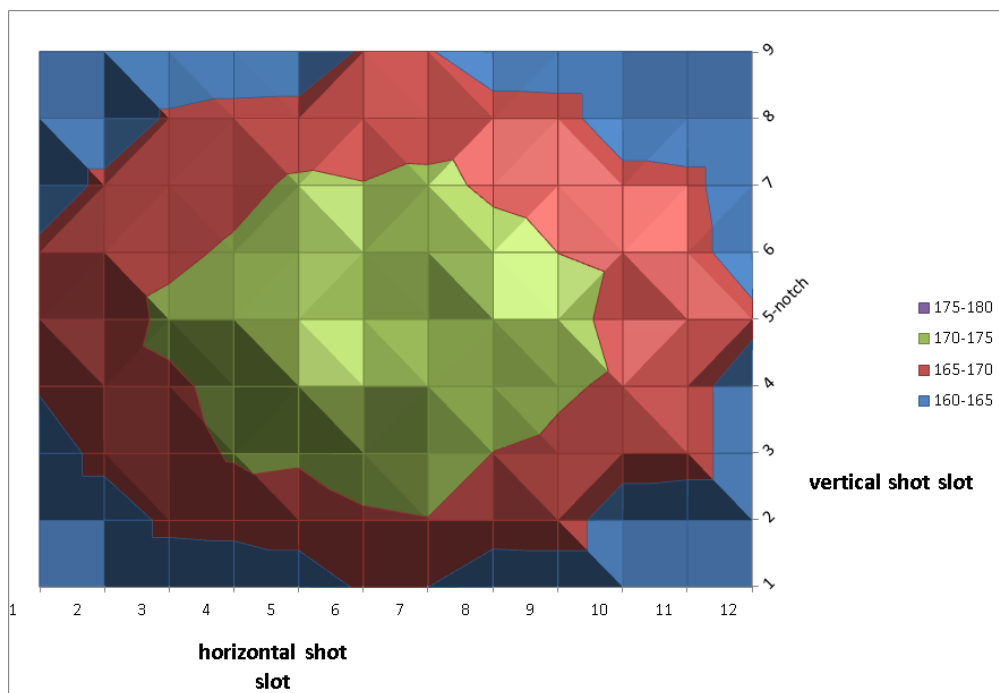


Figure 3.19.: Wafermap of the 385 μm crying group with M170Y

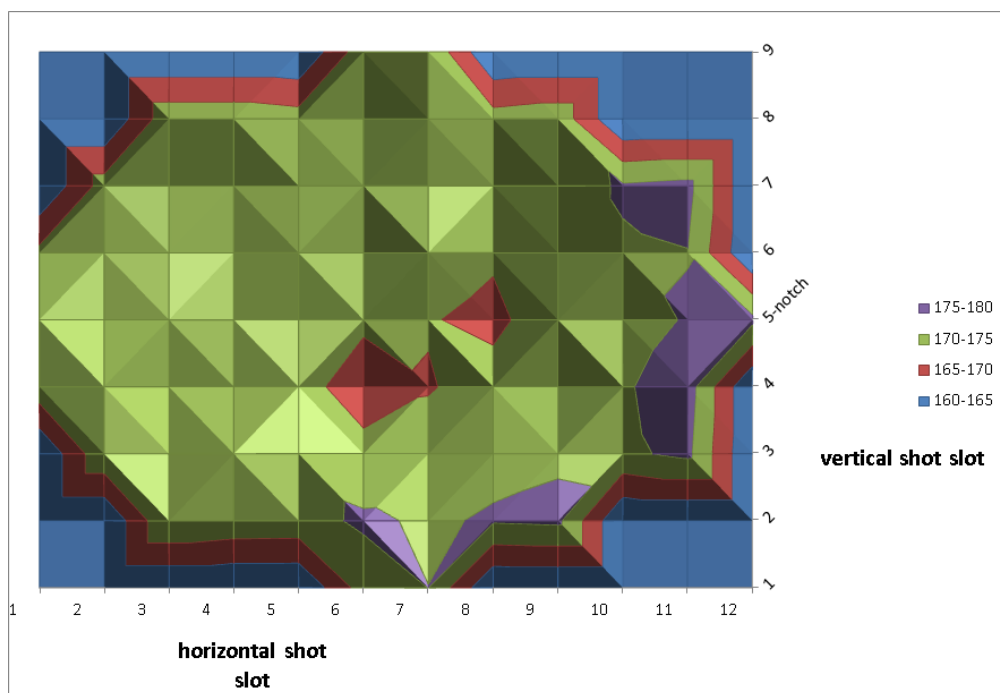


Figure 3.20.: Wafermap of the 255 μm smiling group with M170Y

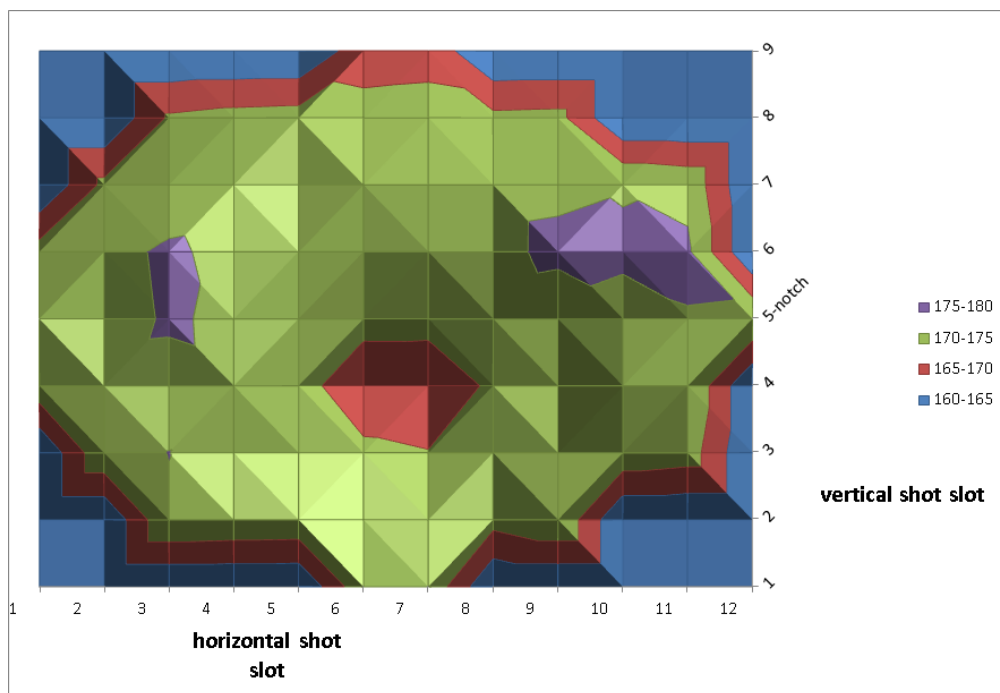


Figure 3.21.: Wafermap of the 370 μm smiling group with M170Y

bow group	bow type	avg CD 3rd	avg CD rep	3σ 3rd	3σ rep
275 μm	crying	166.6 nm	167.9 nm	5.8 nm	6.4 nm
385 μm	crying	167.8 nm	169.2 nm	6.9 nm	7.3 nm
255 μm	smiling	171.6 nm	172.9 nm	9.1 nm	9.4 nm
370 μm	smiling	171.4 nm	173.0 nm	10.0 nm	8.7 nm

Table 3.11.: Average CD and 3σ for the 3rd experiment and its repetition

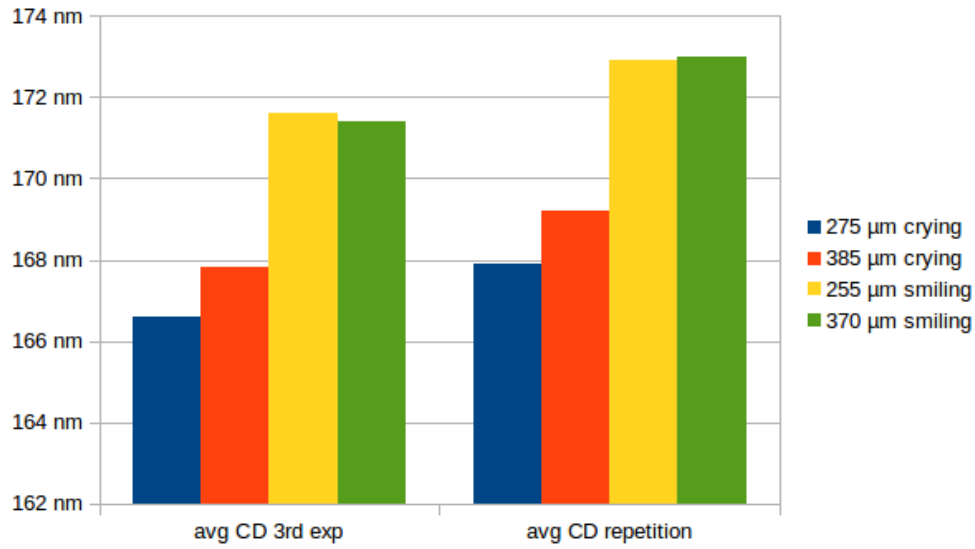


Figure 3.22.: Average CD for the 3rd experiment and its repetition

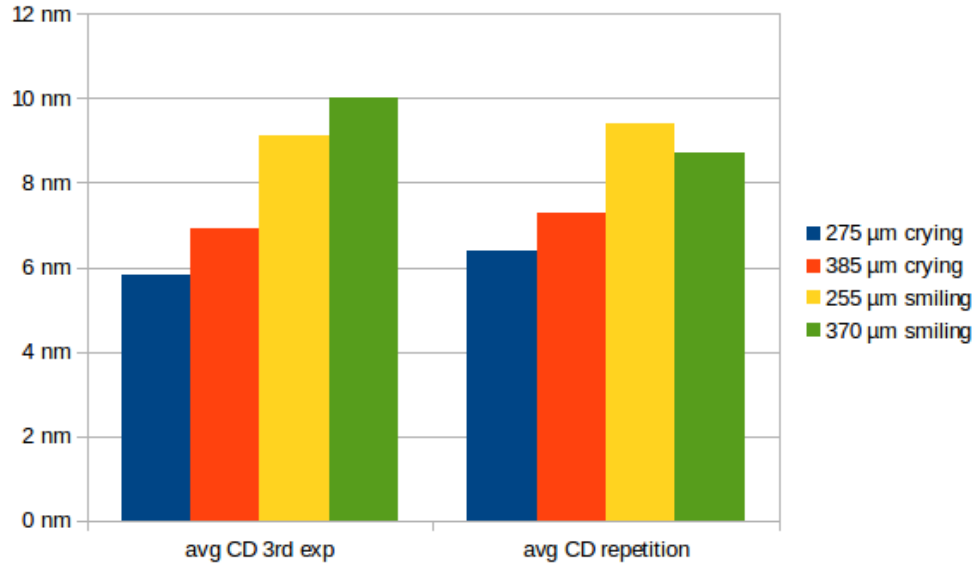


Figure 3.23.: 3σ for the 3rd experiment and its repetition

is larger than the 3σ from the initial experiment (see fig. 3.23). The 3σ of the 255 μm smiling group is larger compared to the initial experiment, while the 3σ of the 370 μm group is smaller.

The crying and smiling groups show different behaviour in regards to reproducibility. The change in 3σ between the experiments for the crying groups is not significant and therefore we consider it repeatable. The smiling groups show an increase of the 3σ for the 255 μm group, but a decrease for the other. When we look at the wafermaps we see that the spots with the largest CD are on different positions from wafer to wafer. This suggests that the position of a smiling wafer on the hot plate is not stable and is different from wafer to wafer. The 3σ for the smiling groups is not significantly different between the experiments. Therefore we conclude that the experiment with smiling wafers has only limited reproducibility.

3.4.4. Fourth experiment

The fourth and fifth experiment are performed on wafers with smaller bow than the previous two experiments. We want to know at if a bow of 130 μm differs significantly from the not bowed wafers. The wafers are taken from the first lot. The frontside of the wafers is blank silicon and the wafers are etched on the backside to reduce the centrebow. 10 wafers were used for the experiment. The centrebow and the oxide thickness of the wafers are shown in table 3.12. There is only 1

wafer	etched side	oxide thickness range	bow type	centrebow
1	backside	0-1 nm	smiling	131.09 μm
2	backside	0-1 nm	smiling	122.13 μm
3	backside	0-1 nm	smiling	122.46 μm
4	backside	0-1 nm	smiling	121.80 μm
5	backside	0-1 nm	smiling	122.27 μm
6	backside	0-1 nm	smiling	131.51 μm
7	backside	0-1 nm	smiling	126.16 μm
8	backside	0-1 nm	smiling	126.12 μm
9	backside	0-1 nm	smiling	125.79 μm
10	backside	0-1 nm	smiling	130.36 μm

Table 3.12.: Properties of the bowed wafers for the fourth experiment 130 nm bow

bow group	bow type	avg CD [nm]	CD-centre [nm]	CD-edge [nm]	3σ [nm]
130 μm	smiling	168.2	163.2	171.0	12.9

Table 3.13.: CD-U values of the fourth M170Y experiment

group in this experiment, 130 μm smiling bow. The parameters of the experiment are shown in table 3.2 with the running number 5.

The results of the experiment are shown in table 3.13. This is a single group experiment, so we can only compare the results with other experiments, this is done in section 3.4.6. The average CD is 168.2 nm. The difference between CD-centre (163.2 nm) and CD-edge (171.0 nm) is large with 7.8 nm. The 3σ is large too with 12.9 nm. The wafermap of the 130 μm is shown in fig. 3.24. The wafermap shows a small CD at the central shots, indicated by the blue spot. At the edge the CD increases and is largest at the notch, indicated by the purple spots.

3.4.5. Fifth experiment

The wafers from the first lot are etched on the backside to further reduce the centrebow. 11 wafers can be used in the experiment after the etch. The centrebow and the oxide thickness of the wafers are shown in table 3.14. There are 2 groups in this experiment, 90 μm smiling bow and 80 μm smiling bow. The parameters of the experiment are shown in table 3.2 with the running number 6.

The results of the fifth experiment are shown in table 3.15. The average CD of the 90 μm smiling group is 166.1 nm and larger than the average CD of the

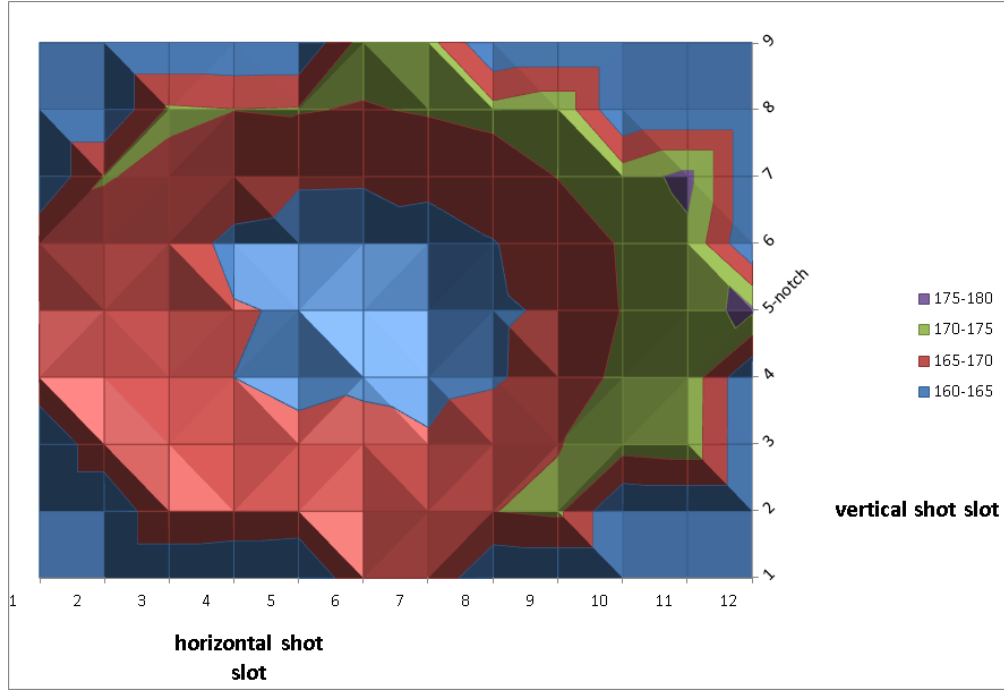


Figure 3.24.: Wafermap of the 130 μm smiling group with M170Y

wafer	etched side	oxide thickness range	bow type	centrebowl
1	backside	0-1 nm	smiling	81.56 μm
2	backside	0-1 nm	smiling	81.73 μm
3	backside	0-1 nm	smiling	80.99 μm
4	backside	0-1 nm	smiling	81.59 μm
5	backside	0-1 nm	smiling	91.05 μm
6	backside	0-1 nm	smiling	90.78 μm
7	backside	0-1 nm	smiling	89.85 μm
8	backside	0-1 nm	smiling	89.50 μm
9	backside	0-1 nm	smiling	89.15 μm
10	backside	0-1 nm	smiling	89.80 μm
11	backside	0-1 nm	smiling	90.57 μm

Table 3.14.: Properties of the bowed wafers for the fourth experiment 90 nm bowl

bowl group	bowl type	avg CD [nm]	CD-centre [nm]	CD-edge [nm]	3σ [nm]
90 μm	smiling	166.1	164.4	167.2	7.3
80 μm	smiling	164.2	163.1	164.7	5.0

Table 3.15.: CD-U values of the fifth M170Y experiment

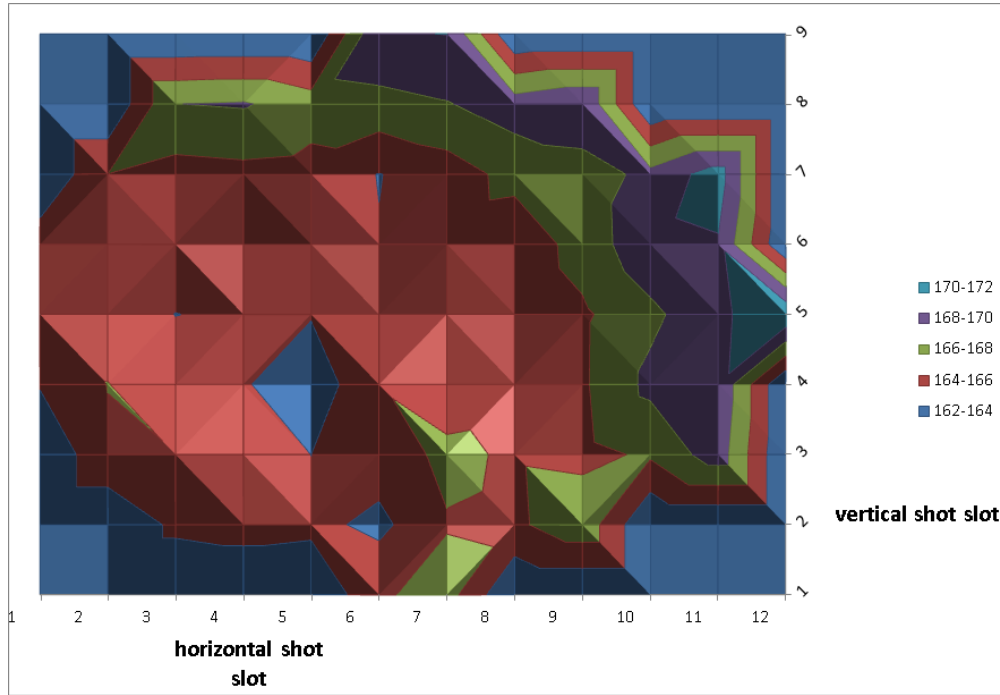


Figure 3.25.: Wafermap of the 90 μm smiling group with M170Y

80 μm smiling group with 164.2 nm. The difference between CD-centre (164.4 nm) and CD-edge (167.2 nm) of the 90 μm smiling group is 2.8 nm. The 80 μm smiling group has a difference between CD-centre (163.1 nm) and CD-edge (164.7 nm) of the 1.4 nm. The 3σ of the 90 μm smiling group is 7.3 nm, while it is 5.0 nm for the 80 μm smiling group.

The wafermap for the 90 μm smiling group in fig. 3.25 shows a small CD near the centre, indicated by the blue spot. The largest CD for the 90 μm smiling group is near the notch, indicated by the blue-green spot. The wafermap for the 80 μm smiling group is shown in fig. 3.26. The largest CD is near the notch, indicated by the golden spot, while the smallest CD is at roughly 9 o'clock. There are many small-CD-spots on the wafermap, indicated by blue color.

3.4.6. Results

The CD-U results of the crying bow groups are compared in fig. 3.27. The group name and the number of the experiment is given in the legend of the graph (3^{rep} stands for the repetition of the third experiment). The groups are lined up with increasing centrebow from left to right. For the crying bow groups we can see an increasing 3σ with increasing centrebow. The crying groups from the first experi-

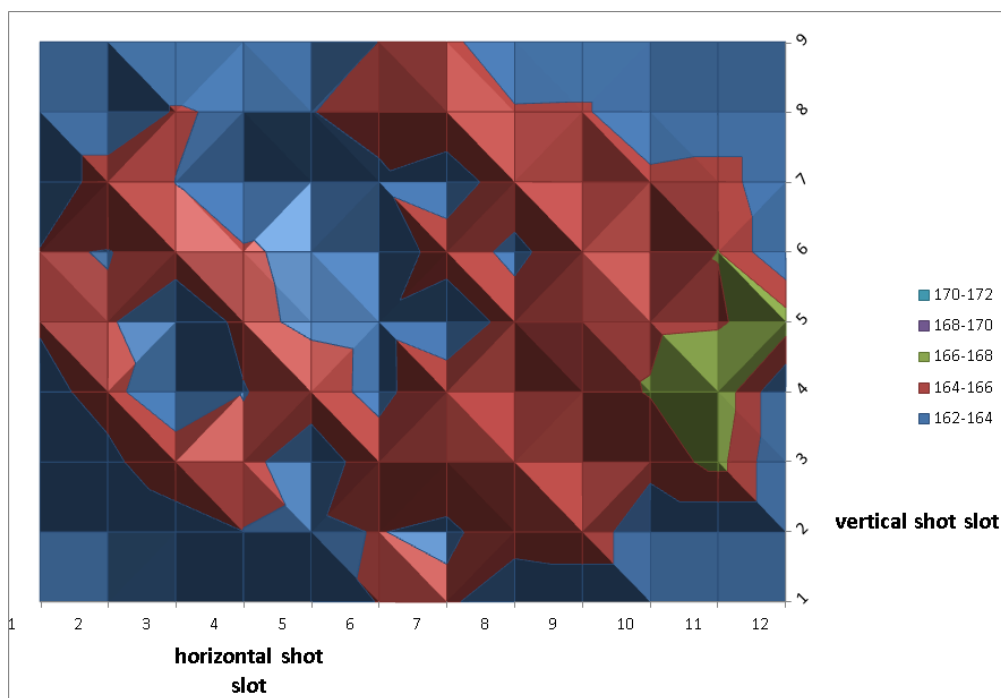


Figure 3.26.: Wafermap of the 80 μm smiling group with M170Y

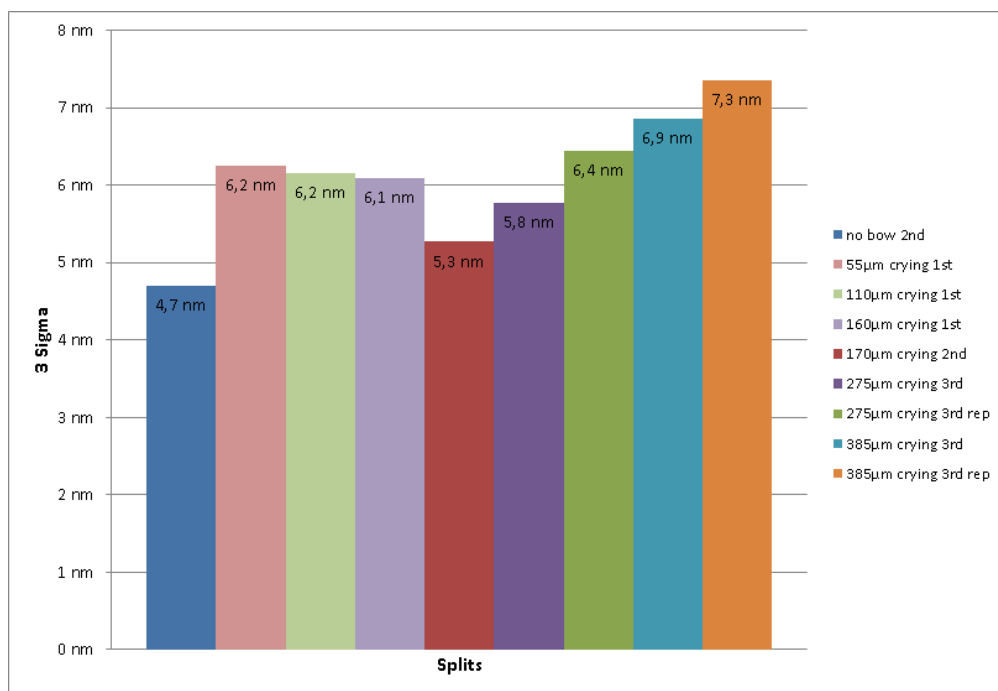


Figure 3.27.: CD-U comparison of the crying bow groups

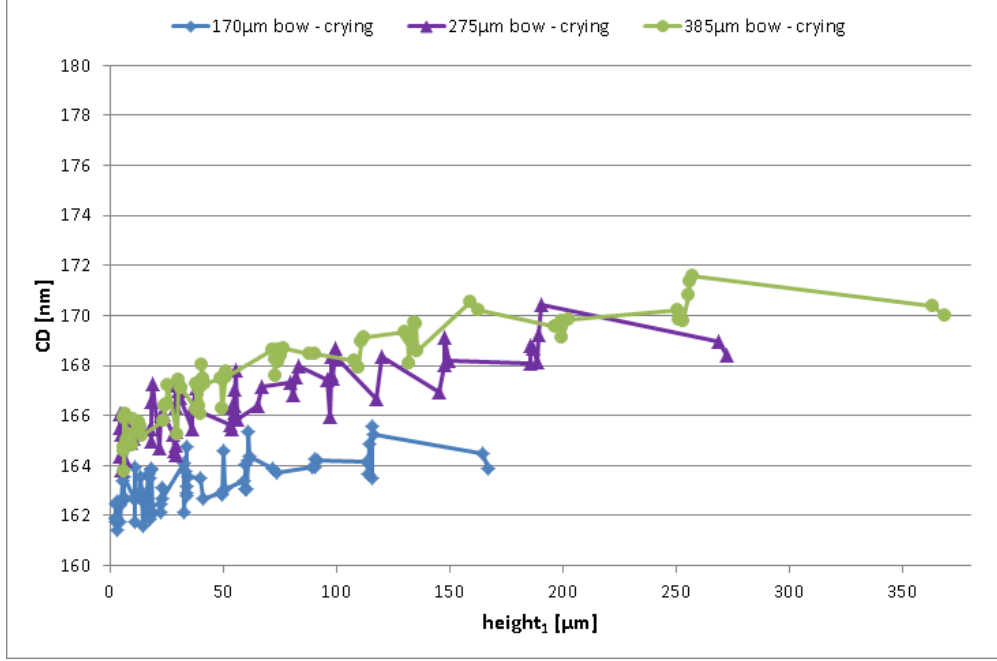


Figure 3.28.: CD over height₁ for the 175 μm, 275 μm and 385 μm crying bow groups

ment are the exception to this observation, this is probably due to a contamination of a coater unit, which caused problems for other experiments as described in chapter 4. The contaminated coater is the reason why the focus of this section is on the second to fifth experiment. From the wafermaps of the experiments we conclude that the 3σ increase is due to the centre-edge-CD-trend. The repetition of the third experiment shows an increase of 3σ , a worse CD-U. It is not understood why the 3σ is larger in the repetition, but the wafermaps, the CD-centre and the CD-edge behave similar to the initial experiment.

$$height = \frac{\kappa \cdot (2 \cdot r)^2}{8} \quad (3.1)$$

$$height_1 = \frac{\kappa \cdot (2 \cdot (150 \text{ mm} - r))^2}{8} \quad (3.2)$$

The defined variable *height* plus the constant height of the gap pins ($= 100 \mu\text{m}$) plus the thickness of the wafer ($800 \mu\text{m}$) is the distance between the shot position on the wafer and the hot plate during the PEB. The expressions for calculating it from the radial position of the shot are given in eq. (3.1) and eq. (3.2). κ is the curvature of the bowed wafer, which is defined as the reciprocal of the radius of a circle. r is the radius from the centre of the wafer to the shot. The smiling

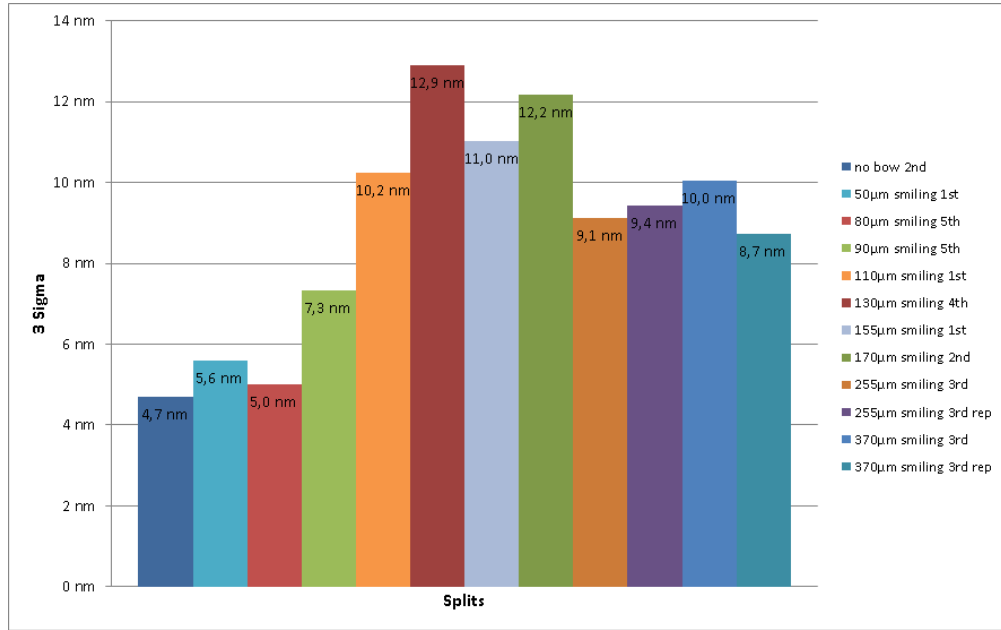


Figure 3.29.: CD-U comparison of the experiments on smiling bow groups

wafers have the shortest distance at the centre of the wafer where the gap pins make contact with the wafer, this is where we want to have $height = 0 \mu m$. The crying wafers are in contact with the gap pins close to the edge of the wafer. Hence the second formula for the height, because we want to have $height_1 = 0 \mu m$ at the edge of the wafer.

The crying bow groups have a similar growth of CD with the $height_1$ as shown in fig. 3.28. The 275 µm crying bow group and the 385 µm crying bow group have the same CD at the first measurement points close to the edge ($height_1 \hat{=} 0 \mu m$). The 175 µm crying bow group is offset by roughly 2.5 nm. The steepness of the curve increases with increasing bow group. We can see smaller CD-values of the 275 µm crying bow group at the height-range=150 µm-270 µm compared to the 385 µm crying group.

The CD-U results of the smiling bow groups are compared in fig. 3.29. The first experiment had some problems with a contaminated coater, so we need to be careful with interpreting the groups of the first experiment. The 3σ increases with increasing centrebow until the 130 nm smiling group. Then the 3σ decreases slowly with increasing centrebow. We assume that the main factor for the 3σ change is the centre-edge-CD-trend. A minor factor is the accuracy of the robot, which handles the wafers onto the hot plate (see the smiling wafer in fig. 3.6). The

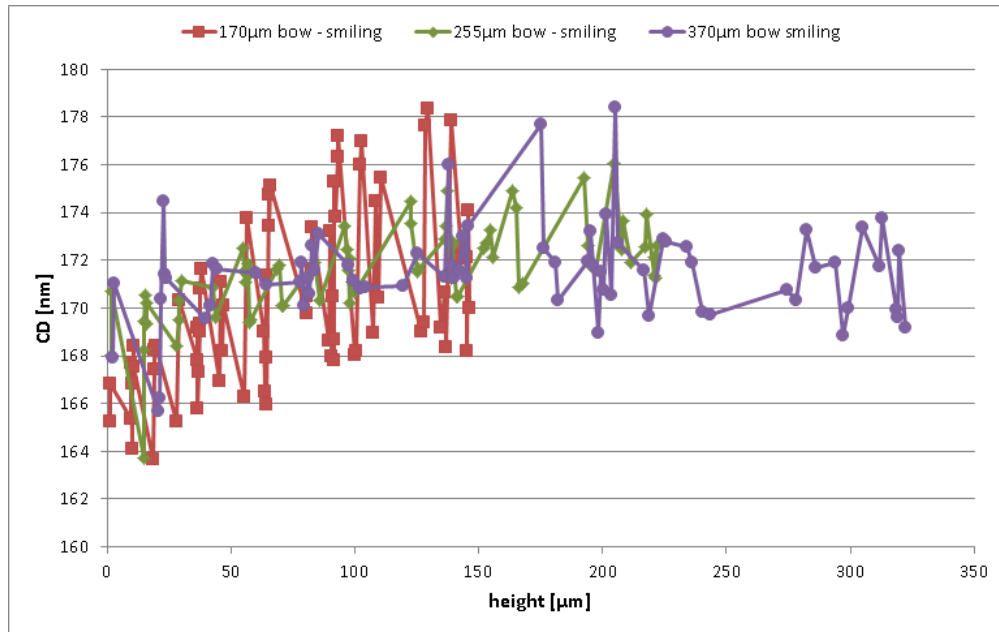


Figure 3.30.: CD over height for the 170 μm , 255 μm and 370 μm smiling bow groups

position is not well defined and seems to be different for every wafer because of the form of the wafer and the single central pin. In the third experiment the 255 μm smiling group has a 3σ of 9.1 nm, while the repetition of the experiment gives us a 3σ of 9.4 nm. The 370 μm smiling group has a 3σ of 10.0 nm, while the repetition of the experiment gives us a 3σ of 8.7 nm. It is not known why the groups vary their 3σ that much, but we can assume that the wafer robot accuracy plays a role.

The smiling bow groups have a similar behaviour with an increase in *height* as shown in fig. 3.30 and fig. 3.31. We see a strong increase of the CD with the *height* up until roughly 130 μm . Then the curves stay flat until about 200 μm and afterwards they decline. The CD in the centre varies for the groups, the smaller the centrebow, the smaller the CD in the centre. The exception is the 130 μm smiling group, which has almost the same CD in the centre as the 80 μm smiling group.

Our assumption for the difference between CD at the centre and CD at the edge is a change in the thermal conditions at the edge of the wafer. A smiling wafer has a larger distance between edge and hot plate than a not bowed wafer and can experience a lower temperature at the edge. A lower temperature and the negative PEB-temperature-coefficient of the M170Y result in an increased CD at the edge.

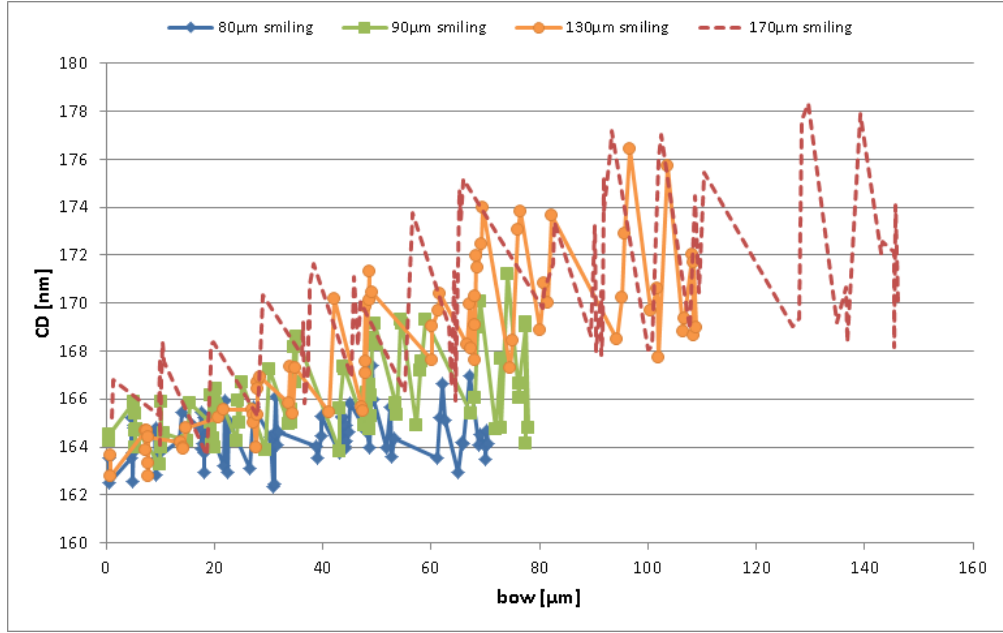


Figure 3.31.: CD over height for the 80 μm , 90 μm , 130 μm and 170 μm smiling bow groups

The graph in fig. 3.32 shows the PEB-temperature calculated with the average CD of the exposure shots, if the PEB-temperature is the only influence on the CD. The CD is averaged over all wafers of the respective group on a fixed exposure shot position for all those positions. The PEB-temperature is calculated with eq. (3.4). A is a constant that shifts the curve up or down on the temperature. The temperature at the bake is 130 $^{\circ}\text{C}$, so A is adjusted to reach this temperature at the centre. The temperature change from centre to edge for the crying group is roughly 1 $^{\circ}\text{C}$, while the same change for the smiling group is estimated with -3.5°C . The CD-values vary strongly for the smiling group, because the PEB-temperature-curve is varying in a similar way. The range of the temperature change at the edge points is -2°C to -6°C .

$$CD = A - 2.2 \text{ nm}/^{\circ}\text{C} \cdot T_{PEB} \quad (3.3)$$

$$T_{PEB} = \frac{(A - CD)}{2.2 \text{ nm}/^{\circ}\text{C}} \quad (3.4)$$

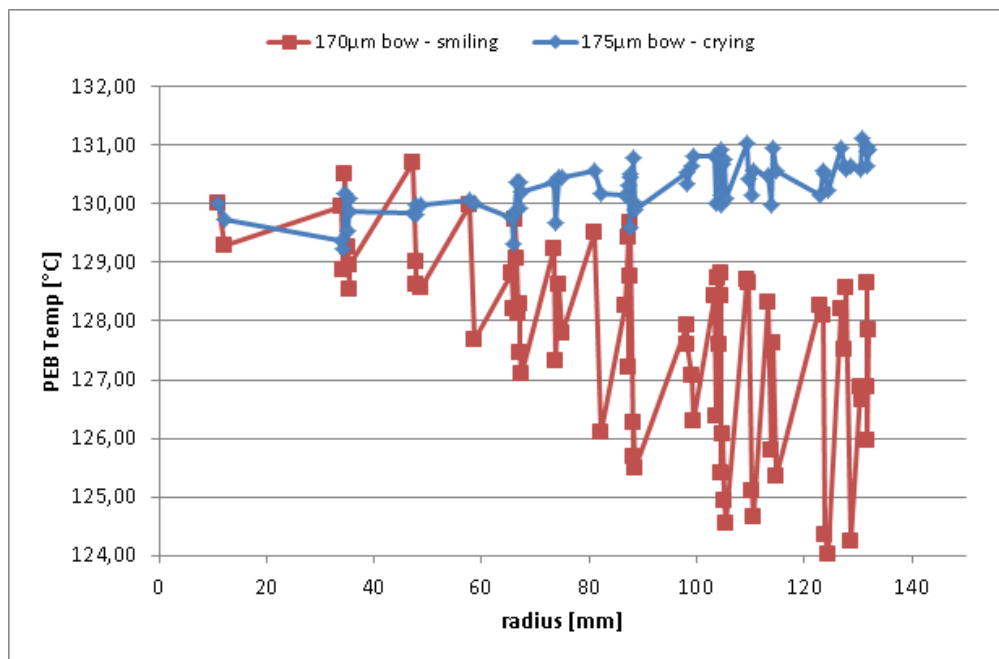


Figure 3.32.: PEB-temperature resulting from the average CD of the exposure shots versus their radial position from the centre (assuming that the PEB is the only influence)

3.5. Experiments with the resist M91Y

3.5.1. First experiment - 414 nm thickness

The following experiment is performed on a second resist, M91Y, which has a different PEB-temperature-coefficient. The goal is to verify if the change in CD and 3σ of the bowed wafer groups can be explained by the different thermal conditions they experience in the PEB. The exposure dose, focus and resist thickness is set to the same values like in the M170Y experiment (see table 3.16 with the running number 7). The lot 1 is used for this experiment and the centrebow and the oxide thickness is shown in table 3.3.

The average CD and 3σ values of the crying groups are similar to the no bow group - 161.8 nm average CD and 7.9 nm 3σ for the no bow group and for instance 160.6 nm average CD and 8.0 nm 3σ for the 160 μm crying group. The 55 μm crying group showed a better CD-U with 7.4 nm than the no bow group. The wafermaps of the no bow and the crying groups are unremarkable and show a mostly statistical CD across the wafer.

The smiling groups show a larger average CD and also a larger 3σ than the crying groups. At first glance this looks similar to the results from the first M170Y-experiment. But the values from CD-centre and CD-edge are not diverging in the same way as in the M170Y experiment. The wafermap of the 155 μm smiling group in fig. 3.33 shows mostly constant CD on the wafer, only the part at 6 o'clock shows a highly increased CD. The 110 μm wafermap as shown in fig. 3.34 looks different than the wafermap of the 155 μm group. The largest CD is at 10:30 position, while the smallest CD parts are at roughly 6 o'clock position.

The expected change of CD with the bow could not be observed in this experiment. It was expected for the smiling groups to have a decreasing CD towards the edge, but this could not be observed.

wafer lot	Nr. of wafers	resist	exposure dose	focus	resist thickness
7	25	M91Y	220 J/m ²	0 μm	414 nm
8	25	M91Y	210 J/m ²	0.1 μm	405 nm
9	18	M91Y	210 J/m ²	0.1 μm	525 nm

Table 3.16.: Parameters of the M91Y wafer bow experiments

bow group	bow type	avg CD [nm]	CD-centre [nm]	CD-edge [nm]	3σ [nm]
no bow	no bow	161.8	162.3	161.4	7.9
55 μm	crying	161.6	159.7	161.3	7.4
110 μm	crying	161.7	160.5	161.2	8.4
160 μm	crying	160.6	159.9	160.6	8.0
50 μm	smiling	164.7	164.7	163.9	8.3
110 μm	smiling	166.3	165.6	165.1	10.4
155 μm	smiling	161.8	161.0	162.2	11.5

Table 3.17.: CD-U values of the first experiment

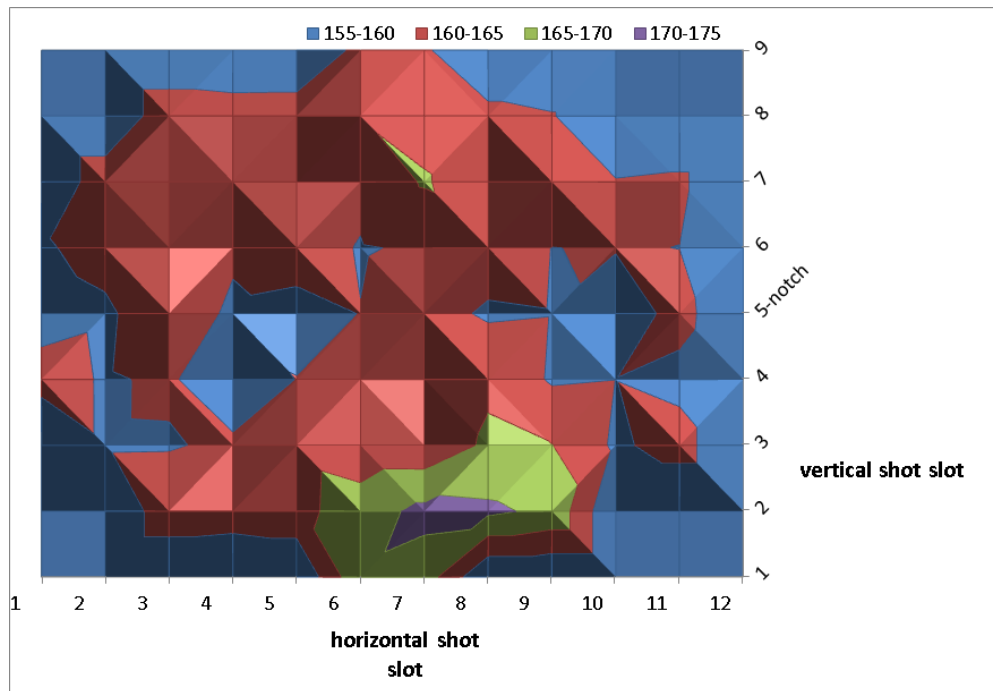


Figure 3.33.: Wafermap of the 155 μm smiling group with M91Y

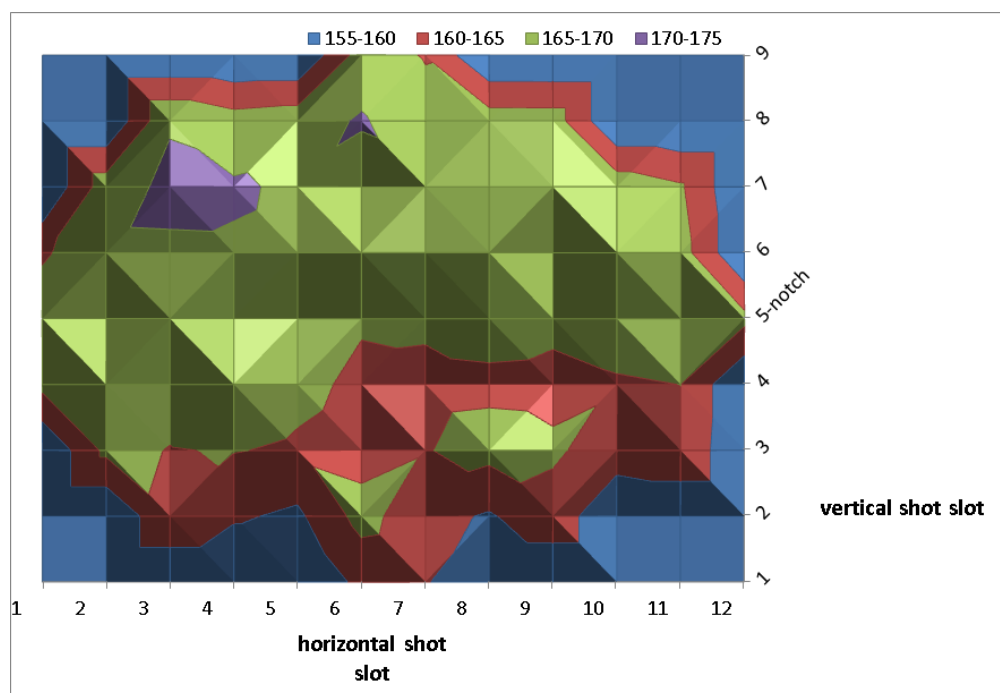


Figure 3.34.: Wafermap of the 110 μm smiling group with M91Y

3.5.2. Second experiment - 405 nm thickness

This experiment uses a smaller resist thickness than the one before, because we wanted to see if we can observe a swing curve effect with a different thickness. Also exposure dose and focus are changed to match usual settings for standard programmes for this resist. The parameters are shown in table 3.16 with the running number 8. The centrebow and the oxide thickness is shown in table 3.3. The same wafers from the previous experiment are used.

The results are shown in table 3.18. The groups of this experiment behave differently than in the experiments before. The average CD, CD-centre and CD-edge do not vary much. The 3σ is bad ($> 7\text{ nm}$) for all the groups, except for the 55 μm crying group with 6.7 nm. Most groups have a better CD-U than the no bow group with 8.3 nm. It was expected that the no bow group shows the best CD-U.

The crying group is inconsistent in the progression of the 3σ with increasing bow. While the 55 μm and 160 μm group have smaller than average 3σ , 6.7 nm and 7.4 nm respectively, the 110 μm group has the largest 3σ from the experiment with 9.0 nm. The smiling group shows a slightly increasing 3σ with increasing bow, from 7.6 nm from the 50 μm group to 8.3 nm from the 155 μm group. But the rate is

bow group	bow type	avg CD [nm]	CD-centre [nm]	CD-edge [nm]	3σ [nm]
no bow	no bow	155.3	155.4	155.1	8.3
55 μm	crying	155.9	155.7	155.2	6.7
110 μm	crying	155.7	154.3	156.1	9.0
160 μm	crying	155.7	154.7	156.1	7.4
50 μm	smiling	154.5	154.6	154.6	7.6
110 μm	smiling	154.9	155.1	154.8	7.8
155 μm	smiling	157.0	157.4	157.4	8.3

Table 3.18.: CD-U values of the second M91Y experiment

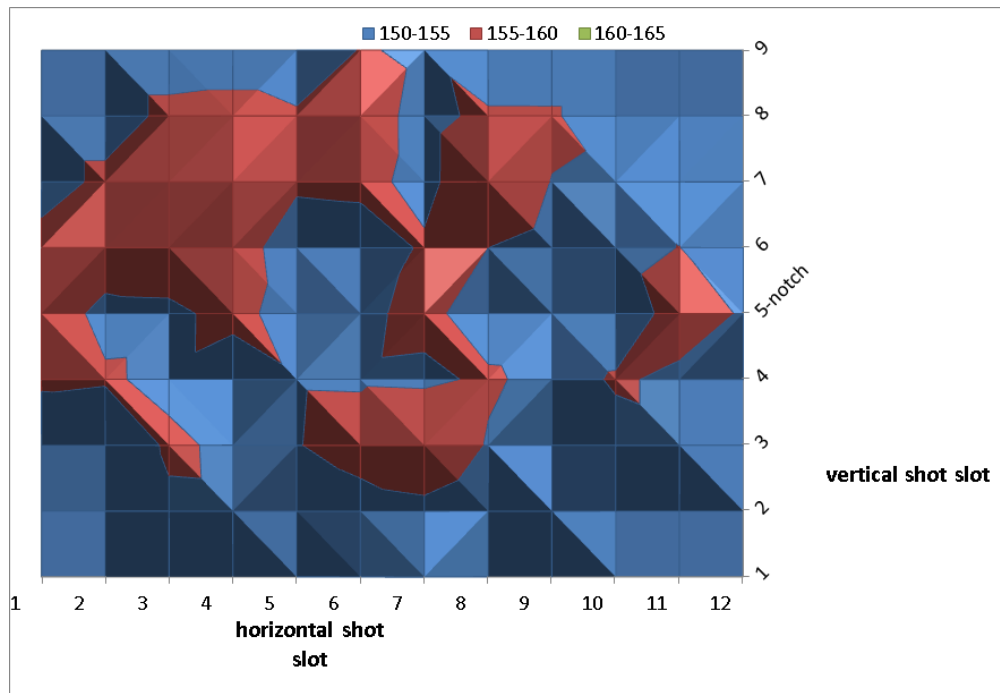


Figure 3.35.: Wafermap of the 110 μm smiling group with M91Y 405 nm

bow group	bow type	avg CD [nm]	CD-centre [nm]	CD-edge [nm]	3σ [nm]
no bow	no bow	163.4	163.0	162.8	6.5
175 μm	crying	162.0	159.8	162.4	6.2
170 μm	smiling	173.2	173.2	173.4	7.0

Table 3.19.: CD-U values of the third M91Y experiment

less than in the experiment before and a centre-edge-CD-difference is not observed.

The wafermap of the 110 μm smiling group is shown in fig. 3.35. The largest CD-values are at roughly 11 o'clock position, but other spots on the wafer have similar CD. The wafer map of the 155 μm smiling group looks similar to the 110 μm smiling group from last experiment (fig. 3.34). The other wafermaps are unremarkable and show mostly constant CD.

3.5.3. Third experiment - 525 nm thickness

The parameters for this experiment are shown in table 3.16 with the running number 9. The dose, focus and resist thickness for the M91Y experiment are changed to adjust the parameters to standard process settings. The centrebow and oxide thickness is shown in table 3.6. This experiment is performed after the wafers were etched again to remove the remaining oxide layers.

The results from the experiment with the resist M91Y are shown in table 3.19. The crying bow group shows a smaller average CD of 162.0 nm in comparison with the no bow group with 163.4 nm. The CD-centre is 159.8 nm for the crying group, while the CD-edge has a larger CD with 162.4 nm, which is still smaller than the no bow groups CD. The wafermap in fig. 3.36 shows this behaviour in more detail. The 3σ is smaller for the crying group with 6.2 nm than for the no bow group with 6.5 nm.

The CD-U of the smiling bow group is 7.0 nm and therefore slightly worse compared to the no bow group with 6.5 nm. The smiling bow group shows an increased average CD of 173.2 nm, but the difference between CD-centre and CD-edge is negligible, 173.2 nm versus 173.4 nm) respectively. The wafermap from the average CD shows the same behaviour, as the CD varies only little across the wafer. But when we look at the wafermaps of single wafers (see fig. 3.38 or the appendix), we can see that there is a small increase of CD from centre to edge, the edge having the larger CD. We suspect that the wafers in this experiment were handled with a different offset by the robot arm in the cluster machine and therefore were placed

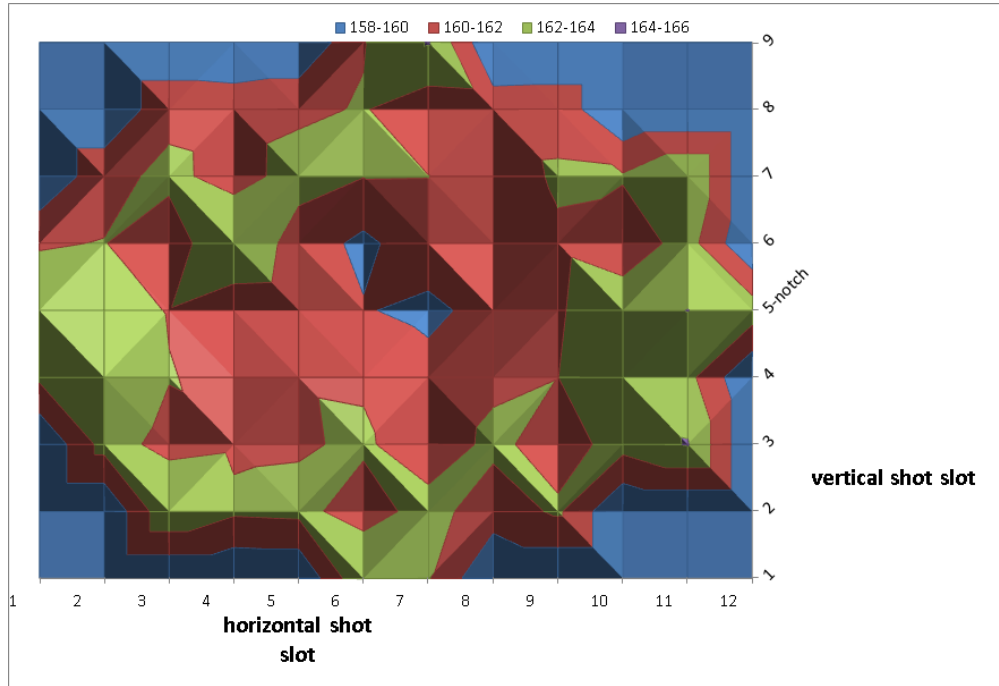


Figure 3.36.: Wafermap of the 175 μm crying group with M91Y

differently on the PEB-hot plate. The single wafermaps show that the largest CD parts on the wafer are not at the same shot-positions. For the first wafermap in fig. 3.38 the largest CD is at 1 o'clock, the second largest CD is at 8 o'clock. It is not clear why the CD is so much larger on the whole wafermap in comparison to the smiling group of the M170Y experiment. At the previous experiment the CD-centre was 166.0 nm, while the CD-centre for the M91Y resist smiling group is 173.2 nm.

3.5.4. Results

The CD-U results of the crying bow groups are compared in fig. 3.39. The bow groups are lined up in order of the experiments. For the crying bow groups we cannot see a distinct pattern with increasing centrebow. We can see no significant change of 3σ in the groups from the first experiment. The second experiment shows 2 crying groups that are better (55 μm , 160 μm) than the no bow group and the 110 μm crying group is worse than the no bow group. In the third experiment the 175 μm crying group shows the best CD-U. The first and second experiment was performed with a contaminated coater which probably worsened the CD-U. Our hypothesis for the influence of the contamination on CD-U is that the contamination causes a variation in the thickness of the BARC. In the results-section of

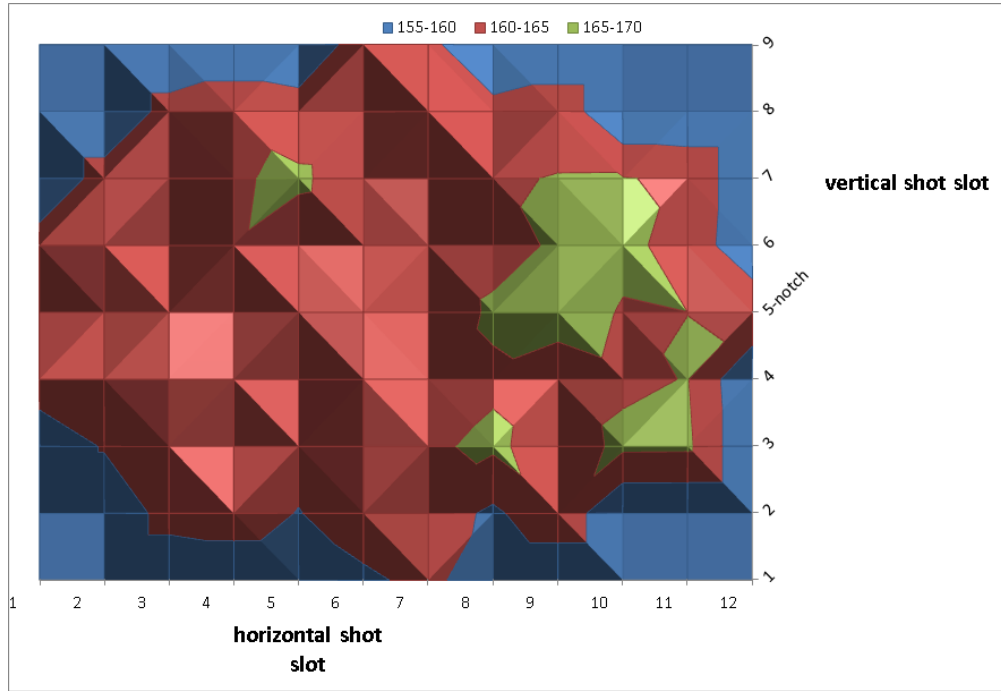


Figure 3.37.: Wafermap of the no bow group with M91Y

the M170Y experiments the *height*-graphs were introduced. For the M91Y resist this plot makes less sense, because we cannot see patterns in the plots as most of the lines are unremarkable.

The CD-U results of the smiling bow groups are compared in fig. 3.40. The first and second experiment were performed on a contaminated coater and contained smiling wafers with an oxide top layer. These properties may have influenced the 3σ of the groups in a way we cannot judge. In the first experiment we see an increase of 3σ with increasing centrebow. The second experiment shows this trend in a reduced way as the increase from the $50\mu\text{m}$ group to the $155\mu\text{m}$ group is smaller. The no bow group has the same 3σ as the $155\mu\text{m}$ smiling group in the second experiment. The third experiment shows the best CD-U of the experiments and the increase from no bow to $170\mu\text{m}$ smiling group is small. We trust the results from the third experiment the most, because there was no influence of the 3σ due to contamination or oxide top layer.

Figure 3.41 shows the CD over the radius from the centre of the wafer to the shot (where the CD was measured). The data for this graph is obtained from the third experiment only, because it had the least side-influences. The plot shows the mostly constant centre-edge-CD-trend for the no bow group. The $175\mu\text{m}$ crying

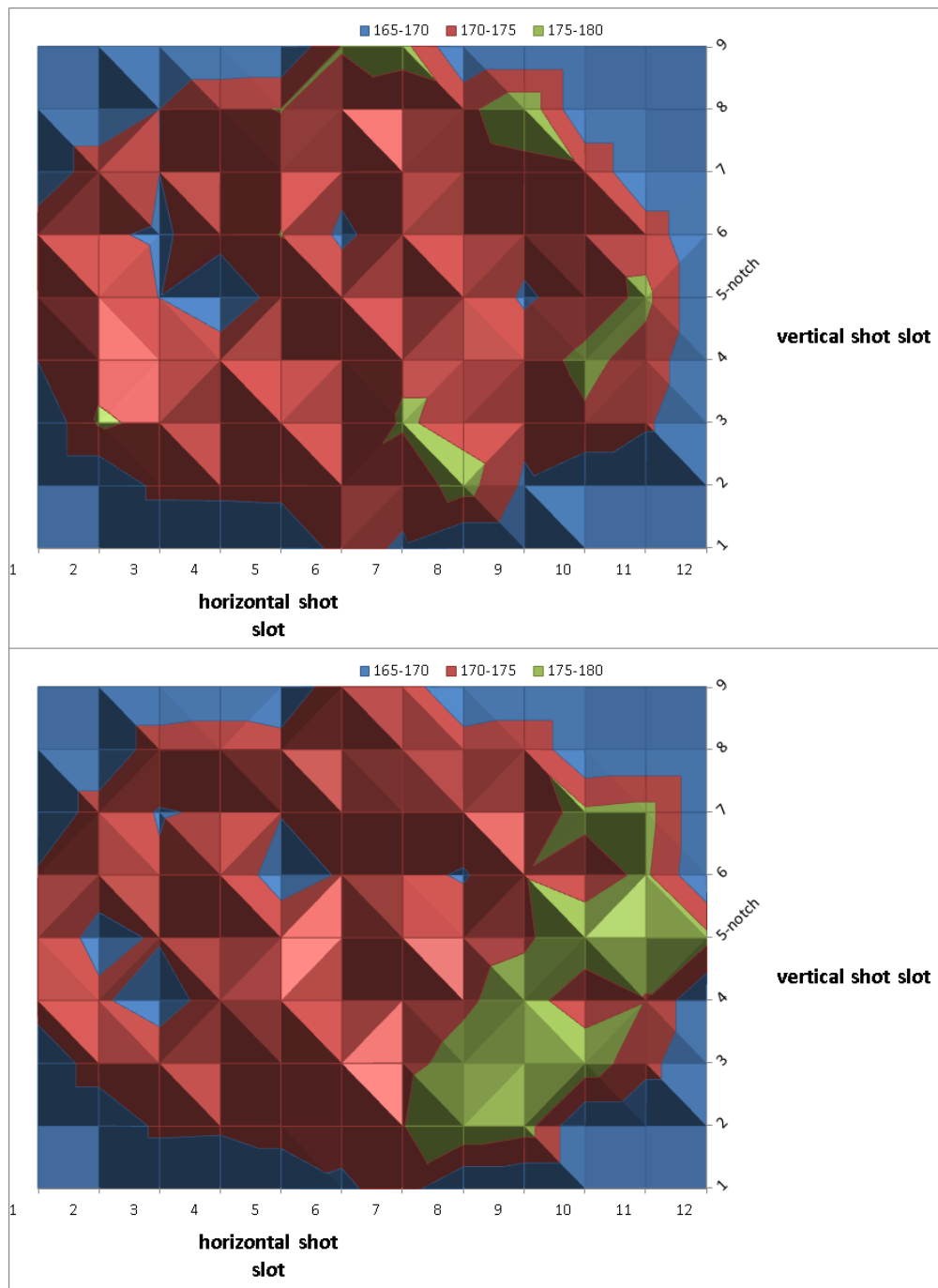


Figure 3.38.: Wafermaps of two 170 μm smiling wafers with M91Y

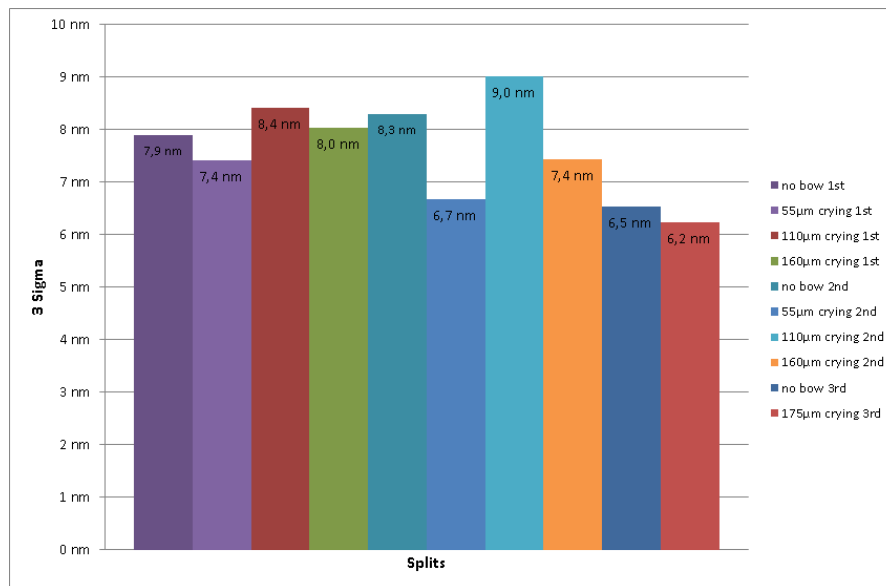


Figure 3.39.: CD-U comparison of the crying bow groups

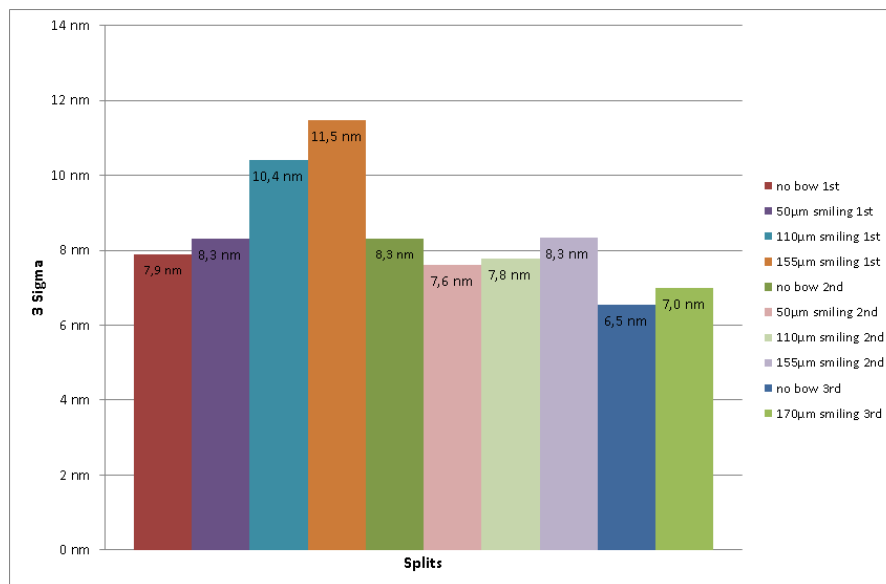


Figure 3.40.: CD-U comparison of the crying bow groups

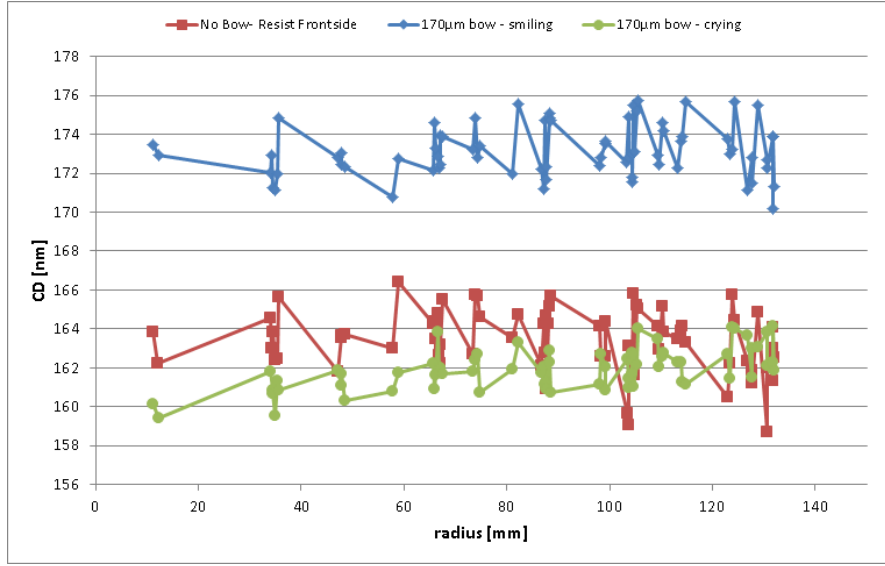


Figure 3.41.: CD over radius for the no bow, 175 µm crying and 170 µm smiling group

group shows an increase of the CD from centre to edge. The 170 µm smiling group shows a small increase of the CD from centre to edge.

3.6. Discussion

3.6.1. F-Test

The F-test is used in this work to indicate if the variance of two compared data-sets is similar and if the difference is statistically significant. The null hypothesis is that the data-sets from the experiments have the same variance. The so-called p -value is the probability that the two compared data-sets have the same variation, but only if the null hypothesis is true. The significance level α is chosen to be 5% and marks the threshold for accepting ($\alpha < p$) or rejecting ($\alpha > p$) the null hypothesis. Furthermore the difference between the data-sets is called statically significant if the null hypothesis is rejected.

It is important to note that the variances (σ^2) for the data-sets are calculated differently than the 3σ given in the tables above. It is not possible to calculate one from the other. The variances (and therefore the f- and p-values) are calculated with every CD-data point in the respective group, while the 3σ of a single wafer is calculated with the data points on a single wafer and the resulting 3σ (used in this work) is the average of all the single wafer 3σ s. The calculation of the F-test

comparison	f-value	p-value (two tail)	$\alpha = 0.05 > p$
First experiment			
no bow vs 55 μm crying	0.77	0.02	yes
no bow vs 110 μm crying	0.85	0.21	no
no bow vs 160 μm crying	0.90	0.35	no
no bow vs 50 μm smiling	0.87	0.22	no
no bow vs 110 μm smiling	0.23	0.00	yes
no bow vs 155 μm smiling	0.21	0.00	yes
Second experiment			
no bow vs 175 μm crying	0.87	0.19	no
no bow vs 170 μm smiling	0.16	0.00	yes
Third experiment (compared to no bow from 2nd exp)			
no bow vs 275 μm crying	0.71	0.00	yes
no bow vs 385 μm crying	0.53	0.00	yes
no bow vs 255 μm smiling	0.28	0.00	yes
no bow vs 370 μm smiling	0.23	0.00	yes
Third experiment repetition (compared to no bow from 2nd exp)			
no bow vs 275 μm crying	0.59	0.00	yes
no bow vs 385 μm crying	0.46	0.00	yes
no bow vs 255 μm smiling	0.27	0.00	yes
no bow vs 370 μm smiling	0.31	0.00	yes
Fourth experiment (compared to no bow from 2nd exp)			
no bow vs 130 μm smiling	0.12	0.00	yes
Fifth experiment (no bow from 2nd)			
no bow vs 90 μm smiling	0.28	0.00	yes
no bow vs 80 μm smiling	0.91	0.54	no

Table 3.20.: F-test evaluation for the wafer bow experiments with M170Y

comparison	f-value	p-value (two tail)	$\alpha = 0.05 > p$
First experiment			
no bow vs 55 μm crying	1.30	0.03	yes
no bow vs 110 μm crying	1.00	0.97	no
no bow vs 160 μm crying	1.10	0.44	no
no bow vs 50 μm smiling	0.94	0.59	no
no bow vs 110 μm smiling	0.66	0.00	yes
no bow vs 155 μm smiling	0.53	0.00	yes
Second experiment			
no bow vs 55 μm crying	1.39	0.01	yes
no bow vs 110 μm crying	0.66	0.00	yes
no bow vs 160 μm crying	1.08	0.51	no
no bow vs 50 μm smiling	1.19	0.15	no
no bow vs 110 μm smiling	1.09	0.49	no
no bow vs 155 μm smiling	0.83	0.08	no
Third experiment			
no bow vs 175 μm crying	0.87	0.23	no
no bow vs 170 μm smiling	1.08	0.46	no

Table 3.21.: F-test evaluation for the wafer bow experiments with M91Y

has to use the former way to calculate the variance, while it is more convenient to calculate the 3σ in the latter way.

The results of the F-Test for the M170Y experiments are shown in table 3.20. Most of the comparisons between not bowed wafers and bowed wafers show a significant difference. This is indicated by the 4th column, a “yes” means that the p-value dropped below the significance level. For the smiling bow groups all groups except the 50 nm group ($p = 0.22$) and the 80 nm group ($p = 0.54$) show a significant difference. For the crying bow groups there are several groups that do not show a significant difference: 110 nm crying, 160 nm crying and 175 nm crying do not show a significant difference.

The results of the F-Test for the M91Y experiments are shown in table 3.21. Most groups do not show a significant difference, as the general variation was large probably due to the contamination. The groups with significant difference are the 55 nm crying group, the 110 nm smiling and the 155 nm smiling for the first experiment and the 55 nm crying group for the second experiment. We believe that the 55 nm crying group is not more critical than the larger crying bow groups, although the group shows significantly different variation in the first and second experiment, while the other crying groups do not show that. We have no explanation why the 110 nm smiling and the 155 nm smiling group in the first experiment are significantly different from the no bow group.

3.6.2. Impacts on CD

Before the experiments were performed, we expected the PEB to be the major factor in the wafer bow experiments. To test this assumption experiments with the resists M170Y and M91Y, which have a different temperature coefficient, were performed. The experiments with the resist M170Y supported this assumption as there is an observable centre-edge-CD-trend for both smiling and crying wafers (see e.g. fig. 3.30 or the M170Y wafermaps). The graph in fig. 3.32 shows the effective PEB temperature of the crying group and smiling group. We assume that only the PEB has influence on the CD to calculate the temperature values. The temperature change for a crying wafer from centre to edge is therefore estimated to be roughly 1°C , while the temperature change for a smiling wafer is estimated with -3.5°C . Firstly we expected the same temperature change for smiling bow and crying bow, as the wafers have similar centrebow and therefore almost the same minimal and maximal distance from the hot plate during the PEB. A second problem is that the value of the temperature change for the smiling group is unbelievably large. We do not believe that an increase of $170\mu\text{m}$ in the distance between hot plate and wafer can have such a strong impact on the felt PEB tem-

perature. Also the third experiment with the resist M91Y of the crying group showed the expected increase of CD towards the edge, while the smiling group showed an unexpected increase of CD towards the edge too. But it was expected to see the reverse trend for the smiling group, a decrease of CD towards the edge, since the PEB temperature coefficient is positive for the M91Y. We conclude that there is at least a second influence, that has an impact on the CD with the increase of centrebow.

The assumption is that the cooling process right after the PEB works against the PEB temperature change due to wafer bow, because the same places where the PEB temperature are the hottest are the best cooled places during the cooling process. The geometry of the wafers and the positioning is the motivation for these thoughts.

The favoured candidate for an influence that impacts the CD is the development process. It is not yet understood how the development process changes with increasing centrebow. We assume that the flow of developer and internal currents cause the developer to remove a different amount of resist than for not bowed wafers. For a smiling wafer we assume that the developer removes more resist when the developer flows toward the wafer centre. The thickness of the developer increases in the centre. For a crying wafer we assume that the developer flows from the centre towards the edge of the wafer and removes more resist at the edge. The development process is needed to clear the exposed resist before the trench structures can be measured in a SEM. This is why we cannot skip the development process for our experiments. Unfortunately it is not trivial to examine the influence of the development on the type and value of bow because the effects cannot be distinguished easily. There is no measurement or setup to test the individual influence of development on the CD. Other influences have been examined, but showed only small to no effect. For further information see section 3.3.

With the impact of development on the CD we can explain why the CD-centre increases with increasing centrebow for smiling wafers (e.g. fig. 3.30). The larger the centrebow, the more developer flows to the centre of the wafer, which removes more resist in the central region of the smiling wafer. The same effect is the reason why the 3σ decreases with a centrebow greater than $130\text{ }\mu\text{m}$. The range of the CD values is decreased when the CD-centre is raised. But it is not clear why the CD does not increase with the *height* above roughly $130\text{ }\mu\text{m}$ and why it declines above roughly $200\text{ }\mu\text{m}$.

The first and second experiment with the resist M91Y are difficult to interpret

because of contamination in the coater cup and the oxide top layer of the smiling wafers make it hard to judge the results properly. We assume that standing waves and swing curve effects on the resist sidewall are why the smiling groups show an increase of 3σ in the first experiment and no dependency on centrebow in the second experiment is observed. The oxide thickness range is large enough to move from the minimum in the swing curve to the maxima. The standing waves and contamination are problems for the first experiment with the resist M170Y too, but we do not observe their impact on CD nor CD-U as much as for the M91Y.

The results of the M170Y experiments are consistent, because the centre-edge-CD-trends in fig. 3.30 and fig. 3.31 overlap. We do not have enough proper experiments with the M91Y to draw clear conclusions for this resist at the time.

4. Development process parameters

During development the exposed resist is removed by a developer, which is a solution of 2.38 % Tetra Methyl Ammonium Hydroxide in water. The exposed resist is removed in this process and forms the patterns in the resist. An important process-parameter is the development time. A low development time doesn't permit the fluid to totally remove the exposed resist. The so-called dark film loss is low. The other case is a long development time in which the fluid might dissolve the unexposed structures in a way that is difficult to control. Both of these effects affect CD & CD-U.

The cluster tool employed for the experiments uses puddle development as the preferred development method. A rectangle-shaped arm with valves pours down the developer while moving across the wafer (see fig. 4.1). This means that one side of the wafer receives the developer earlier than the other side. Therefore the developer rests longer on one side than the other side. After developer-deployment a developer-puddle forms on the substrate (see fig. 4.2). It is possible to create a puddle, remove it and create another one. This technique is called double puddle. A chuck fixes the position of the wafer during the development by sucking the wafer with vacuum-pressure. The wafer can be turned at any point in the process because the chuck is rotatable, but this option is usually not used. Therefore parameters like nozzle distance, agitation - rotation of the wafer during development - and usage of double puddle influence cleanliness and CD on the wafer. The goal of the following experiments is to optimize these parameters regarding CD-U.

The standard programme (50 s development) looks like this:

- 5.5 s developer deposition by the robot arm, but only ca. 4.7 s deposition on the wafer (fig. 4.1)
- 50 s development time without rotating the wafer
- 18 s water rinse to remove the developer puddle while the wafer is rotated at 1200 rpm, at the same time the backside is rinsed to remove contamination

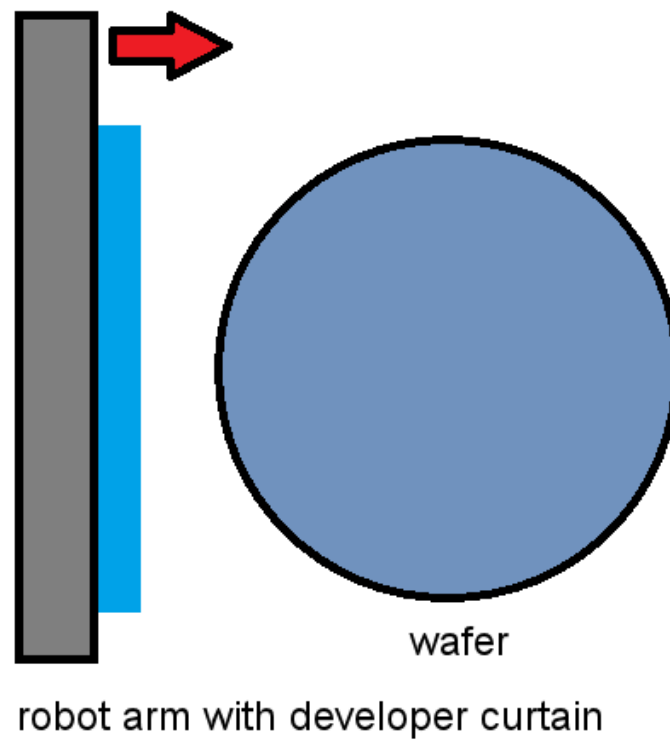


Figure 4.1.: Deposition of the developer on the wafer, the red arrow indicates the movement of the robot arm

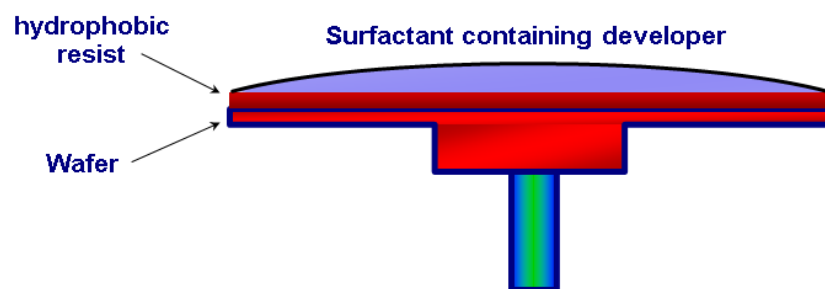


Figure 4.2.: Puddle on a wafer for development [6, p.84]

4.1. Experiments on development time

After the developer is applied on the wafer, the developer is given some time to remove the exposed resist on the wafer. The longer the developer stays on the wafer, the more resist is removed. The purpose of this experiment is to show how fast the developer removes the resist on a large area. There are 2 questions we want to answer in this experiment.

The first question is how fast can the developer dissolve the exposed resist. A large area of exposed resist is needed for this task. To do that the scanner exposes with an open frame job, that means that there is no reticle in the tool and the wafer is completely exposed. The wafer will have no structures on it, instead the whole shot region is freed of exposed resist if the development time is long enough. After exposure the wafer goes through the development step. Programs with low development time are prepared. The thickness of the resist (M170Y) is 414 nm after spin coating. Also the BARC coating step is replaced by applying an adhesion promoter to measure the correct resist thickness, otherwise we would measure the thickness of BARC + resist.

The second question is how the development time affects CD and CD-U. We use a reticle with 180 nm space and 650 nm pitch to generate the space-CD-target of 160 nm with an exposure dose of 220 J/m² and a focus of 0 μ m. The used development times are 20 s, 30 s and 50 s. 50 s is the current standard.

4.1.1. Open frame wafers

The purpose of this experiment is to look for the lower limits of exposure dose and development time. Table 4.2 shows the performed experiments regarding open frame and development time. The wafers 1 – 4 are processed with a dose series, the starting dose is 150 J/m² and increases from row to row with an increment of 20 J/m². The dimensions of the open frame exposure shot regions are 26 mm \times 33 mm (23.32 mm \times 32.66 mm for the other experiments in this work). Every shot region is cleared of resist, so more experiments are needed to see the limitations of the exposure dose and the development time. The next experiments are done with 5 s development time, because this time is enough to develop the wafer fully as the cleared exposure shot regions on wafer 4 show.

Wafer 5 shows a new dose series starting from 30 J/m² with an increment of 20 J/m² with an increase from row to row. The exposure unit has a lower limit for the exposure dose of 25 J/m². A lower value brings a large variation in the exposure dose and the unit does not permit that by popping up an error message and stop-

wafer	development time	exposure dose	avg. thickness after dev.	3σ
1	50 s	150 – 350 J/m ²	0 nm	-
2	15 s	150 – 350 J/m ²	0 nm	-
3	10 s	150 – 350 J/m ²	0 nm	-
4	5 s	150 – 350 J/m ²	0 nm	-
5	5 s	30 – 230 J/m ²	0 nm ¹	-
6	5 s	25 J/m ²	394.4 nm	2.8 nm
7	5 s	40 J/m ²	335.9 nm	25.9 nm
8	5 s	45 J/m ²	296.8 nm	75.1 nm
9	5 s	60 J/m ²	0 nm	-

Table 4.2.: Open frame experiments overview

¹The shot regions with 30 J/m² had some resist remaining, but the thickness measurement unit did not measure these shots because they were too far on the outside.

experiment	Nr. of wafers	dev. time	exposure dose	focus
1	12	50 s	220 J/m ²	0 μ m
	13	30 s	220 J/m ²	0 μ m
2	12	50 s	220 J/m ²	0 μ m
	13	20 s	220 J/m ²	0 μ m

Table 4.3.: Parameters of the development time experiments

ping the process. From 50 J/m² upward, the shot regions are clear of resist. Only the 30 J/m² shot regions show unexposed resist. This suggests a dose-to-clear of somewhere between 30 J/m² and 50 J/m².

The wafers 6 – 9 are used to further determine at which dose the shot regions are cleared of resist. The wafers 6 – 8 use a exposure dose less than 50 J/m² and are not clear of resist after development. Therefore the dose-to-clear is approximately 50 J/m² as seen in the dose series from wafer 5. Wafer 9 confirms that a dose of 60 J/m² is able to expose the resist completely. The wafers 6 – 8 show that the resist thickness decreases as the exposure dose increases. This is just as we expect when nearing the dose-to-clear.

	50 s development time	30 s development time	difference
Maximum	164.0 nm	162.2 nm	1.8 nm
Minimum	151.3 nm	149.6 nm	1.7 nm
Average	159.0 nm	156.5 nm	2.5 nm
3σ	5.1 nm	5.1 nm	0.0 nm

Table 4.4.: CD-U evaluation for 50 s versus 30 s development time

	50 s development time	20 s development time	difference
Maximum	171.2 nm	169.9 nm	1.4 nm
Minimum	161.4 nm	158.5 nm	2.9 nm
Average	166.7 nm	163.6 nm	3.1 nm
3σ	4.5 nm	4.8 nm	−0.3 nm

Table 4.5.: CD-U evaluation for 50 s versus 20 s development time

4.1.2. Experiments with a reticle

50s versus 30s

The first experiment is used to compare 50 s development time with 30 s development time. The lot is split in 2 groups: 12 wafers are processed with 50 s development time, the remaining 13 wafers are processed with 30 s development time (see table 4.3).

The results in table 4.4 show that the CD-U is the same for 50 s development time as it is for 30 s development time. The average CD with 30 s development time is 2.5 nm less than the average CD with 50 s development time. This is not a problem, because a larger exposure dose is able to adjust the CD to larger values.

50s versus 20s

The second experiment shows a change in CD-U with the development time. The lot is split in 2 groups: 12 wafers are processed with 50 s development time, the remaining 13 wafers are processed with 20 s development time (see table 4.3).

The results in table 4.5 show that the CD-U with 50 s development time is better than the CD-U with 20 s development time. The difference is 0.3 nm in 3σ . The average CD with 20 s development time is 3.1 nm less than the average CD with 50 s development time. The first experiment's CD gap is less between the average

CD of the groups.

4.2. Dependency of the development process on position

The orientation of the wafer in the development unit is fixed during the developer dispense. A robot arm distributes the developer like a water curtain across the whole wafer with a scan speed of 64 mm/s. The removal of resist could be unequally distributed, because the fluid lasts different times on the surface of the wafer.

The following charts are based on the data from the experiment on development time (50 s vs 30 s, section 4.1.2). Each value in the graphs (fig. 4.3 & fig. 4.4) represents an exposure shot region in which an average CD is calculated from the CD measurement which is performed by a SEM.

The graph showing the 50 s development (fig. 4.3) shows that the CD increases in value in the same row from vertical shot 9 to vertical shot 1. The hypothesis is that the CD increases where the developer fluid stays a longer time on the surface. This could indicate that the developer is lasting longer in vertical shot 1 than in vertical shot 9.

The 30 s development shows a larger CD in the centre of the wafer, while at the border of the wafer (fig. 4.4) there is a lower CD, with a few exceptions. This result is against our expectations, because the developer application time takes a relatively longer time in the development process for the 30 s development than for the 50 s development. We rather expected the same graph for 30 s development as for the 50 s development, but with a wider range of values and a steeper slope. The relatively large standard deviation may play a role with these observations.

Figure 4.5 and fig. 4.6 show the radial progression of the CD. The average CD is plotted versus the radius from the centre for each shot. The standard deviation is indicated with error bars (1σ up and 1σ down, in total 2σ). In the graphs the standard deviation σ is an average of 1.8 nm for both groups and therefore large enough that the minimal and maximal CD lie within the other measurement points deviation. This weakens the observations of the CD-trends from above, the increase of CD vertically for 50 s development and the increase of CD towards the centre in 30 s development. The wafermaps and the radial progression proved to be useful tools in the analysis of the Impact of wafer bow on CD and CD-U in

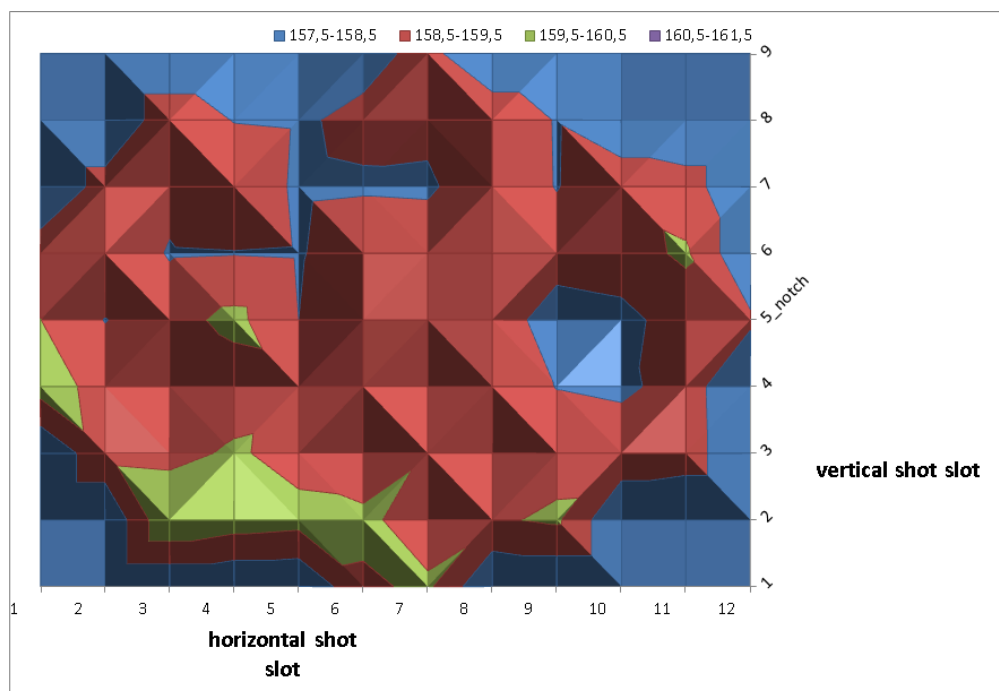


Figure 4.3.: Average CD of 12 wafers with 50 s development time

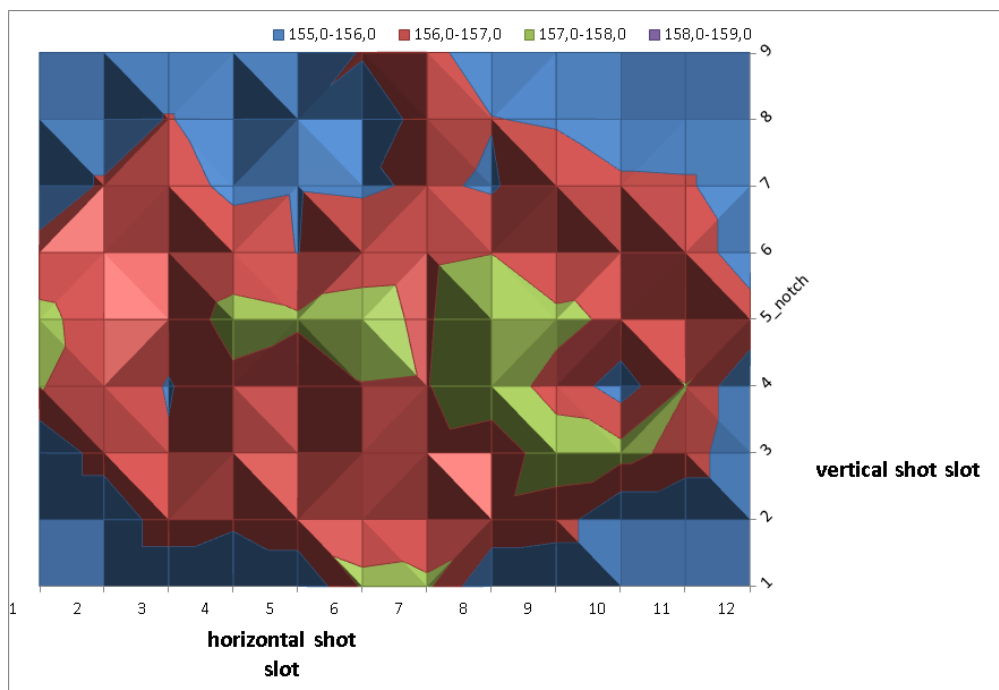


Figure 4.4.: Average CD of 13 wafers with 30 s development time

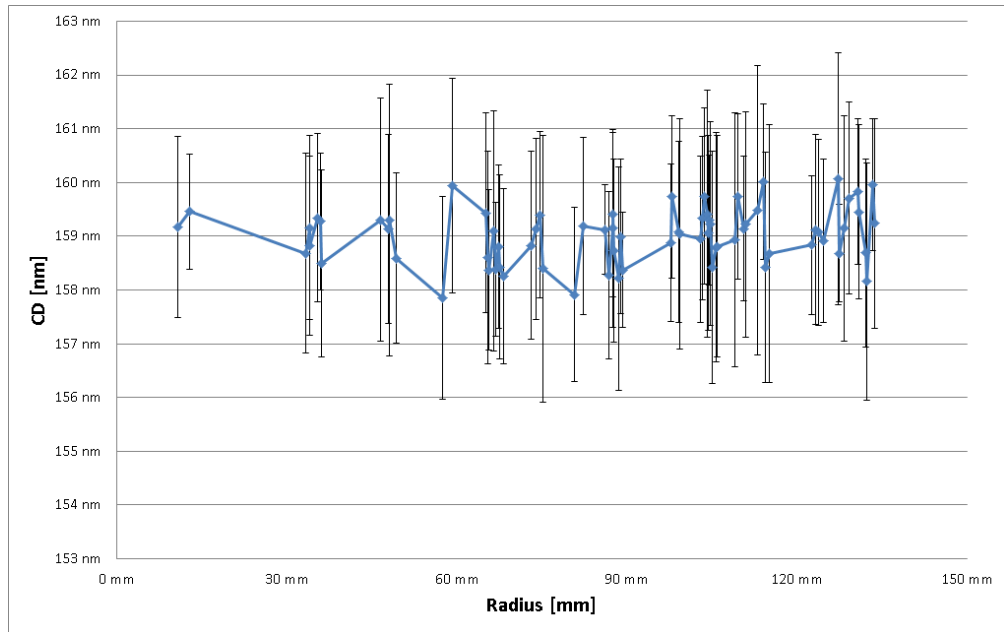


Figure 4.5.: Radial progression of CD and standard deviation for every shot for the 50 s development time

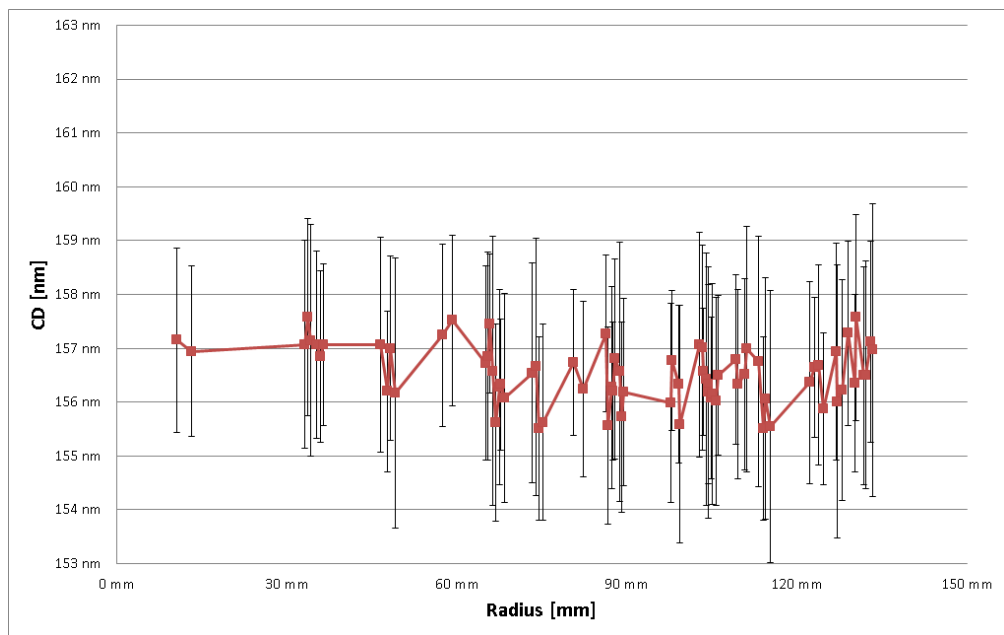


Figure 4.6.: Radial progression of CD and standard deviation for every shot for the 30 s development time

chapter 3. But the data in this experiment shows too large standard deviation compared with the range between minimal and maximal CD to observe changes on the wafermap. The same radial graphs like in fig. 4.5 and fig. 4.6 were plotted for all the development parameter experiments but showed similar standard deviations. The following sections do not use wafermaps and radial progression plots because of the large standard deviation and thus the insignificance of the plots.

4.3. Experiments with agitation

A previous experiment showed that a 30 s development has a similar quality (CD-U) as a 50 s development. The next question is if a low development time and agitation - movement of the wafer - can deliver the same or a better uniformity. The experiments compare 30 s development with 20 s development with and without agitation.

An increase of the 3σ was noticed from an experiment to the next one. It was found, that a coater was contaminated and that this is the reason for the increase of the 3σ . We assume that the contamination caused thickness variation in the BARC. The agitation experiments are performed with the contaminated coater. We compare the experiments despite the bad CD-U, because we assume that all groups are affected the same way by the contamination. After the experiments with agitation the coater was cleaned and the experiments in the next sections showed better CD-U.

The development time groups are split into a second pair of groups. The difference between them is agitation - rotating the wafer - during the development. The agitation groups are “no rotation”, “ $\frac{1}{4}$ -rotation” and “continuous rotation”. The parameters of the split groups of the two experiments are shown in table 4.6 and table 4.7. We expect to have a different CD if the wafer is turned during the development, the goal of the experiments is to find out if CD-U is affected too and by how much. The reason of the CD-change is that the movement agitates the developer fluid. Internal fluid currents increase the removal of resist in comparison to a resting developer. The agitation modes are:

- no rotation: the wafer rests during the whole development time, it is not turned
this is the standard
- 20 s – $\frac{1}{4}$: a quarter turn every 4.6 s with 30 rpm in a 0.5 s period
- cont: continuous rotation with 15 rpm during the whole development time
- 30 s – $\frac{1}{4}$: a quarter turn every 7.1 s with 30 rpm in a 0.5 s period

group	20 s – $\frac{1}{4}$	20 s–cont	30 s – $\frac{1}{4}$	30 s–cont
Nr. of wafers	6	6	6	6
dev. time	20 s	20 s	30 s	30 s
exposure dose	220 J/m ²	220 J/m ²	220 J/m ²	220 J/m ²
focus	0 μ m	0 μ m	0 μ m	0 μ m
agitation	$\frac{1}{4}$	cont	$\frac{1}{4}$	cont

Table 4.6.: Parameters of the first agitation experiment

group	20 s	20 s–cont	30 s	30 s–cont
Nr. of wafers	6	6	6	6
dev. time	20 s	20 s	30 s	30 s
exposure dose	220 J/m ²	220 J/m ²	220 J/m ²	220 J/m ²
focus	0 μ m	0 μ m	0 μ m	0 μ m
agitation	no rot	cont	no rot	cont

Table 4.7.: Parameters of the second agitation experiment

	20 s – $\frac{1}{4}$	20 s–cont	30 s – $\frac{1}{4}$	30 s–cont
Maximum	160.2 nm	161.1 nm	161.5 nm	161.4 nm
Minimum	148.5 nm	149.7 nm	151.1 nm	149.5 nm
Average	154.3 nm	155.1 nm	155.6 nm	155.9 nm
3σ	5.9 nm	5.7 nm	5.8 nm	5.5 nm

Table 4.8.: CD-U evaluation for the first agitation and development time experiment

	20 s	20 s—cont	30 s	30 s—cont
Maximum	159.6 nm	160.8 nm	161.2 nm	162.2 nm
Minimum	148.9 nm	150.1 nm	150.5 nm	150.3 nm
Average	154.7 nm	154.8 nm	156.1 nm	155.9 nm
3σ	5.5 nm	5.9 nm	5.7 nm	6.2 nm

Table 4.9.: CD-U evaluation for the second agitation and development time experiment

4.3.1. First experiment, $\frac{1}{4}$ -rotation vs continuous rotation

The results of the first experiment are shown in table 4.8. The best 3σ is 5.5 nm by the 30s-continuous group. But the difference between the groups in regards of CD-U is small. We can see that the 30s groups both show better 3σ , than their agitation-counterparts with 20s development time. Continuous rotation is the better agitation mode for both development times by 0.2 nm to 0.3 nm in 3σ . The difference in CD-U is not significant for any of these groups.

The average CD of the 30 s groups are similar with 155.6 nm and 155.9 nm. The 20 s — $\frac{1}{4}$ group has a CD of 154.3 nm and the 20 s—continuous group has a CD of 155.1 nm.

4.3.2. Second experiment, no rotation vs continuous rotation

The results of the second experiment are shown in table 4.9. The first major point is that we see that the split group continuous rotation behaves differently in the second experiment compared to the first one. While the first experiment shows us 5.7 nm 3σ for 20 s and 5.5 nm 3σ for 30 s, the second experiment shows us 5.9 nm 3σ for 20 s and 6.2 nm 3σ for 30 s. While in the first experiment the 30 s continuous split group gave the best result, it gives the worst in the second experiment. This result is probably due to the contamination in the coater unit.

The CD-U in the second experiment is overall worse than in the first experiment. The 3σ of the 20 s development time groups are better by 0.2 nm (no rotation) and 0.3 nm (continuous) compared to the 30 s group. The differences between “no rotation” and continuous groups are 0.4 nm (20 s) and 0.5 nm (30 s) in favour of the “no rotation” development. This shows that 20 s “no rotation” development is the best split group of this experiment.

The average CD of the 20 s groups is similar with around 154.7 nm. The 30 s groups have a similar average CD of 156.1 nm. It was expected that the agitation increases the CD, but that could not be proven. It was only shown that the CD-U is worse for agitation groups.

4.4. Experiments with double puddle development

The double puddle is a method where the first developer-puddle is removed and a second puddle is poured on the wafer instead of pouring developer on the substrate only once. The differences in the groups for the experiments is the method of removal for the first puddle and the waiting time between the deposition of the puddles. The groups are called “replace-1”, “centrifuge-1”, “rinse-1”, “replace-2”, “centrifuge-2” and “rinse-2”. The modes are described in the following list. Waiting time is the time between the deposition of the first puddle and the second puddle.

- replace-1: the first puddle is applied, then the second puddle is applied onto the first one without delay, pushing it down.
- centrifuge-1: the first puddle is applied, but before the second puddle is applied, the wafer is spun rapidly for 1 second.
- rinse-1: the first puddle is applied, but before the second puddle is applied, the wafer is spun rapidly and rinsed for 1 second. This program is not used, because in a test run the robot arm collided with the nozzle.
- replace-2: the first puddle is applied, then the puddle rests for 10 seconds. Afterwards the second puddle is applied onto the first one, pushing it down.
- centrifuge-2: the first puddle is applied, then the puddle rests for 10 seconds. The wafer is spun rapidly for 1 second before the second puddle is applied.
- rinse-2: the first puddle is applied, then the puddle rests for 10 seconds. The wafer is spun rapidly and rinsed for 1 second before the second puddle is applied.

group	replace-1	centrifuge-1	replace-2	centrifuge-2	rinse-2
Nr. of wafers	5	5	5	5	5
dev. time	25 s	26 s	26 s	26 s	26 s
exposure dose	220 J/m ²	220 J/m ²	220 J/m ²	220 J/m ²	220 J/m ²
focus	0 μm	0 μm	0 μm	0 μm	0 μm
waiting time	0 s	0 s	10 s	10 s	10 s
spin/rinse	none	spin	none	spin	spin & rinse

Table 4.10.: Parameters of the double puddle experiment

group	replace-1	centrifuge-1	50 s	30 s
Nr. of wafers	6	6	6	6
development time	25 s	26 s	50 s	30 s
exposure dose	220 J/m ²	220 J/m ²	220 J/m ²	220 J/m ²
focus	0 μ m	0 μ m	0 μ m	0 μ m
time between puddles	0 s	0 s	single	single
spin/rinse	none	spin	none	none

Table 4.11.: Parameters of the single puddle & double puddle experiment

	replace-1	centrifuge-1	replace-2	centrifuge-2	rinse-2
Maximum	168.3 nm	169.5 nm	170.3 nm	169.7 nm	169.9 nm
Minimum	158.9 nm	160.1 nm	160.0 nm	155.8 nm	159.9 nm
Average	164.2 nm	164.5 nm	164.5 nm	163.9 nm	165.6 nm
3σ	4.3 nm	4.4 nm	4.7 nm	4.4 nm	4.6 nm

Table 4.12.: CD-U evaluation for the first double puddle experiment

4.4.1. First experiment - different double puddle programs

The first experiment compares the five recipes described above. The goal is to find out the best two groups for the second experiment. The results of this experiment are shown in table 4.12. The CD-U is good and similar for all the double puddle groups. The replace-1 group has the best CD-U with a 3σ of 4.3 nm, while the replace-2 has the worst CD-U with 4.7 nm 3σ . Both centrifuge groups have the same 3σ of 4.4 nm. The average CD is similar for both replace groups and both centrifuge groups with around 164.2 nm average. Rinse-2 has a larger average CD of 165.6 nm.

The recipes chosen for the comparison in the next experiment are replace-1 and centrifuge-1. Replace-1 is chosen because it has the best CD-U. Centrifuge-1 is chosen over centrifuge-2 because it is more comparable with replace-1 because of the same waiting time before the second puddle is applied.

4.4.2. Second experiment - comparing with single puddle programs

The second experiment takes the 2 best recipes from the first experiment and compares them with 30 s development time and the standard recipe (50 s development time). The 50 s group (standard recipe) has the best CD-U with a 3σ of 4.5 nm.

	replace-1	centrifuge-1	50 s	30 s
Maximum	164.2 nm	165.4 nm	167.6 nm	163.9 nm
Minimum	154.8 nm	155.5 nm	158.4 nm	154.6 nm
Average	159.3 nm	159.6 nm	162.6 nm	159.5 nm
3σ	4.9 nm	4.8 nm	4.5 nm	5.1 nm

Table 4.13.: CD-U evaluation for the second double puddle experiment

The 30 s group had the same 3σ as the 50 s group in the development time experiment (see table 4.4), but in this experiment it is worse than the 50 s group with the same value as in the previous experiment, 5.1 nm. Both double puddle groups show a similar CD-U with around 4.8 nm 3σ . In this experiment the replace-1 group is slightly worse than the centrifuge-1 group, in the previous experiment it was vice-versa.

The average CD is similar for the replace-1, centrifuge-1 and 30 s groups with 159.3 nm, 159.6 nm and 159.5 nm CD, respectively. The total development time is similar for the replace-1, centrifuge-1 and 30 s groups, hence the similar average CD. The 50 s group exhibits a larger CD of 162.6 nm because of the additional 20 s development time.

4.4.3. Resist profile cross section for 30s single puddle and centrifuge-1 double puddle

The resist profile is important for further characterization, because some operations demand a good CD-U but in addition a processable resist sidewall. The sidewall angle is the main concern for operations, but other properties like a symmetrical profile, standing waves and general condition (cracks, deformation) have to be considered too. The wafers have been carefully cut perpendicular to the structure lines, in order to be able to observe the profile. A SEM takes the following images from the cross section of the wafer.

In fig. 4.7 we can see profiles taken from wafers from the second experiment with double puddle from section 4.4.2. The bottom part of the picture is filled with information about the magnification and a scale. The part above the information bar is the silicon bulk. On top of the silicon substrate is the BARC with approximately 80 nm thickness. The top layer in the picture is the resist M170Y with roughly 380 nm thickness showing the repeating pattern of line (resist) and space (clear region).

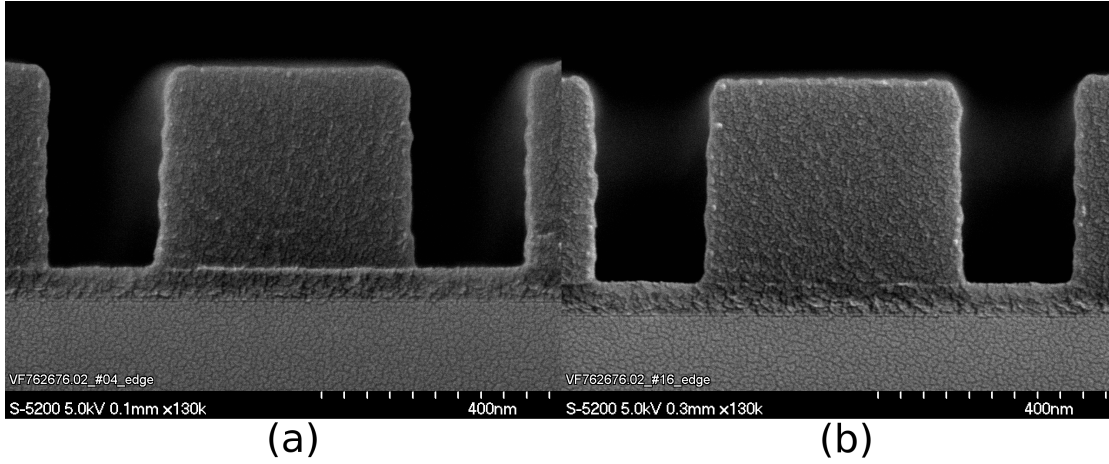


Figure 4.7.: (a) Resist profile for single puddle 30 s development time
(b) Resist profile for double puddle (centrifuge-1)

Both resist profiles show steep sidewall angles. The sidewalls have wave-like formations on them. The formations are due to the standing waves effect. The steep sidewall angle is good. An ideal angle would be 90° for most applications. Both resist show no cracks or other deformations on the sidewall. A small footing is observed at the contact area of resist and BARC. The footing varies across the wafer and is not the same on every position along the line structure. The sidewalls for the double puddle profile (fig. 4.7 (b)) look mostly symmetrical, while the sidewalls for the single puddle profile (fig. 4.7 (a)) seem to have a smaller sidewall angle on the left side than on the right side. The right side seems to have smaller wave-like formations for the single puddle profile.

Further investigation is needed to find out if the wave-formations are standing waves and why the single puddle resist profile has an asymmetric profile.

4.5. Discussion

The open frame experiments in this chapter show that the resist M170Y is cleared in 5 s and has a dose-to-clear of roughly 50 J/m^2 for the given bake temperature, bake times and developer concentration. That indicates that it is possible to reduce the development time of 50 s of the standard process drastically.

The experiments after the open frame experiments are performed to show what an impact the reduction of the development time has on CD and CD-U. The first

comparison between 50 s and 30 s development time shows the same 3σ for both groups, while the average CD is decreased by 2.5 nm for the 30 s group. A later experiment within the double puddle experiments with a smaller group size comes to a different result, where the 50 s group has a significantly better CD-U than the 30 s group.

The 50 s and 20 s development time groups are compared in a second experiment and show an increased 3σ for the 20 s group. The 50 s group has a 3σ of 4.5 nm and the 20 s has a 3σ of 4.8 nm. The average CD is increased by 3.1 nm for the 20 s group.

We looked for trends of the CD in wafermaps, but the standard deviation of the data is too large to make reliable statements.

The agitation experiments have an increased 3σ because of contamination in the coater, this may have influenced the first 50 s versus 30 s experiment too. The first agitation experiment is done to determine the best groups, which are continuous groups. The second experiment compares 20 s and 30 s continuous rotation groups with 20 s and 30 s “no rotation” groups and shows that the agitation modes are worse in regards of CD-U than the “no rotation” groups. The conclusion is that agitation worsens the CD-U. The F-test in the following section shows that the 20 s continuous group is significantly worse than the 20 s (no rotation) group.

The purpose of the first double puddle experiment is to find the best groups for a comparison with single puddle groups, which is performed in the second experiment. It shows that the replace-1, one of the double puddle groups, is significantly worse than the 50 s (no rotation) group. The other double puddle group, centrifuge-1, has a worse 3σ than the 50 s group, but this is not significantly so.

The reduction from 50 s to 20 s development time causes an insignificant change in CD-U, but increases the throughput by a lot. An increase of throughput is sought to reduce the time of wafers in the tools and decrease the costs of the final products.

4.5.1. F-Test

The results from the F-test are shown in table 4.14. Most of the experiment groups showed a similar 3σ , so it is not surprising to see that most of the comparisons accept the hypothesis. Only 3 comparisons are statistically significantly different: 20 s: no rotation vs continuous from the agitation experiment, 50 s vs 30 s and 50 s vs replace-1 from the double puddle experiment. The agitation experiment has

comparison	f-value	p-value (two tail)	$\alpha = 0.05 > p$
50 s vs 30 s	0.90	0.11	no
50 s vs 20 s	0.87	0.06	no
20 s: $\frac{1}{4}$ vs continuous	1.04	0.65	no
30 s: $\frac{1}{4}$ vs continuous	1.08	0.40	no
$\frac{1}{4}$: 20 s vs 30 s	1.07	0.49	no
continuous: 20 s vs 30 s	1.11	0.28	no
20 s: no rotation vs continuous	0.83	0.049	yes
30 s: no rotation vs continuous	0.87	0.16	no
no rotation: 20 s vs 30 s	0.88	0.20	no
continuous: 20 s vs 30 s	0.93	0.46	no
replace-1 vs replace-2	0.89	0.29	no
centrifuge-1 vs centrifuge-2	0.82	0.07	no
replace-1 vs centrifuge-1	1.06	0.59	no
replace-2 vs centrifuge-2	0.97	0.77	no
replace-1 vs centrifuge-1	1.12	0.25	no
50 s vs 30 s	0.83	0.047	yes
50 s vs replace-1	1.26	0.02	yes
50 s vs centrifuge-1	1.13	0.22	no

Table 4.14.: F-test evaluation for the development parameter experiments

a generally increased 3σ due to contamination. Both no rotation vs continuous comparisons show a small p-value (20 s: $p = 0.049$ and 30 s: $p = 0.16$) and therefore it is concluded that there is indeed a significant difference between the “no rotation” and continuous groups. The 50 s vs 30 s comparison is rejected in the double puddle experiment and had a small p-value in the first development time experiment ($p = 0.11$). The 50 s vs 20 s comparison has a small p-value of 0.06, close to rejection. A significant difference between the 50 s and lower development time groups, especially the 30 s group, is noted. The 50 s vs replace-1 comparison is rejected, while the 50 s vs centrifuge-1 comparison is accepted and has a decent p-value of 0.22. Further investigation is needed to conclude if the double puddle recipes are viable or not.

5. Conclusion

5.1. Impact of wafer bow

Wafer bow affects the CD-U as bowed wafers have an increased variation of CD. The experiments showed that smiling bow is more critical than crying bow, because the CD-U is worse with smiling bow wafers. The progression of the CD with increasing centrebow was evaluated for the resist M170Y. The smiling bow wafers showed an increasing CD from centre to roughly 130 μm height and then a decline of the CD. The crying bow wafers showed a decreasing CD from centre to edge. The wafer bow examination with the resist M91Y shows that this resist has smaller variations in the CD than samples with the resist M170Y. This different behaviour was expected because the resists have different impact of PEB on the CD.

We suspect that the wafer bow does not only show its influence in the PEB. The cooling process and the development, both steps happen after the PEB, are potential candidates that could not be examined independently from the PEB. Another influence is needed to explain why the trends in CD from centre to edge do not invert as expected with a switch from M170Y to M91Y. Additional experiments are needed to clarify which processes are affected by wafer bow and how strong they are impacted.

Experiments with a wafer with temperature sensors on it should allow to show us how hot the wafer gets with a certain distance to the hot plate. For this we need to be able to adjust the height of the position with the support pins. Additional experiments with bowed wafers with a reduced development time or a reduced PEB temperature should be able to show us how strong the impact of the wafer bow is on the process steps.

Vacuum hot plates are able to avoid the impact of the PEB on the CD for bowed wafers, because the vacuum sucks the wafer-bottom close to the hot plate. Therefore the wafer bow is counteracted. The contact between wafer and hot plate causes additional contamination on the wafer bottom side.

5.2. Development process parameters

We showed that the standard process with 50 s development time is the best process in regard of CD-U. It is possible to reduce the development time to 20 s or 30 s, when the process is not critical, to increase the throughput of the machine.

The experiments with agitation during development and double puddle development showed a worse CD-U in comparison with the 50 s development time, but the differences were not significant for most experiment groups.

The resist profiles for the 30 s development and the centrifuge-1 double puddle development were examined and showed wave-like formations that look like standing waves. Also the 30 s development picture shows a slight asymmetric profile. Further investigation is needed to conclude if the examined programmes are of interest for future use in the production line.

Bibliography

- [1] Jan Albers. *Grundlagen integrierter Schaltungen*. 2nd ed. Carl Hanser, 2010. ISBN: 978-3-446-42232-2.
- [2] Ao.Univ.Prof. Dipl.-Ing. Dr.techn. Christoph Eisenmenger-Sittner. Technische Universität Wien. URL: <https://tiss.tuwien.ac.at/person/46247>.
- [3] Michael Raj Marks, Zainuriah Hassan and Kuan Yew Cheong. “Characterization Methods for Ultrathin Wafer and Die Quality: A Review”. In: *IEEE Transactions on components, packaging and manufacturing technology* 4.12 (2014), pp. 2042–2057. URL: <http://ieeexplore.ieee.org/document/6948353/>.
- [4] Bernhard Hoppe. *Mikroelektronik 2*. 1st ed. Vogel, 1998. ISBN: 978-3-8023-1588-X.
- [5] Chris Mack. *Fundamental Principles of Optical Lithography - The Science of Microfabrication*. 1st ed. John Wiley & Sons, 2007. ISBN: 978-0-470-72730-0.
- [6] Erin Casey Olaf Nootbaar. *Photoresist Technology*. Shipley.
- [7] Renato Škrapec. “Evaluation of the photoresist M170Y regarding the possible minimal structures”. MA thesis. Universitätsring 1, 1010 Wien: Universität Wien, 2016. URL: <http://ubdata.univie.ac.at/AC13398739>.
- [8] Landis Stefan. *Lithography*. 1st ed. ISTE Ltd, John Wiley & Sons, 2011. ISBN: 978-1-848-21202-2.
- [9] *Theory of Operation Manual - Coater/Developer CLEAN TRACK™ LITHIUS™ Series*. Akasaka Biz Tower, 5-3-1 Akasaka, Minato-ku Tokyo 107-6325: Tokyo Electron Limited, 2010.
- [10] *Wafer Geometry Characteristics*. Eichhorn und Hausmann Metrology.

List of Figures

2.1. Lithography process steps [5, p.13]	4
2.2. Exposure methods [5, p.19]	5
2.3. Scanners and steppers [5, p.20]	6
2.4. Step-and-scan [5, p.21]	6
2.5. Interference of light waves with (right) and without (left) BARC (not drawn to scale)	9
2.6. Standing waves on circular structures [6, p.109]	9
2.7. Swing curve of the dose-to-clear [6, p.91]	10
2.8. Diffraction on a single slit [1, p.120] (altered into English language)	11
2.9. Diffraction with light going through 2 slits and a projection system [1, p.123] (altered into English language)	12
2.10. Impact of focus on the shape of the end of an isolated line [5, p.359]	13
2.11. Definition of bow on a crying wafer [3, p.2043]	14
2.12. Measurement principle [10, p.3]	15
2.13. Thin film optical measurement [1, p.110] (altered into English lan- guage)	16
2.14. Definitions of space, line, pitch, CD - top & CD - bottom (not drawn to scale)	17
2.15. Overview of the structures on the substrate	18
2.16. SEM CD measurement with the measured CD, the punctured line follows the CD-bottom	18
3.1. PEB sensitivity curve for a positive DUV resist with a negative temperature dependency [8, p.284]	20
3.2. Preparation of the bowed wafers	21
3.3. Process steps to generate a bow on the wafers for the first experiment	22
3.4. Wafer bow measurement on the MX2012 for a wafer from the 160 μm bow crying group	22
3.5. hot plate inside the cluster machine (the exhaust ventilation was removed for this photo)	23
3.6. Positioning of the bowed wafers on the hot plate (not drawn to scale)	25
3.7. Resist thickness measurement on a not bowed (16) and two smiling wafers (3 & 4)	28
3.8. Necessary process window over radius	29

3.9. CD over focus to determine the process window of the resist M170Y - borders of the chosen process window in orange	29
3.10. Wafermap of the 155 μm smiling group with M170Y	34
3.11. Oxide thickness measurement of a 155 μm smiling wafer (wafer no.25)	36
3.12. Wafermap of the 175 μm crying group with M170Y	39
3.13. Wafermap of the 170 μm smiling group with M170Y	39
3.14. Wafermap of the 275 μm crying group with M170Y	42
3.15. Wafermap of the 385 μm crying group with M170Y	42
3.16. Wafermap of the 255 μm smiling group with M170Y	43
3.17. Wafermap of the 370 μm smiling group with M170Y	43
3.18. Wafermap of the 275 μm crying group with M170Y	45
3.19. Wafermap of the 385 μm crying group with M170Y	45
3.20. Wafermap of the 255 μm smiling group with M170Y	46
3.21. Wafermap of the 370 μm smiling group with M170Y	46
3.22. Average CD for the 3rd experiment and its repetition	47
3.23. 3σ for the 3rd experiment and its repetition	48
3.24. Wafermap of the 130 μm smiling group with M170Y	50
3.25. Wafermap of the 90 μm smiling group with M170Y	51
3.26. Wafermap of the 80 μm smiling group with M170Y	52
3.27. CD-U comparison of the crying bow groups	52
3.28. CD over height ₁ for the 175 μm , 275 μm and 385 μm crying bow groups	53
3.29. CD-U comparison of the experiments on smiling bow groups	54
3.30. CD over height for the 170 μm , 255 μm and 370 μm smiling bow groups	55
3.31. CD over height for the 80 μm , 90 μm , 130 μm and 170 μm smiling bow groups	56
3.32. PEB-temperature resulting from the average CD of the exposure shots versus their radial position from the centre (assuming that the PEB is the only influence)	57
3.33. Wafermap of the 155 μm smiling group with M91Y	59
3.34. Wafermap of the 110 μm smiling group with M91Y	60
3.35. Wafermap of the 110 μm smiling group with M91Y 405 nm	61
3.36. Wafermap of the 175 μm crying group with M91Y	63
3.37. Wafermap of the no bow group with M91Y	64
3.38. Wafermaps of two 170 μm smiling wafers with M91Y	65
3.39. CD-U comparison of the crying bow groups	66
3.40. CD-U comparison of the crying bow groups	66
3.41. CD over radius for the no bow, 175 μm crying and 170 μm smiling group	67
4.1. Deposition of the developer on the wafer, the red arrow indicates the movement of the robot arm	74

4.2. Puddle on a wafer for development [6, p.84]	74
4.3. Average CD of 12 wafers with 50 s development time	79
4.4. Average CD of 13 wafers with 30 s development time	79
4.5. Radial progression of CD and standard deviation for every shot for the 50 s development time	80
4.6. Radial progression of CD and standard deviation for every shot for the 30 s development time	80
4.7. (a) Resist profile for single puddle 30 s development time (b) Resist profile for double puddle (centrifuge-1)	87
A.1. Normal distribution showing the percentiles of covered values in reach of 1,2 and 3 σ	ii
A.2. M170Y no bow wafermaps	iv
A.3. M170Y 55 μm crying wafermaps	v
A.4. M170Y 110 μm crying wafermaps	v
A.5. M170Y 160 μm crying wafermaps	vi
A.6. M170Y 50 μm smiling wafermaps	vi
A.7. M170Y 110 μm smiling wafermaps	vii
A.8. M170Y 155 μm smiling wafermaps	vii
A.9. M91Y 414 nm no bow wafermaps	viii
A.10. M91Y 414 nm 55 μm crying wafermaps	ix
A.11. M91Y 414 nm 110 μm crying wafermaps	ix
A.12. M91Y 414 nm 160 μm crying wafermaps	x
A.13. M91Y 414 nm 50 μm smiling wafermaps	x
A.14. M91Y 414 nm 110 μm smiling wafermaps	xi
A.15. M91Y 414 nm 155 μm smiling wafermaps	xi
A.16. M91Y 405 nm no bow wafermaps	xii
A.17. M91Y 405 nm 55 μm crying wafermaps	xiii
A.18. M91Y 405 nm 110 μm crying wafermaps	xiii
A.19. M91Y 405 nm 160 μm crying wafermaps	xiv
A.20. M91Y 405 nm 50 μm smiling wafermaps	xiv
A.21. M91Y 405 nm 110 μm smiling wafermaps	xv
A.22. M91Y 405 nm 155 μm smiling wafermaps	xv
A.23. M170Y no bow wafermaps	xvi
A.24. M170Y 175 μm crying wafermaps	xvii
A.25. M170Y 170 μm smiling wafermaps	xviii
A.26. M91Y 525 nm no bow wafermaps	xix
A.27. M91Y 525 nm 175 μm wafermaps	xx
A.28. M91Y 525 nm 170 μm smiling wafermaps	xxi
A.29. M170Y 275 μm crying wafermaps	xxii
A.30. M170Y 385 μm crying wafermaps	xxiii

A.31.M170Y 255 μm smiling wafermaps	xxiv
A.32.M170Y 370 μm smiling wafermaps	xxv
A.33.M170Y 130 μm smiling wafermaps	xxvi
A.34.M170Y 80 μm smiling wafermaps	xxvii
A.35.M170Y 90 μm smiling wafermaps	xxviii
A.36.M170Y 275 μm crying wafermaps (repetition)	xxix
A.37.M170Y 385 μm crying wafermaps (repetition)	xxx
A.38.M170Y 255 μm smiling wafermaps (repetition)	xxxi
A.39.M170Y 370 μm smiling wafermaps (repetition)	xxxii

List of Tables

3.1. Resist thickness d on bowed wafers	27
3.2. Parameters of the M170Y wafer bow experiments	31
3.3. Properties of the bowed wafers for the first experiment	32
3.4. CD-U values of the first M170Y experiment	33
3.5. Results of the oxide thickness measurement	35
3.6. Properties of the bowed wafers for the second experiment	37
3.7. CD-U values of the second M170Y experiment	38
3.8. Properties of the bowed wafers for the third experiment	40
3.9. CD-U values of the third M170Y experiment	40
3.10. CD-U values of the repetition of the third M170Y experiment . . .	41
3.11. Average CD and 3σ for the 3rd experiment and its repetition	47
3.12. Properties of the bowed wafers for the fourth experiment 130 nm bow	49
3.13. CD-U values of the fourth M170Y experiment	49
3.14. Properties of the bowed wafers for the fourth experiment 90 nm bow	50
3.15. CD-U values of the fifth M170Y experiment	50
3.16. Parameters of the M91Y wafer bow experiments	58
3.17. CD-U values of the first experiment	59
3.18. CD-U values of the second M91Y experiment	61
3.19. CD-U values of the third M91Y experiment	62
3.20. F-test evaluation for the wafer bow experiments with M170Y	68
3.21. F-test evaluation for the wafer bow experiments with M91Y	69
4.2. Open frame experiments overview	76
4.3. Parameters of the development time experiments	76
4.4. CD-U evaluation for 50 s versus 30 s development time	77
4.5. CD-U evaluation for 50 s versus 20 s development time	77
4.6. Parameters of the first agitation experiment	82
4.7. Parameters of the second agitation experiment	82
4.8. CD-U evaluation for the first agitation and development time ex- periment	82
4.9. CD-U evaluation for the second agitation and development time experiment	83
4.10. Parameters of the double puddle experiment	84
4.11. Parameters of the single puddle & double puddle experiment	85

4.12. CD-U evaluation for the first double puddle experiment	85
4.13. CD-U evaluation for the second double puddle experiment	86
4.14. F-test evaluation for the development parameter experiments	89

Acknowledgements

I want to thank Professor Eisenmenger-Sittner for all his support during this thesis and for accepting his supervision in the first place.

My deepest thanks to my supervisor Dr. Behrendt Andreas at Infineon. He was always ready to help me in my many troubles. I learned a lot from his stories as they bear life experience from difficult situations. A comment by Andreas regarding the topic of wafer bow:

“Und die Moral von der Geschicht: Biege deine Wafer nicht!” *Behrendt Andreas, 13.06.2017, 11:40*

Lots of thanks to my many colleagues at Infineon Villach for supporting me during my thesis. Without their help this thesis wouldn't have been possible.

Thanks to my family as they rarely caught a glimpse of me during my diploma thesis.

I want to thank my dear colleagues at the Vienna University of Technology. Especially my learning group for their endless motivation during our hard study time.

I want to thank Chris Mack for his great book on lithography and cite this part from his book:

“**Lithographer** 1. A practitioner of lithography. 2. A harmless drudge.

Example: *The overworked and underappreciated lithographer paused for a moment and daydreamed, 'Will Moore's Law ever end?'*” [5, p.474]

On one side a funny note, but on the other side a hidden truth as lithography is the working horse driving IC dimensions down as far as possible. Thanks to the lithographers worldwide.

Special thanks to Russian Circles for their *Guidance*.

A. Appendix

A.1. Formulas

$$avg\ CD = \frac{\sum_{i=1}^N CD^i}{N} \quad (A.1)$$

$$\overline{CD}_{x,y} = \frac{\sum_{i=1}^n CD_{x,y}^i}{n} \quad (A.2)$$

$$3\sigma = 3 \cdot \sqrt{\frac{1}{N} \sum_{i=1}^N (CD_i - \overline{CD})^2} \quad (A.3)$$

$$CD = A + 0.7\text{ nm}/^\circ\text{C} \cdot T_{PEB} \quad (A.4)$$

$$\text{CD-centre} = \frac{\overline{CD}_{6,5} + \overline{CD}_{7,5}}{2} \quad (A.5)$$

$$\text{CD-edge} = \frac{\overline{CD}_{12,4} + \overline{CD}_{12,5} + \overline{CD}_{12,6} + \overline{CD}_{11,7} + \overline{CD}_{10,8} + \text{and so on}}{26} \quad (A.6)$$

$$height = \frac{\kappa \cdot (2 \cdot r)^2}{8} \quad (A.7)$$

The formulas used in this thesis are mostly of statistical origin. The formulas and variables are explained in the following paragraphs.

The avg CD stands for average critical dimension and is used throughout the work. CD_i is the i -th measured CD of a wafer or group. In this formula we do not care which position it is in. N is the total number of measurement points.

$\overline{CD}_{x,y}$ is the average CD on a specific point on the wafer. x is the horizontal shot slot and y is the vertical shot slot. n is the number of wafers measured. $\overline{CD}_{x,y}$ is used for curves that show the radial trend of the CD across the wafer. It is mostly used in the wafer bow chapter.

The 3σ is simply put just 3 times the standard deviation. The factor 3 is used

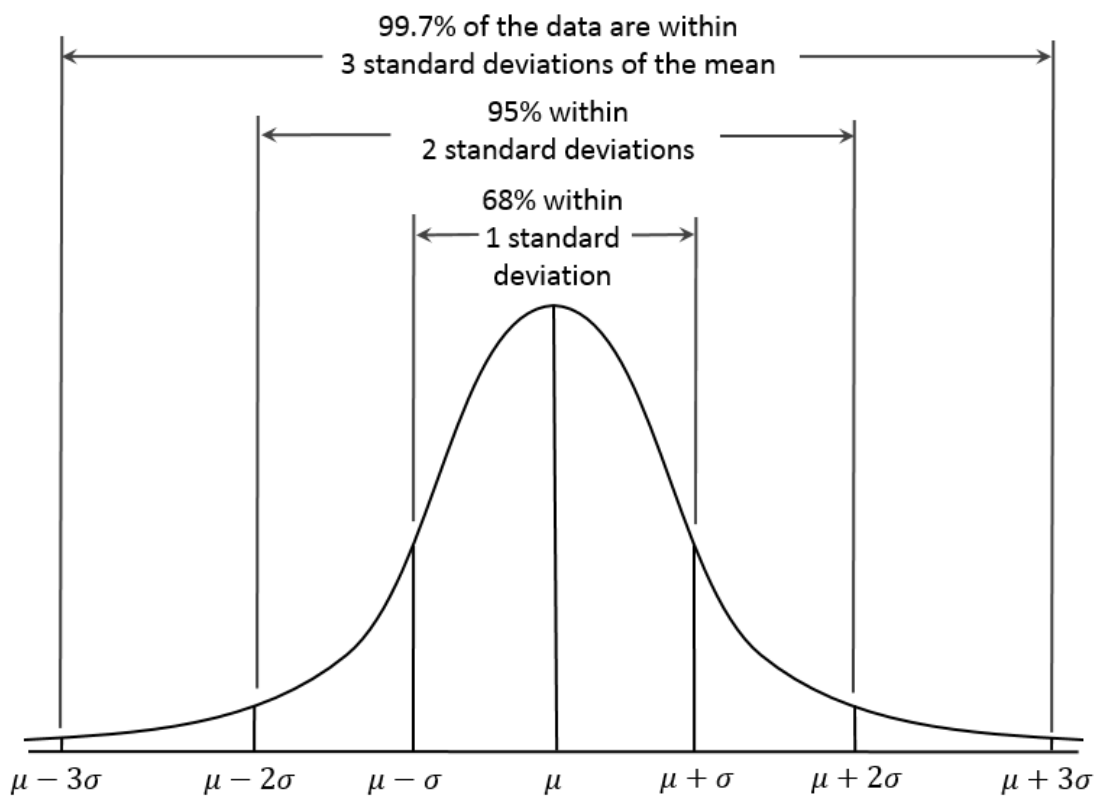


Figure A.1.: Normal distribution showing the percentiles of covered values in reach of 1,2 and 3 σ

because the IC production is interested to have no failures and the 3σ indicates the specification limits of an operation. The reason why 3σ is used instead of 1σ in this work is because in manufacturing it is important to set specification limits (in our case CD-limits) for processes. Programs watch over measurement results to notice if there is a change in the measured variable. $\pm 1\sigma$ is not enough for a specification limit, because roughly 32% of the results of a stable process would violate the limit. With $\pm 3\sigma$ only roughly 0.3% would violate the limit (see fig. A.1).

The PEB-temperature has an influence on the CD. In the wafer bow chapter this formula is used to relate the CD-change caused by the bow to a heat budget difference in the PEB. The 2 resists in this work have different coefficients: M170Y has $-2.2 \text{ nm}/^\circ\text{C}$ and M91Y has $0.7 \text{ nm}/^\circ\text{C}$ as taken from [7, p.73-82].

CD-centre and CD-edge are the averages of the measurement points of the centre and edge respectively. For the CD-centre only the 2 measurement points in the shot slot closest to the centre are taken. The positions of these measurement points are at roughly 11 mm radius. The CD-edge measurement points are 26 in number at lie at roughly 132 mm.

The *height* is a defined variable to measure the vertical distance from the centre of the wafer to the position of the shot slot. That means that *height* = 0 at the centre. The formula bases on the trigonometry of the sector of a circle. To deviate the formula the approximation of $\cos(\alpha) = 1 - \frac{\alpha^2}{2}$ had to be used and therefore is not exact. The error is of order α^4 , the largest α in this thesis is 0.006° . κ is the curvature of the wafer, which is a result of the bow. The radius r is calculated from the shot slot position and is the radial distance from the shot slot to the centre of the wafer. There is another version of the formula used for crying wafers with the difference that the *height* = 0 at the edge. For that a simple substitution of r with $150 \text{ mm} - r$ is done.

A.2. Wafermaps of bowed wafers

The following graphs show the so called wafermaps, the CD of the structures is illustrated in respect to their position on the wafer in the shot slots. The units in the wafermaps are given in nm when the first digit is a 1, otherwise it is μm (when there is a 0,xxx).

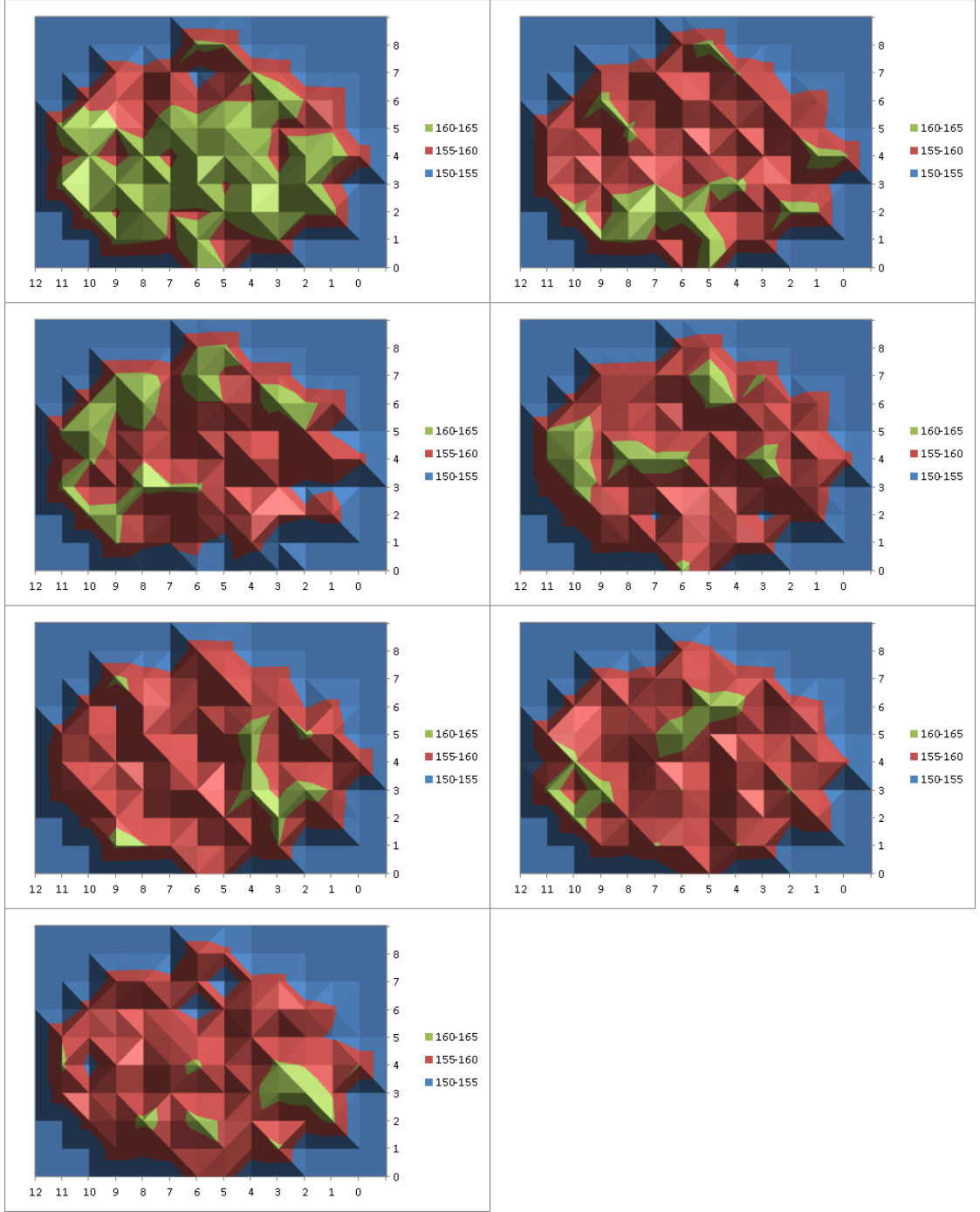


Figure A.2.: M170Y no bow wafermaps

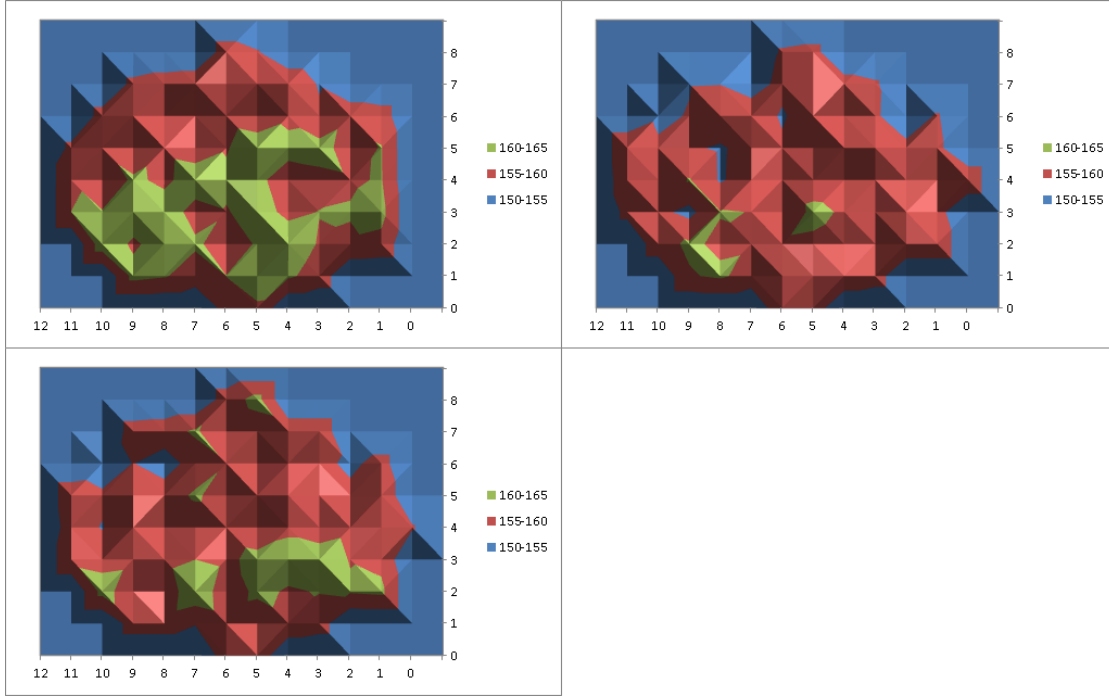


Figure A.3.: M170Y 55 μm crying wafermaps

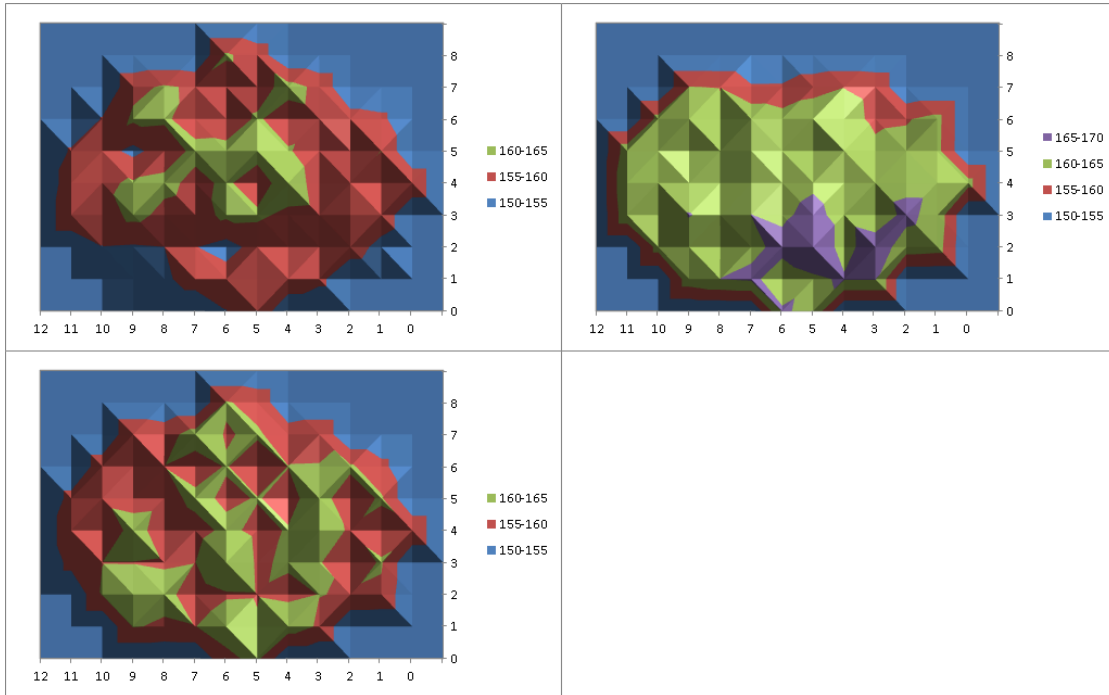


Figure A.4.: M170Y 110 μm crying wafermaps

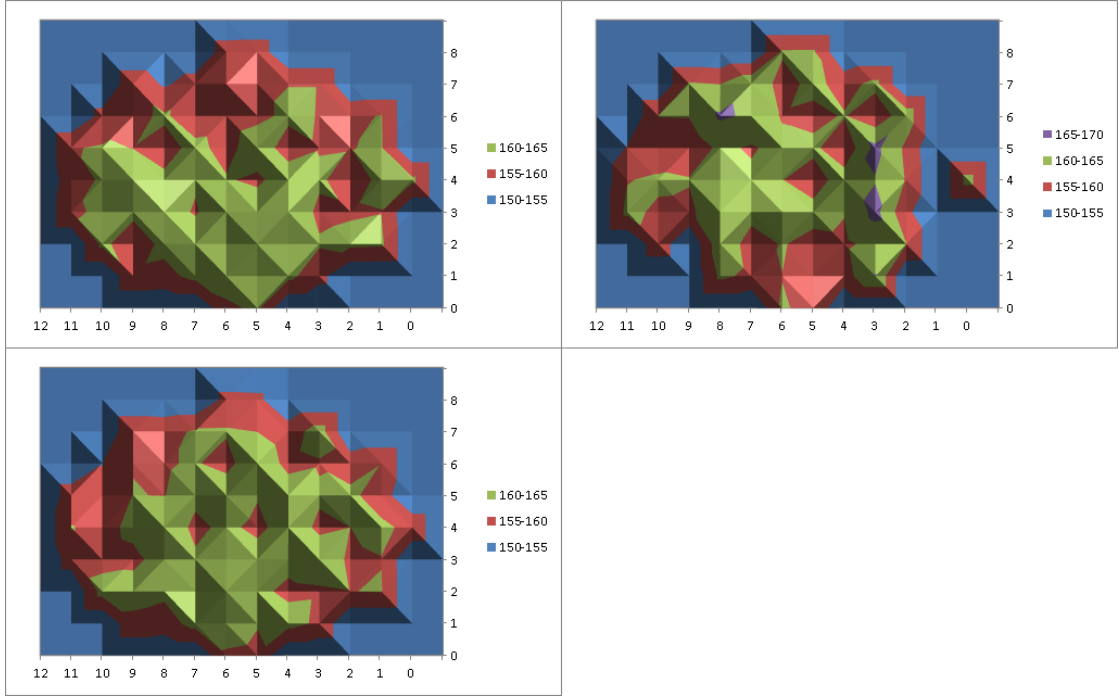


Figure A.5.: M170Y 160 μm crying wafermaps

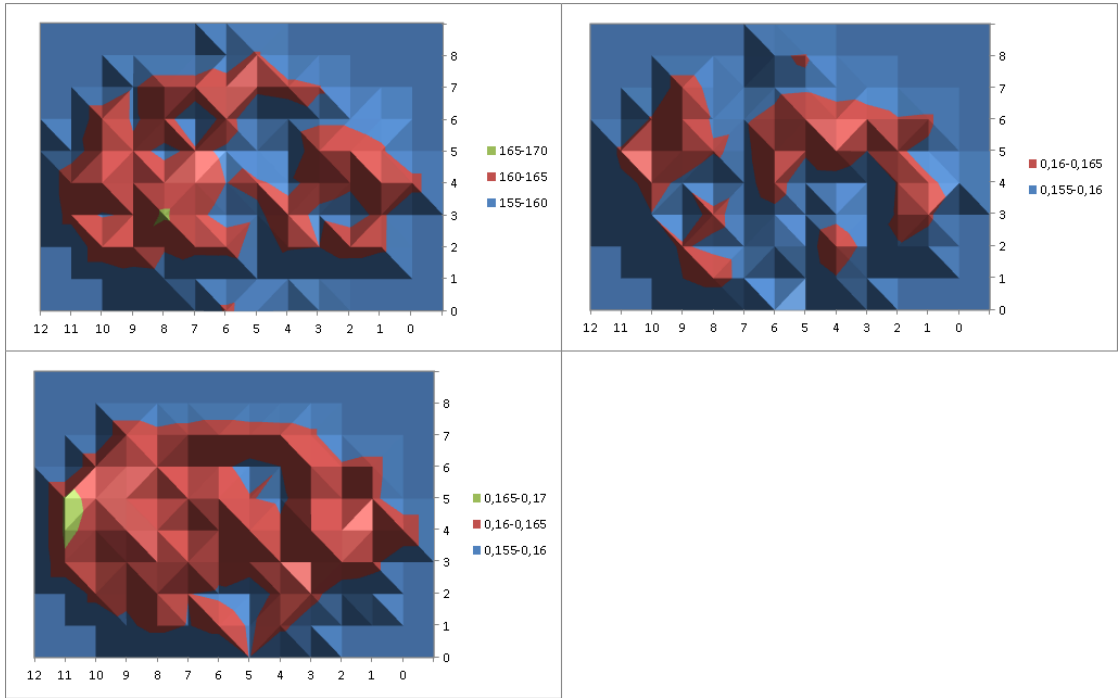


Figure A.6.: M170Y 50 μm smiling wafermaps

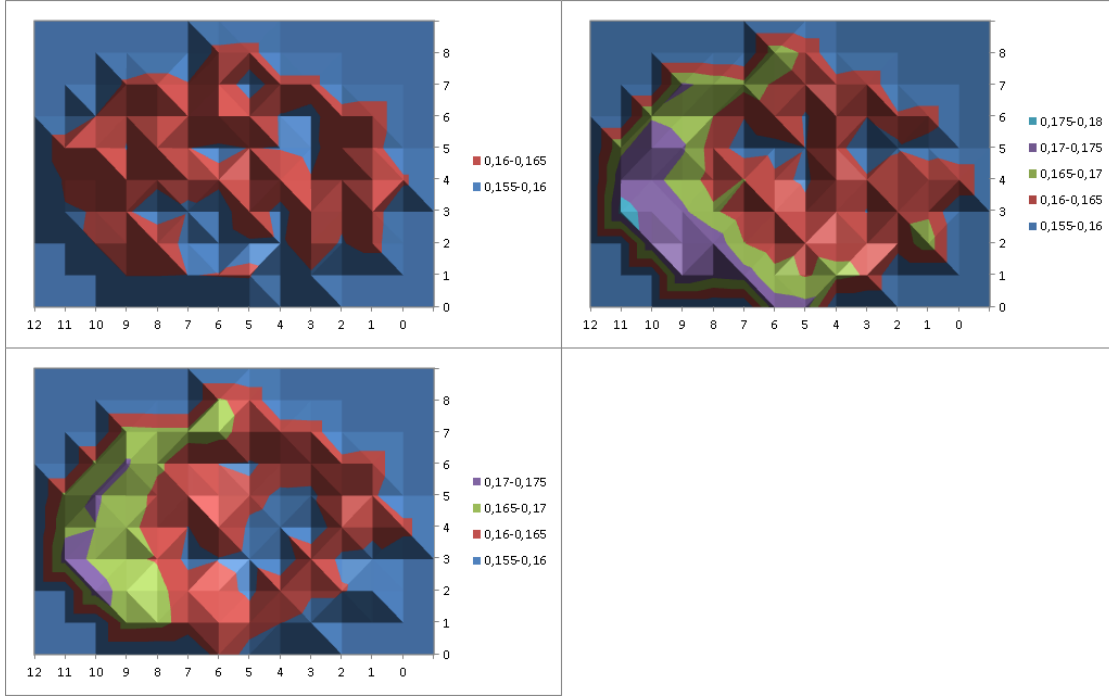


Figure A.7.: M170Y 110 μm smiling wafermaps

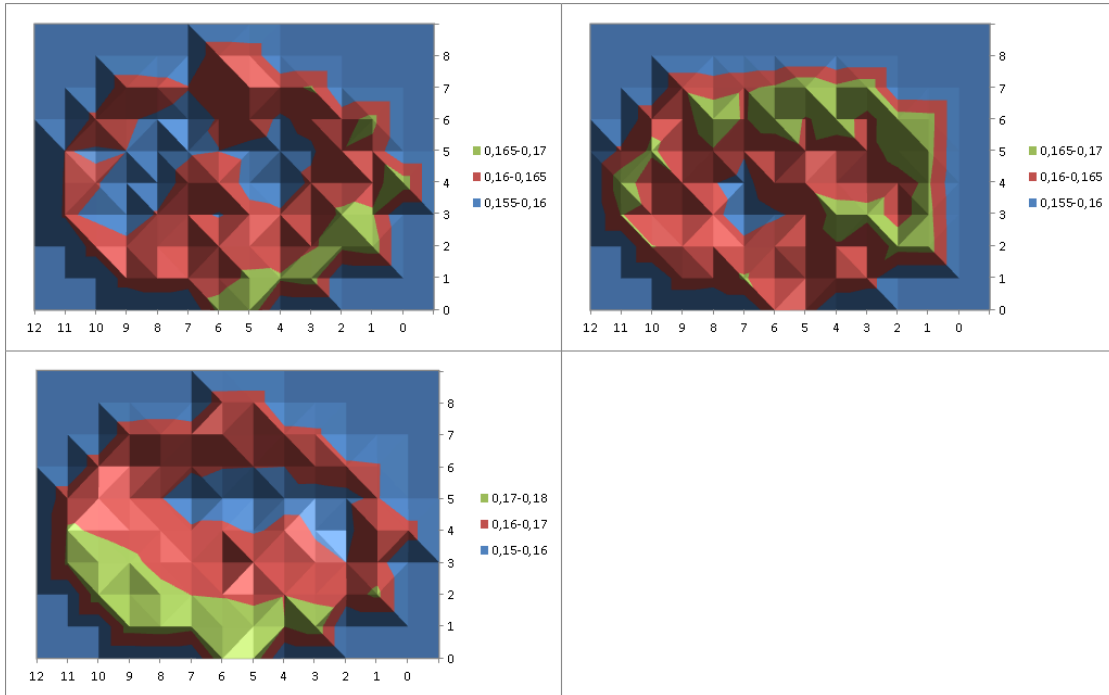


Figure A.8.: M170Y 155 μm smiling wafermaps

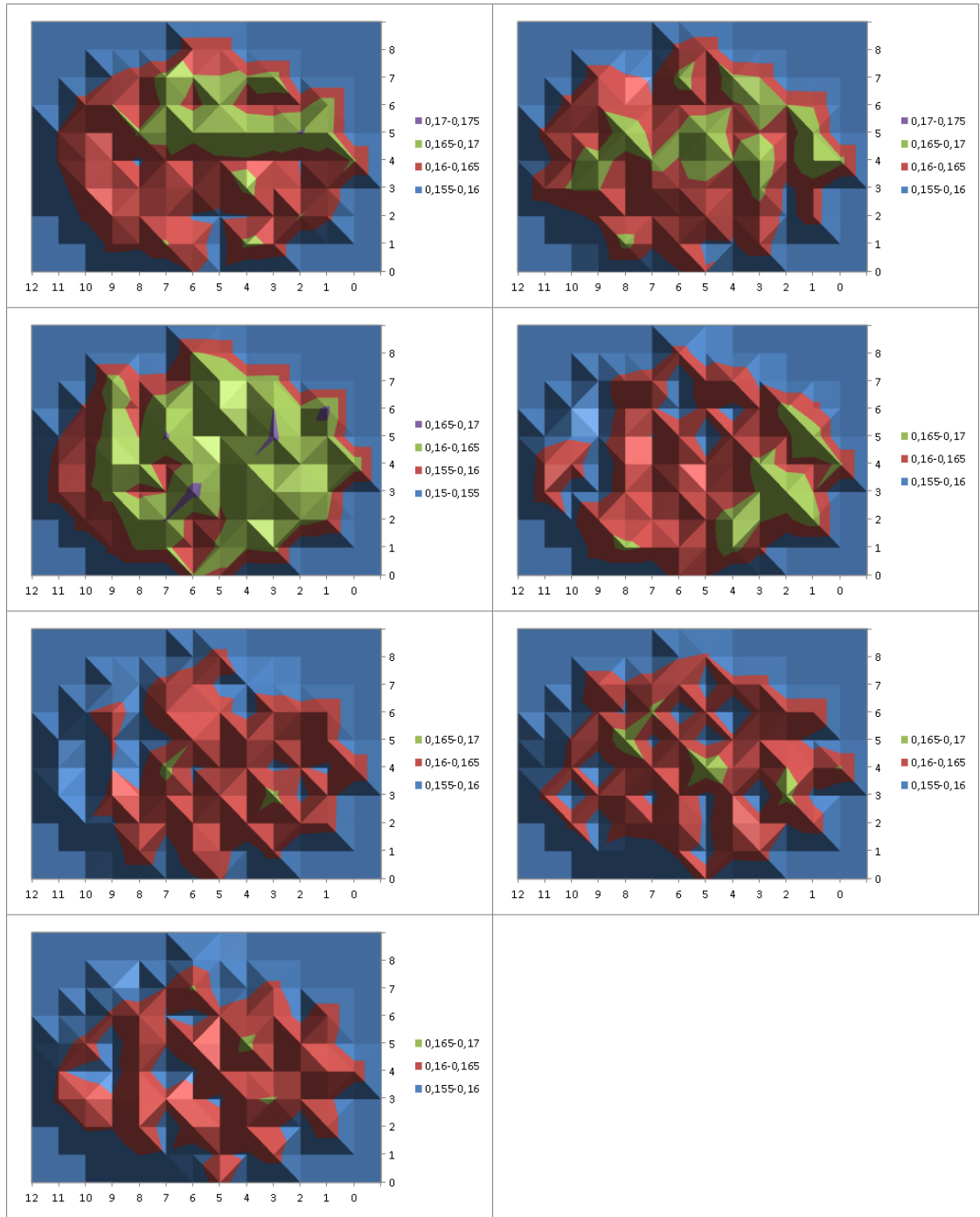


Figure A.9.: M91Y 414 nm no bow wafermaps

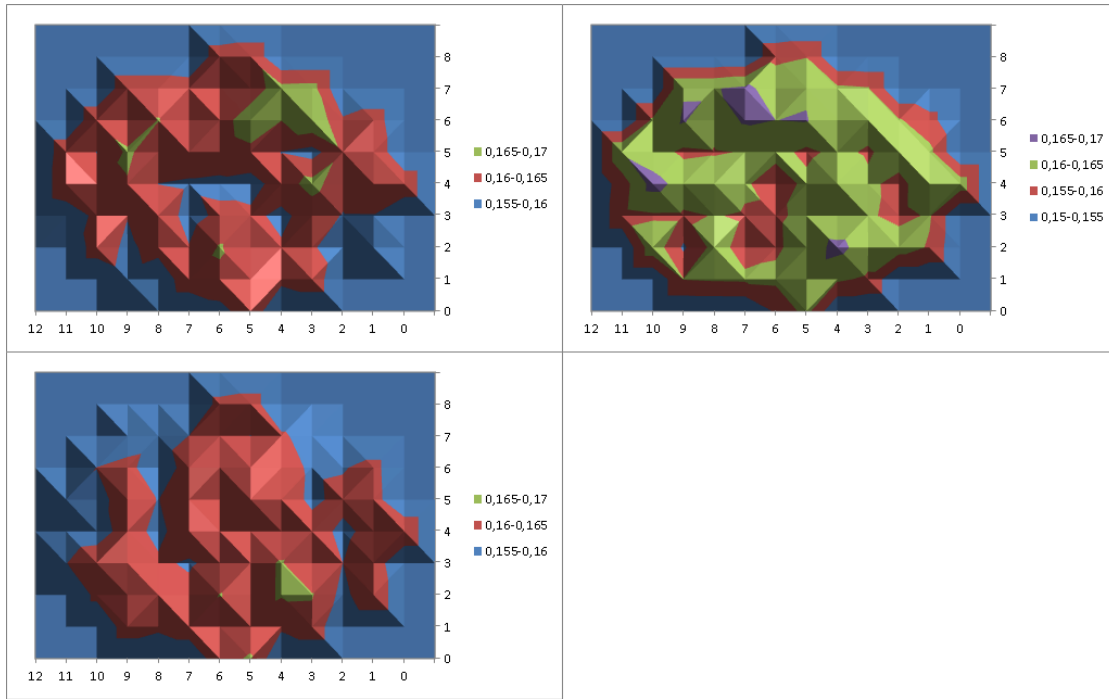


Figure A.10.: M91Y 414 nm 55 μ m crying wafermaps

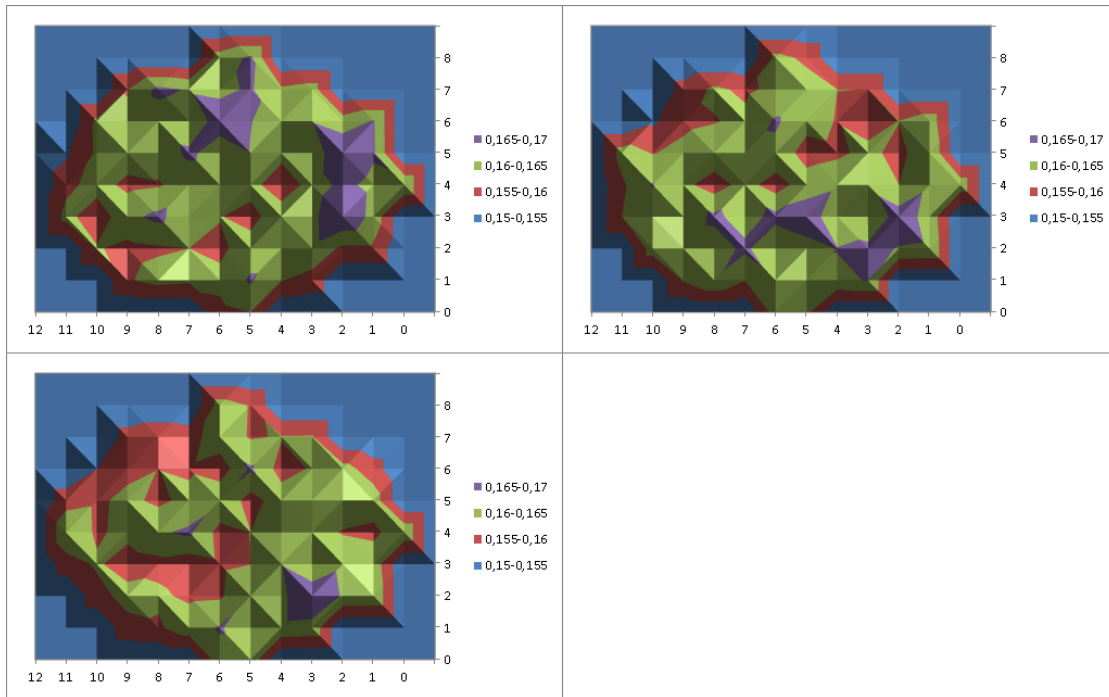


Figure A.11.: M91Y 414 nm 110 μ m crying wafermaps

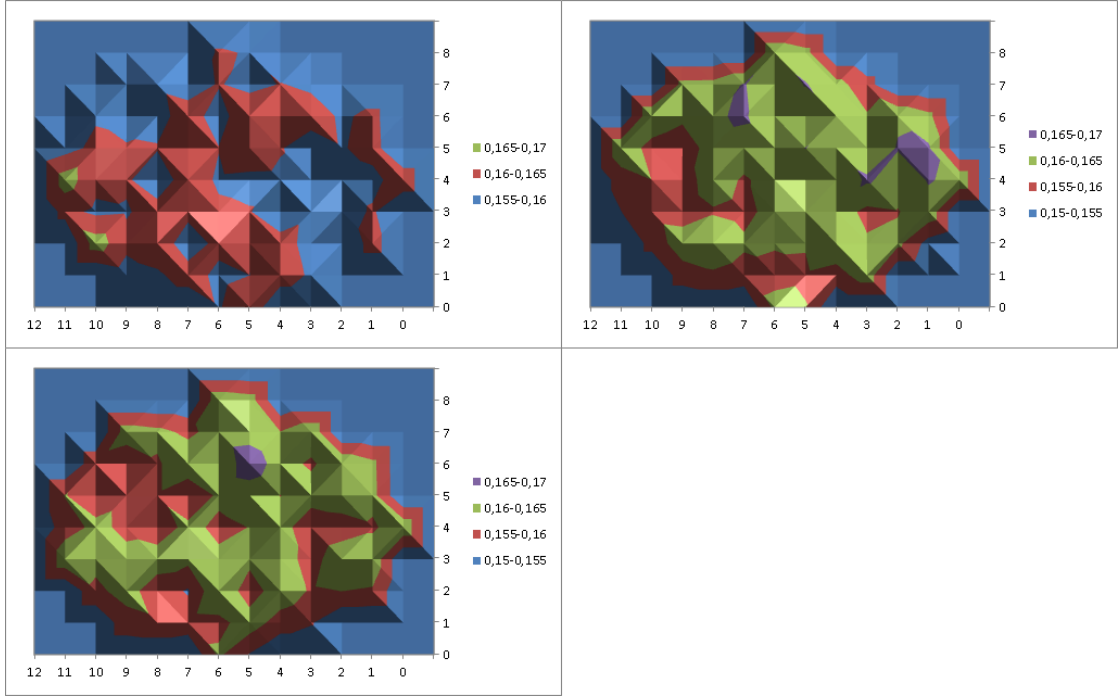


Figure A.12.: M91Y 414 nm 160 μ m crying wafermaps

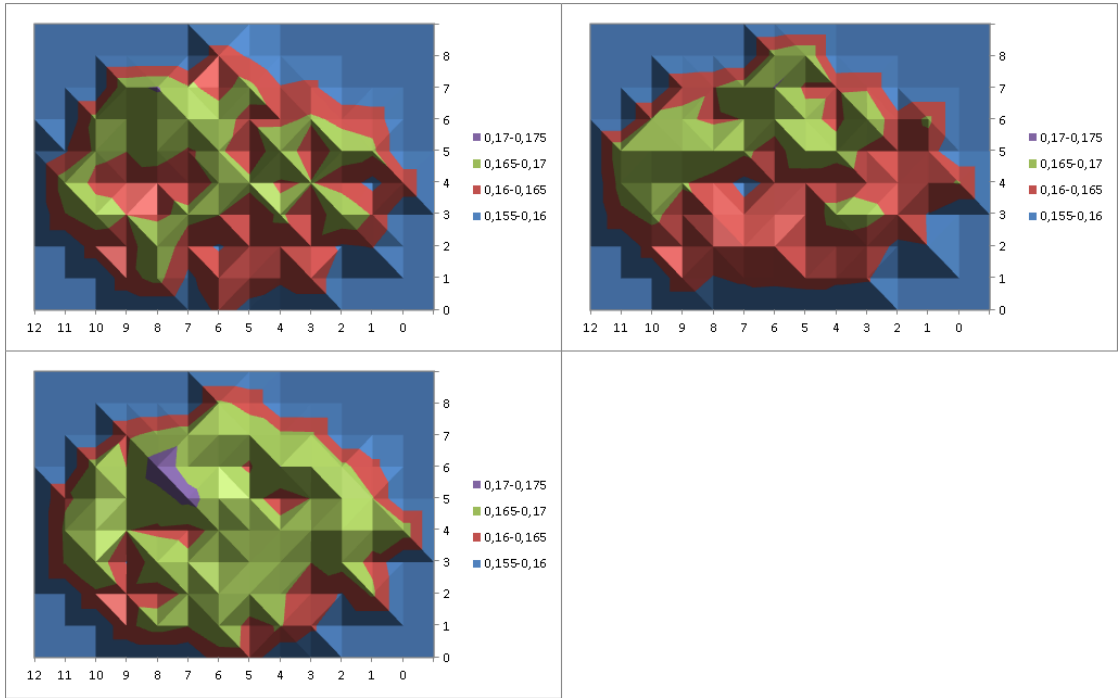


Figure A.13.: M91Y 414 nm 50 μ m smiling wafermaps

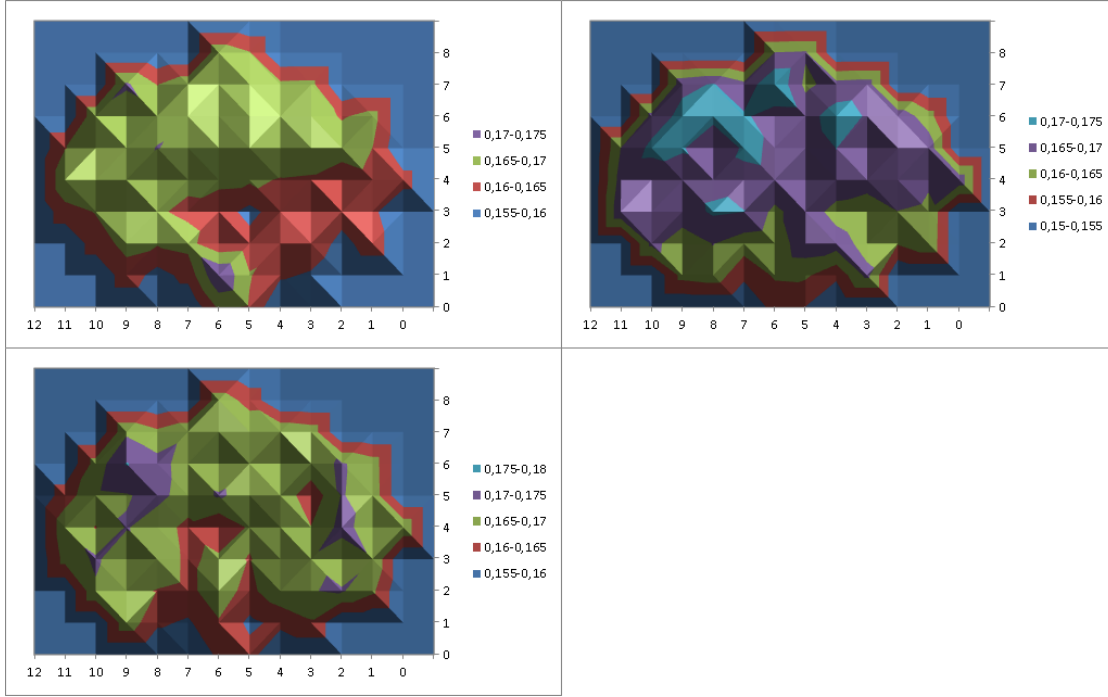


Figure A.14.: M91Y 414 nm 110 μm smiling wafermaps

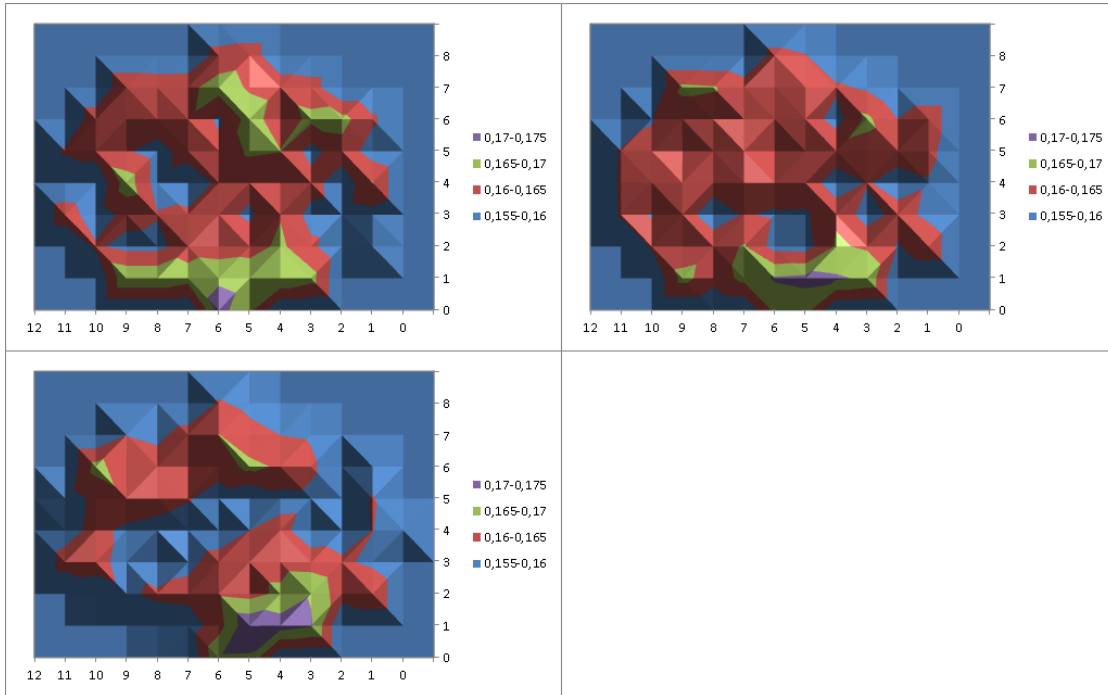


Figure A.15.: M91Y 414 nm 155 μm smiling wafermaps

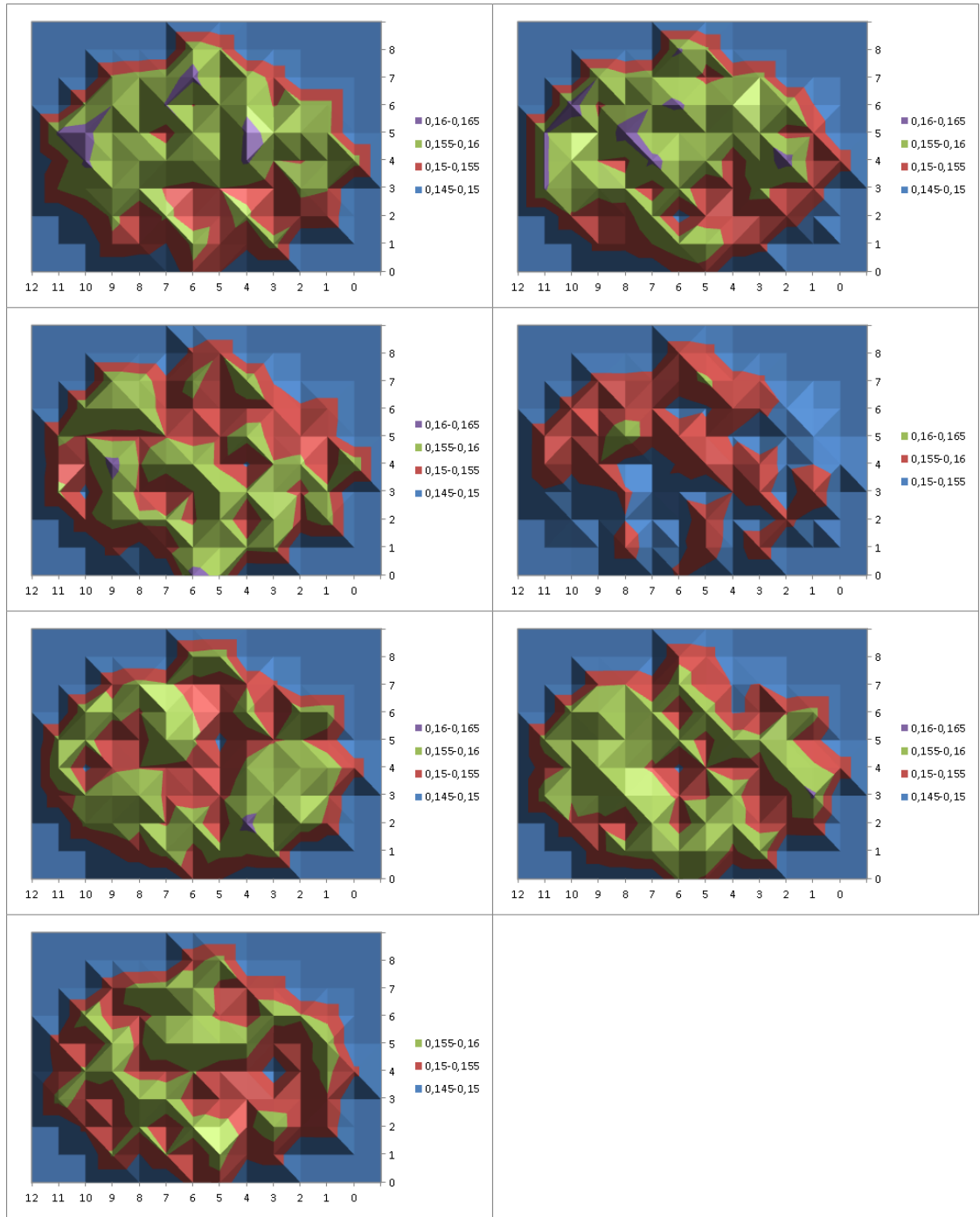


Figure A.16.: M91Y 405 nm no bow wafermaps

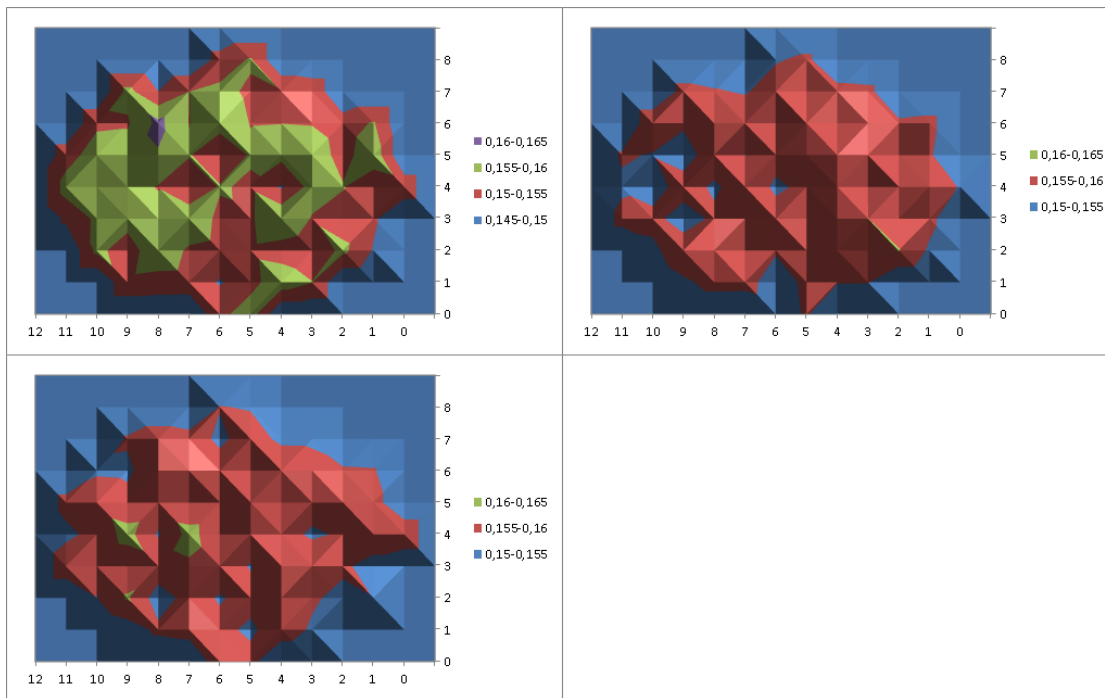


Figure A.17.: M91Y 405 nm 55 μ m crying wafermaps

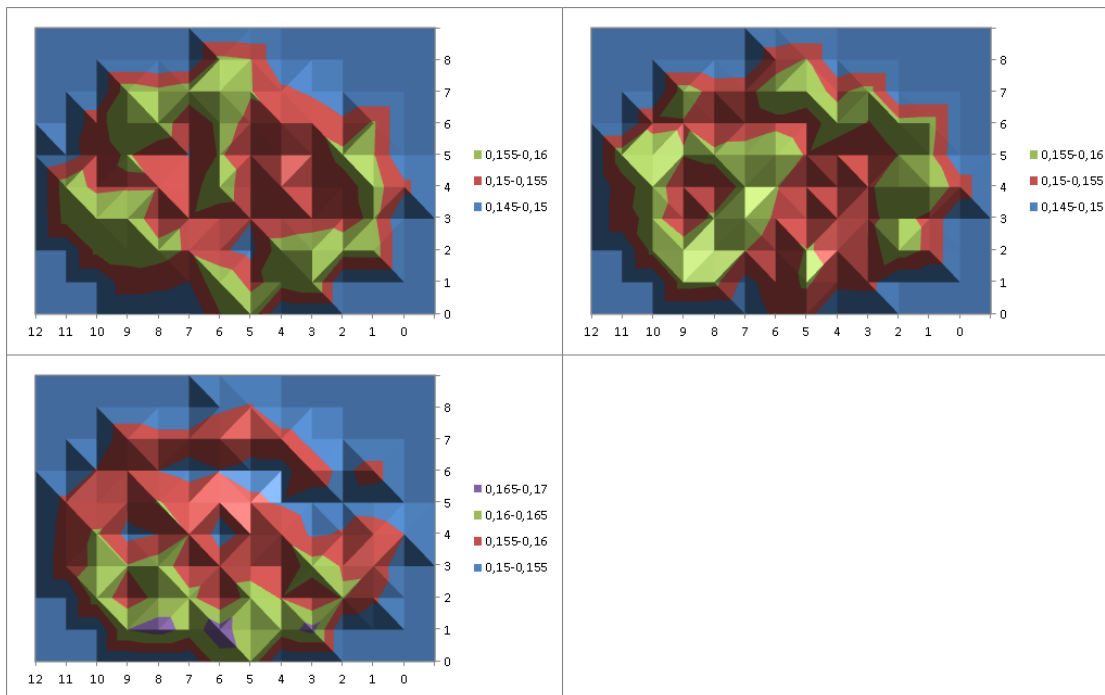


Figure A.18.: M91Y 405 nm 110 μ m crying wafermaps

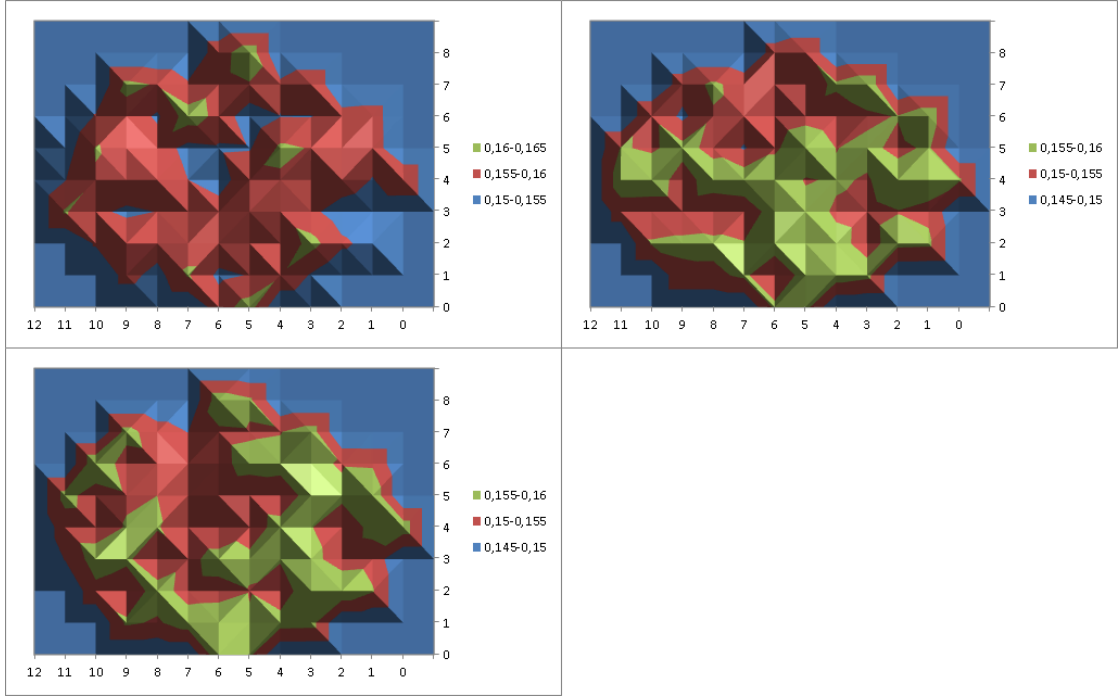


Figure A.19.: M91Y 405 nm 160 μm crying wafermaps

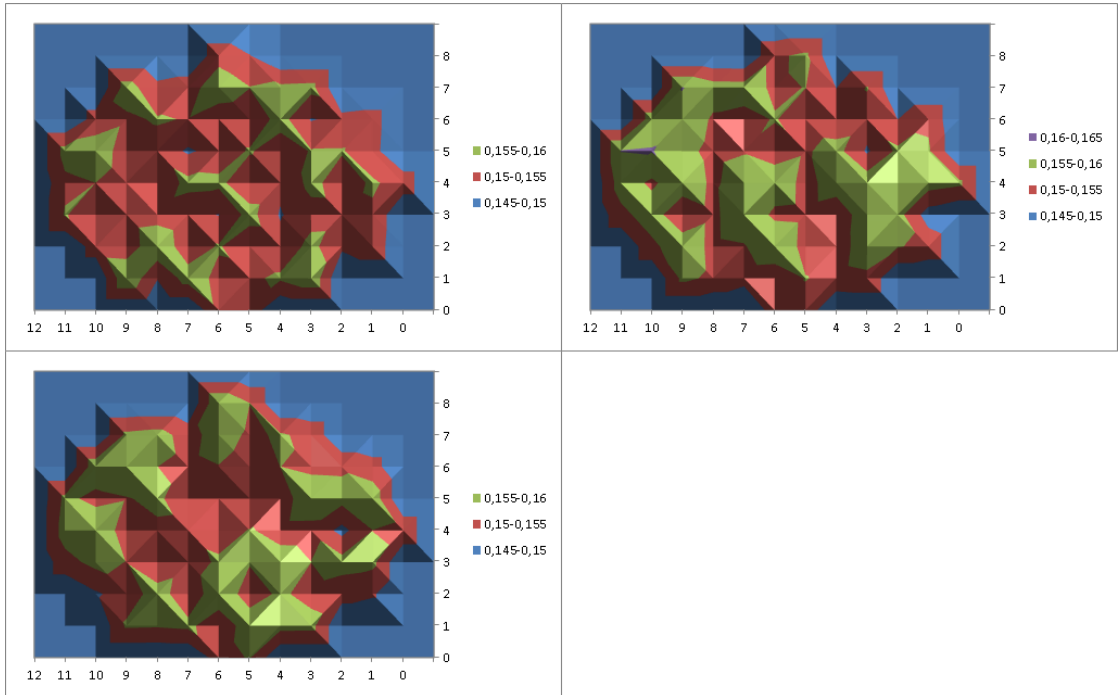


Figure A.20.: M91Y 405 nm 50 μm smiling wafermaps

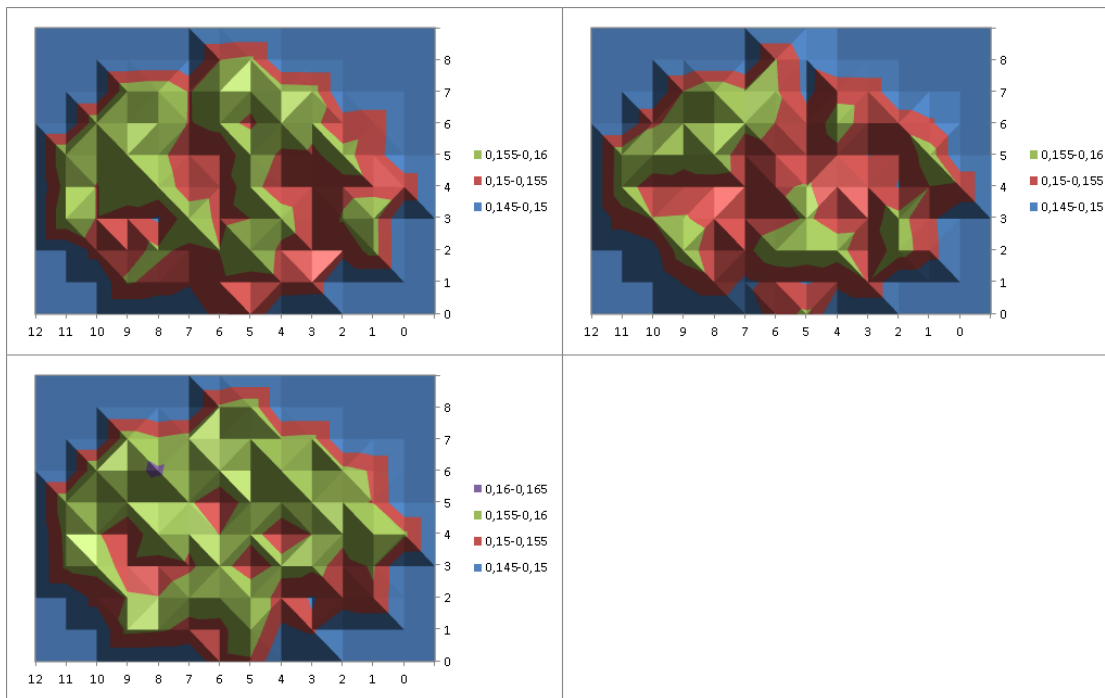


Figure A.21.: M91Y 405 nm 110 μm smiling wafermaps

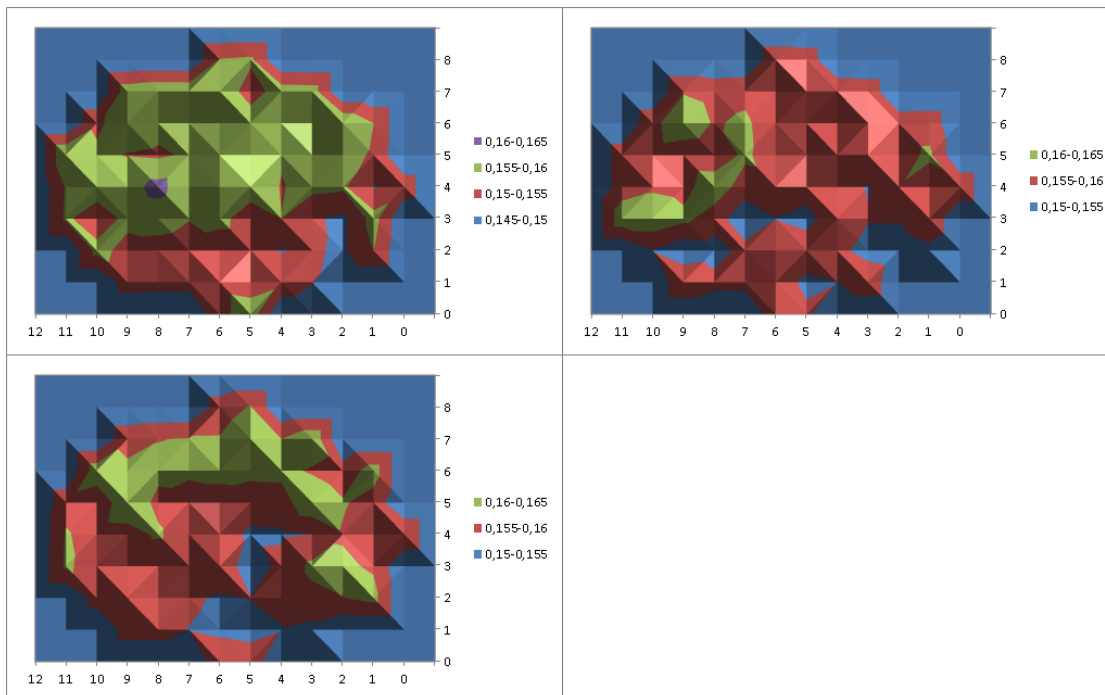


Figure A.22.: M91Y 405 nm 155 μm smiling wafermaps

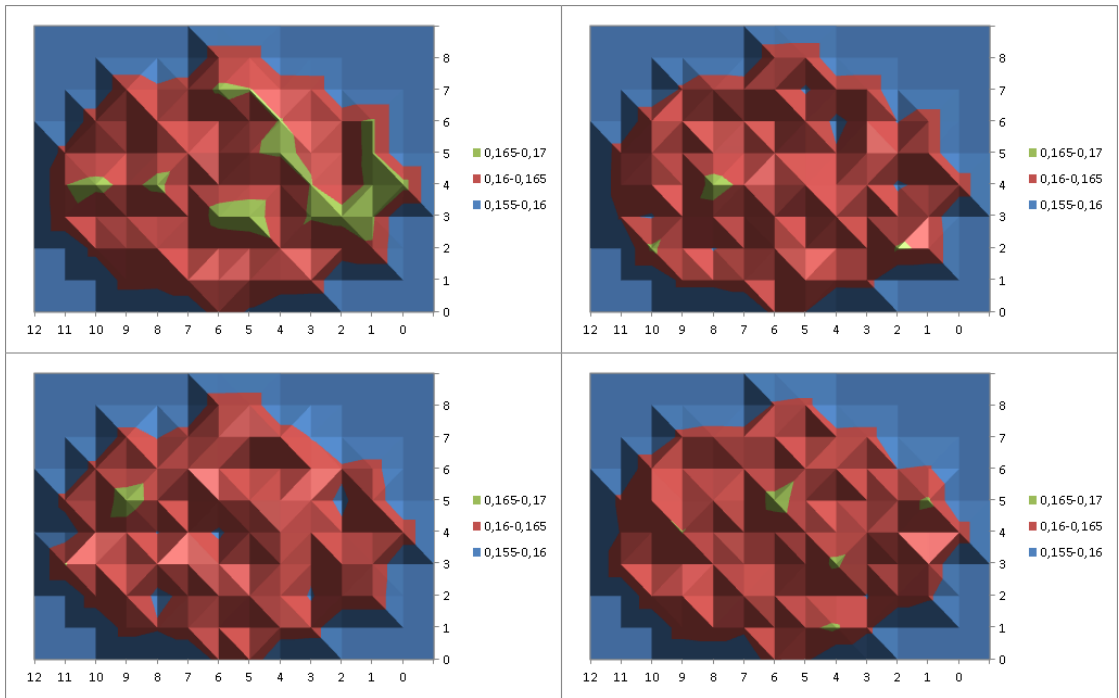


Figure A.23.: M170Y no bow wafermaps

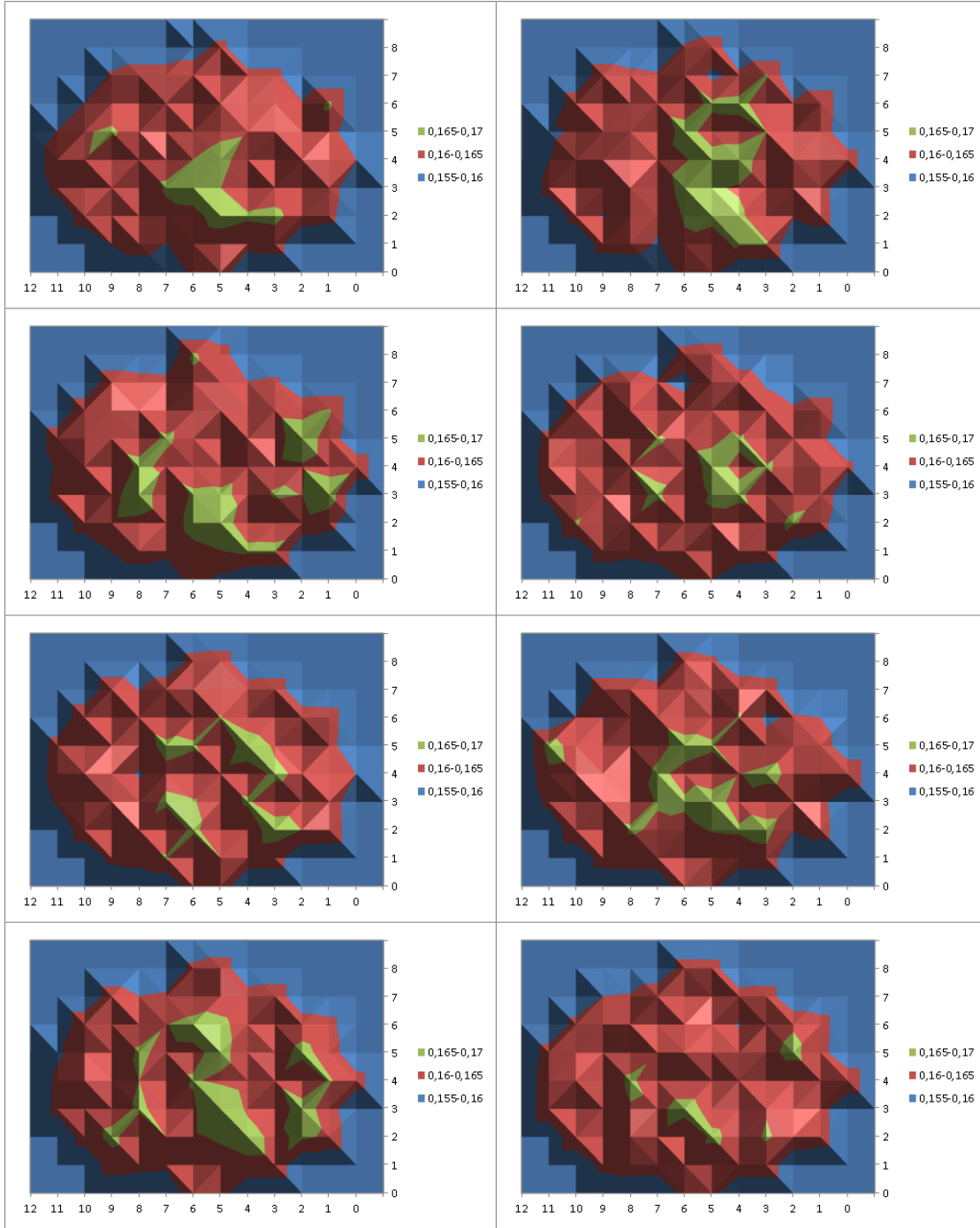


Figure A.24.: M170Y 175 μm crying wafermaps

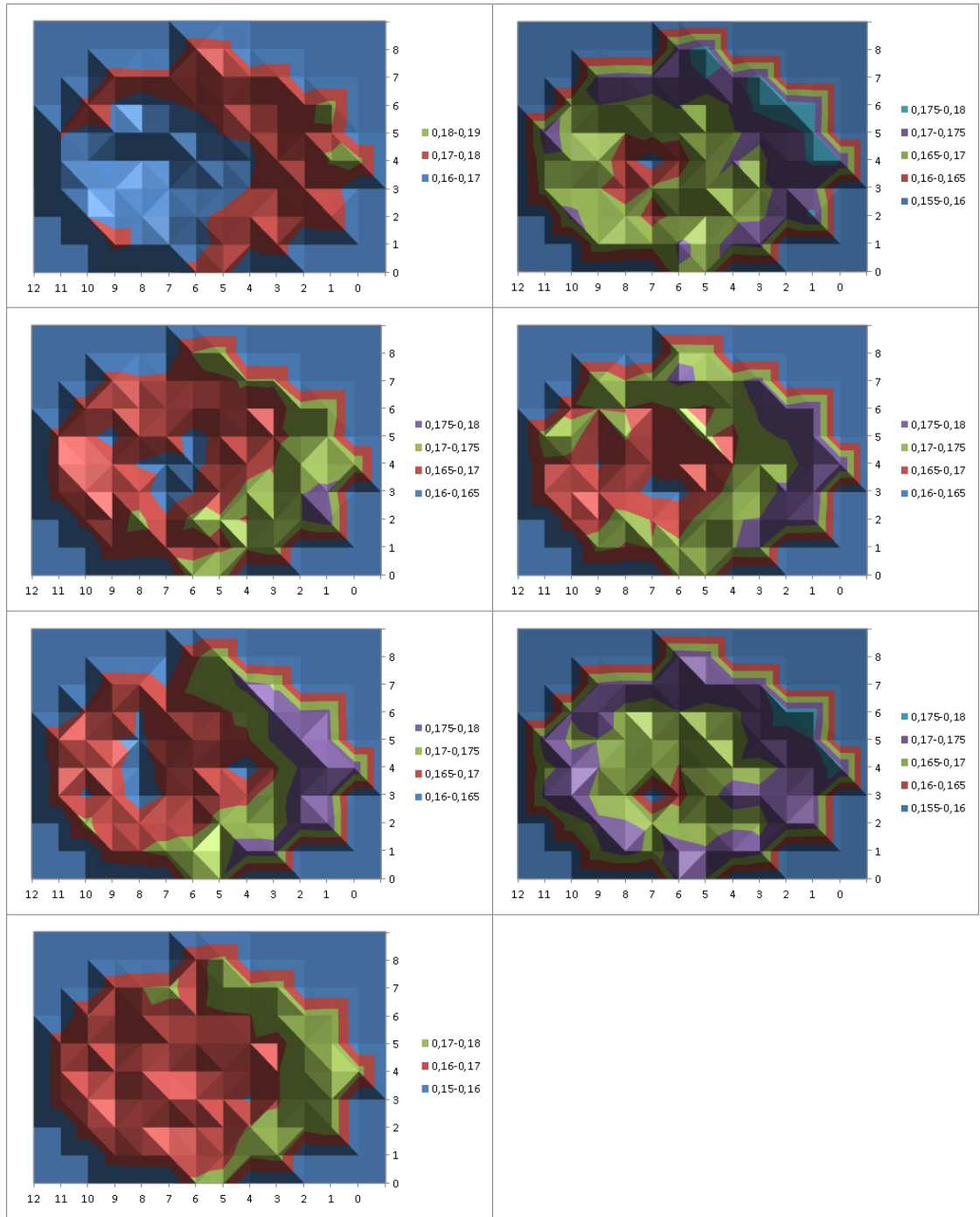


Figure A.25.: M170Y 170 μm smiling wafermaps

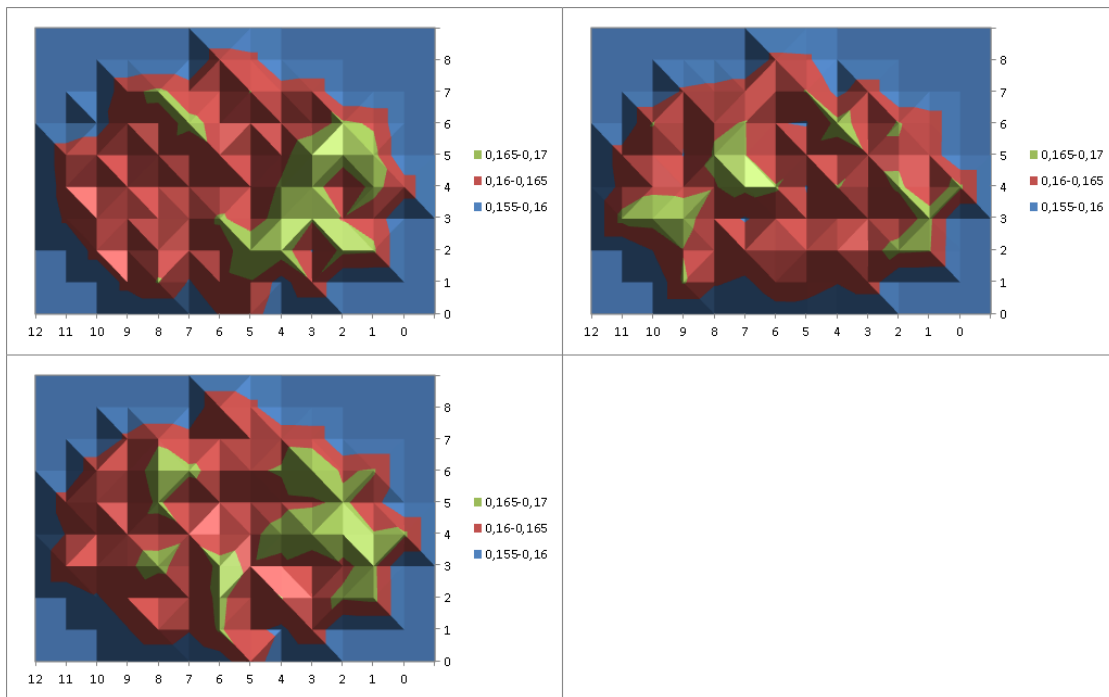


Figure A.26.: M91Y 525 nm no bow wafermaps

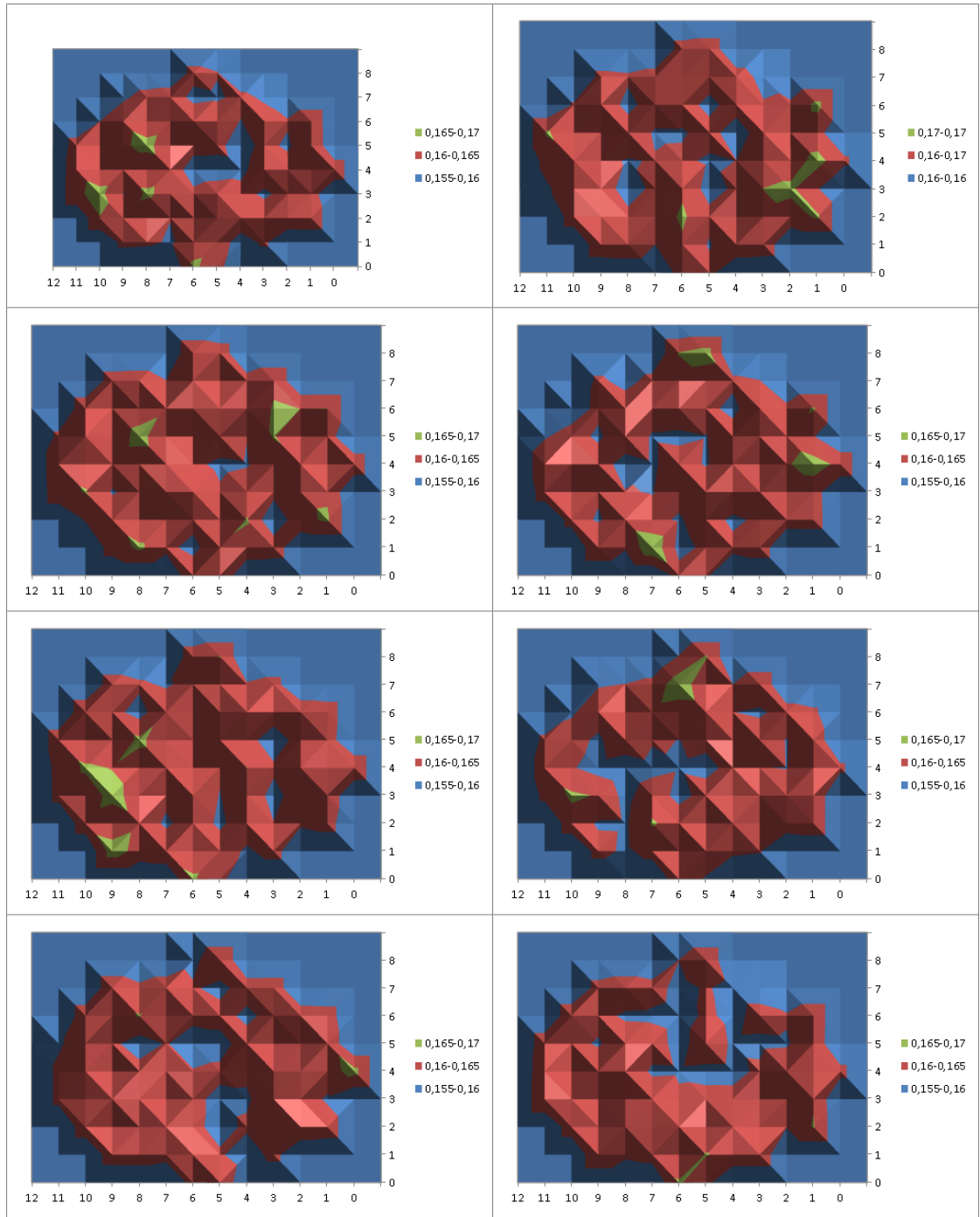


Figure A.27.: M91Y 525 nm 175 μm wafermaps

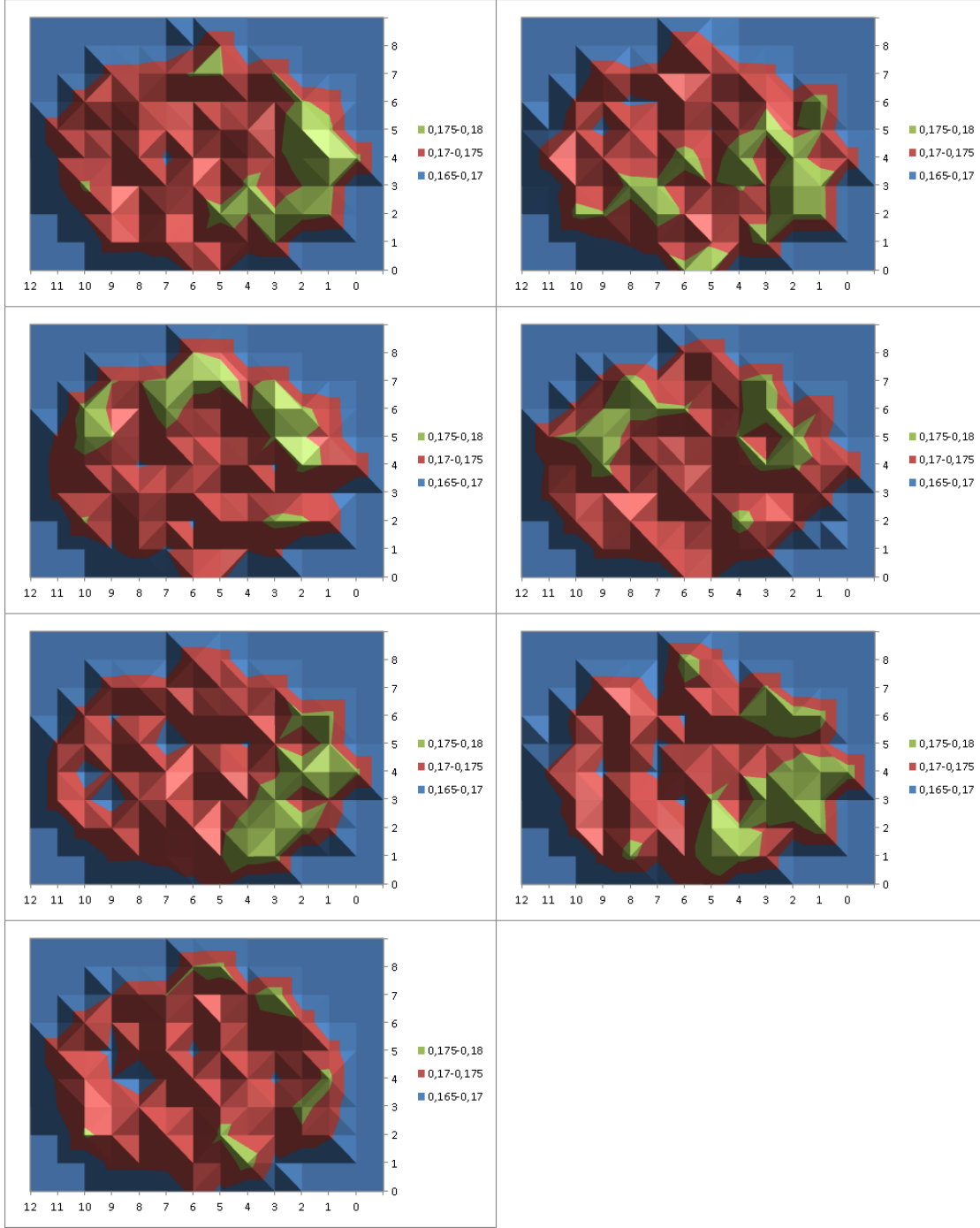


Figure A.28.: M91Y 525 nm 170 μm smiling wafermaps

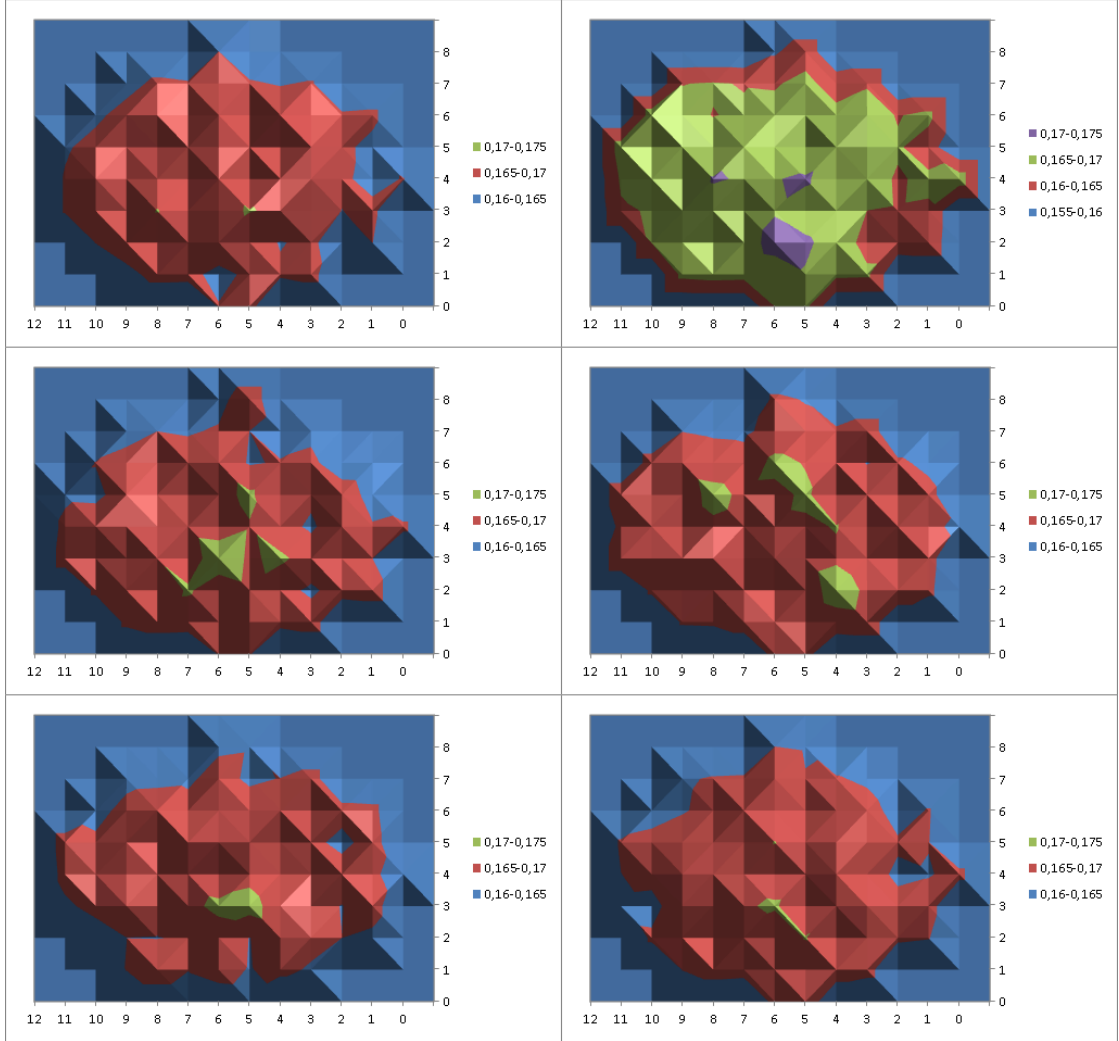


Figure A.29.: M170Y 275 μm crying wafermaps

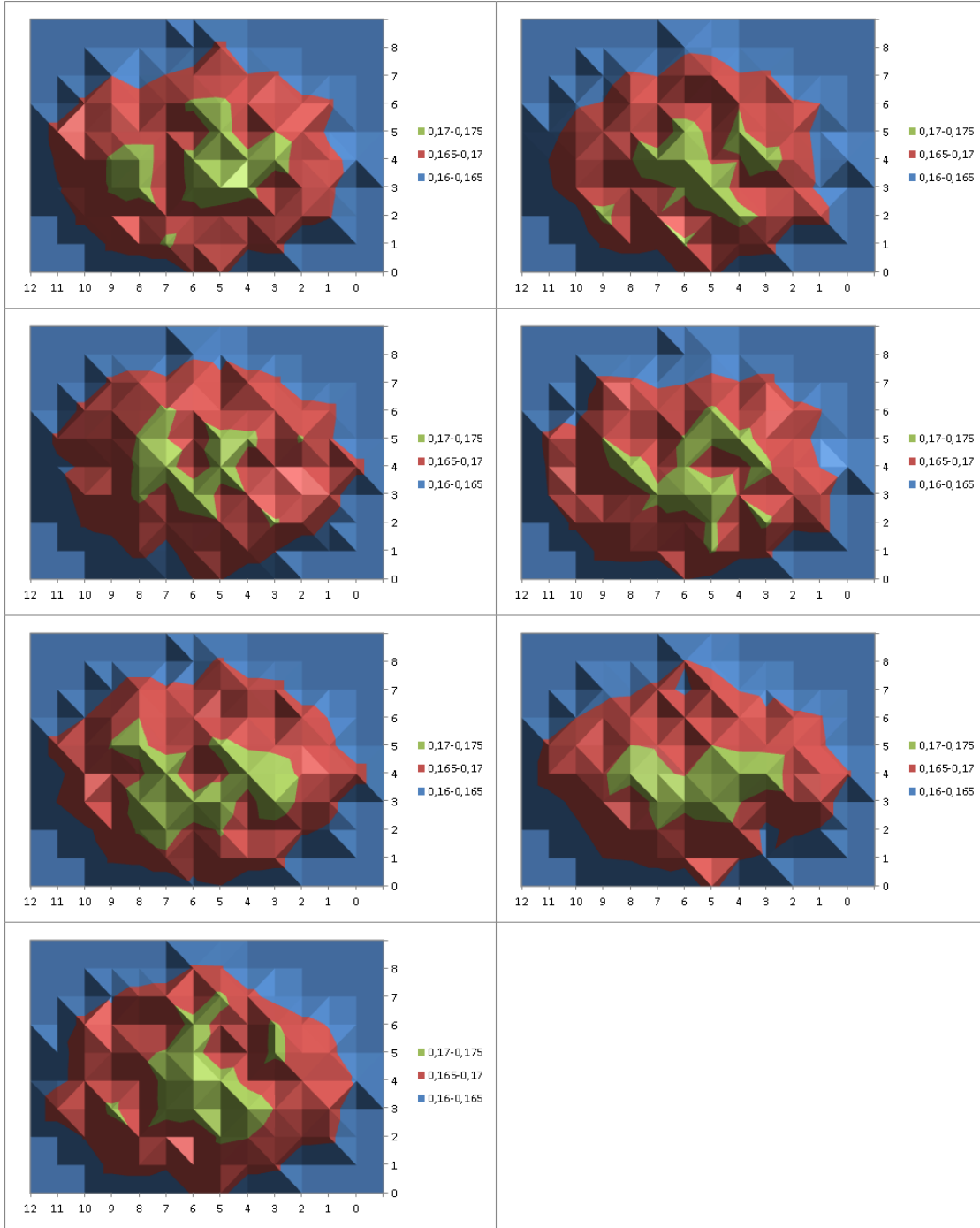


Figure A.30.: M170Y 385 μm crying wafermaps

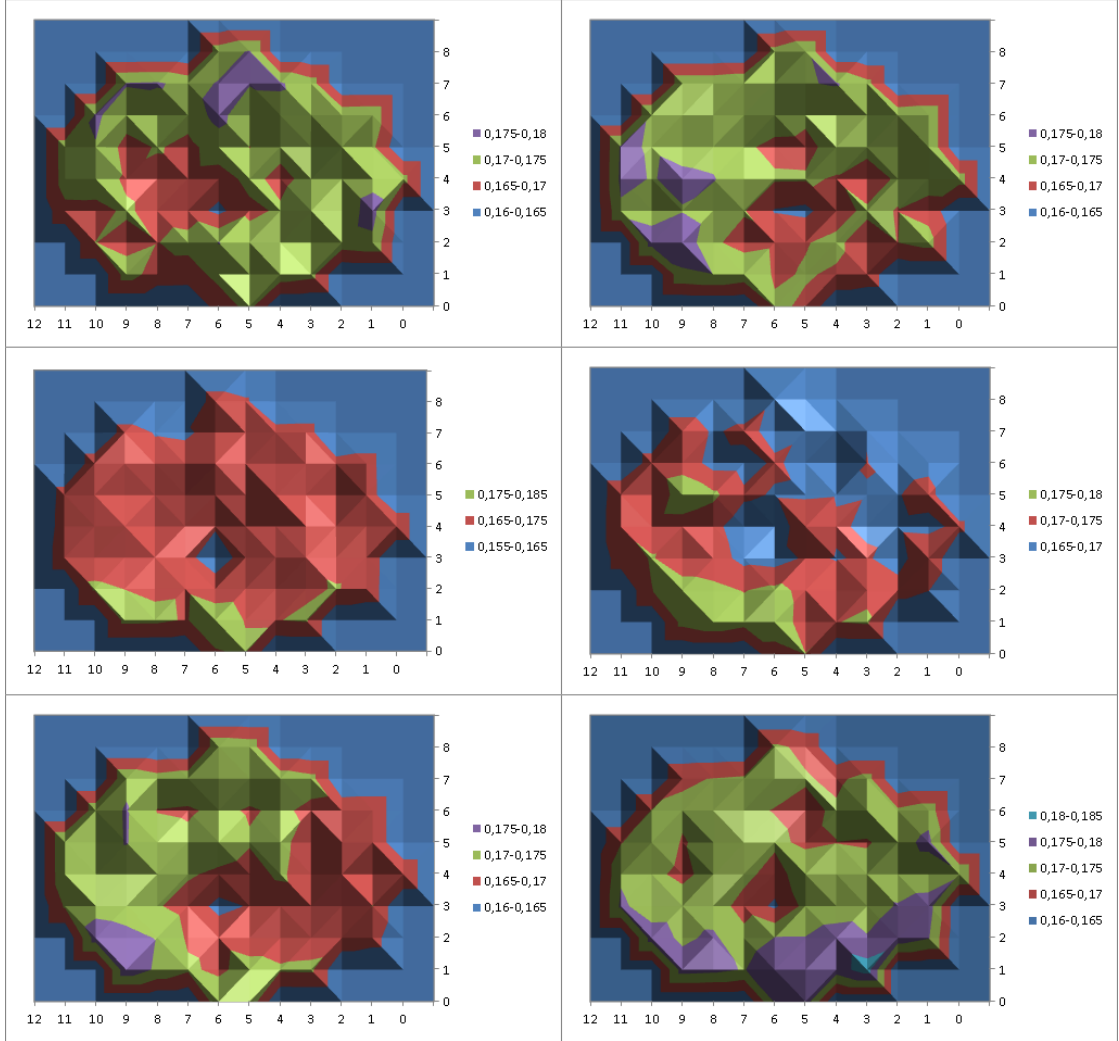


Figure A.31.: M170Y 255 μm smiling wafermaps

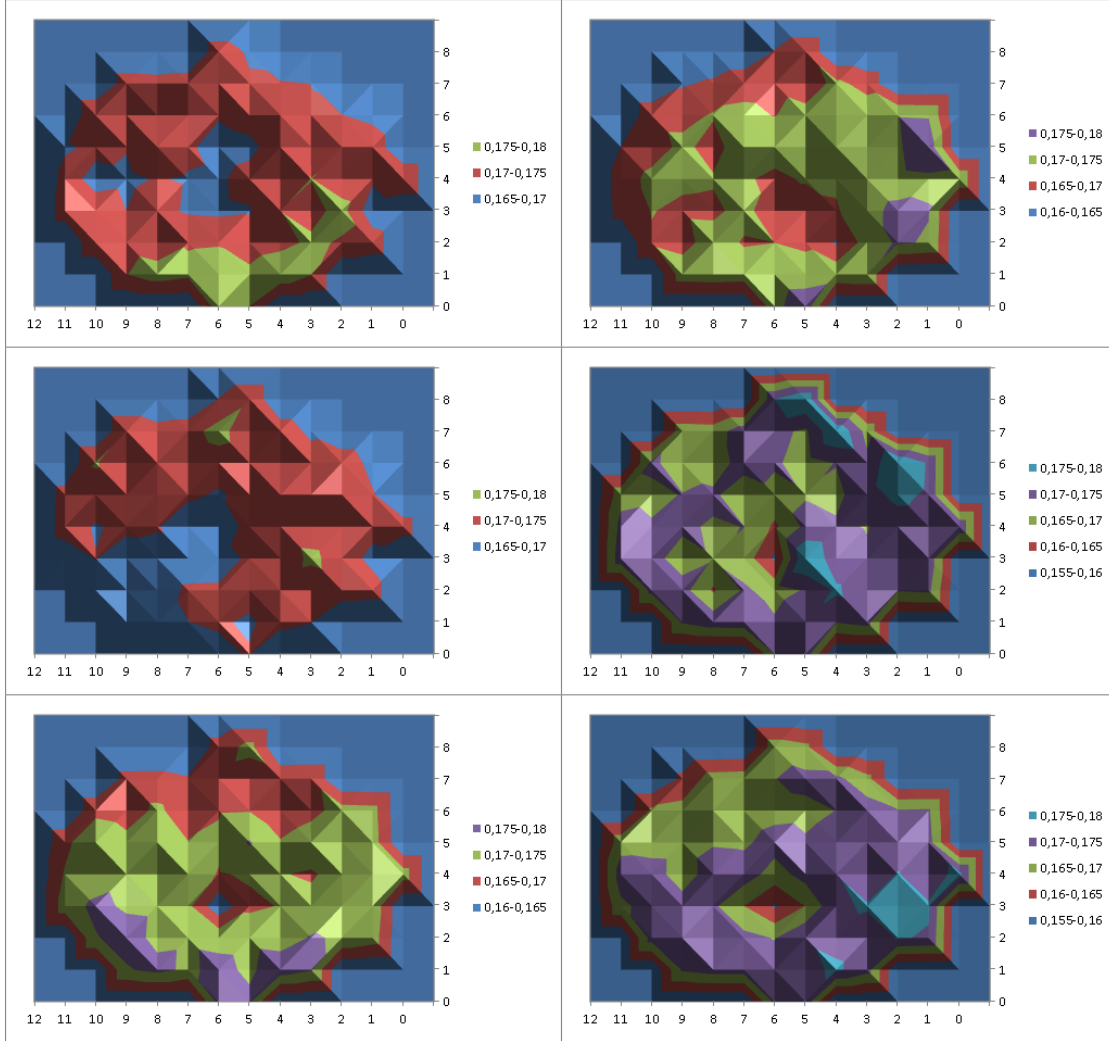
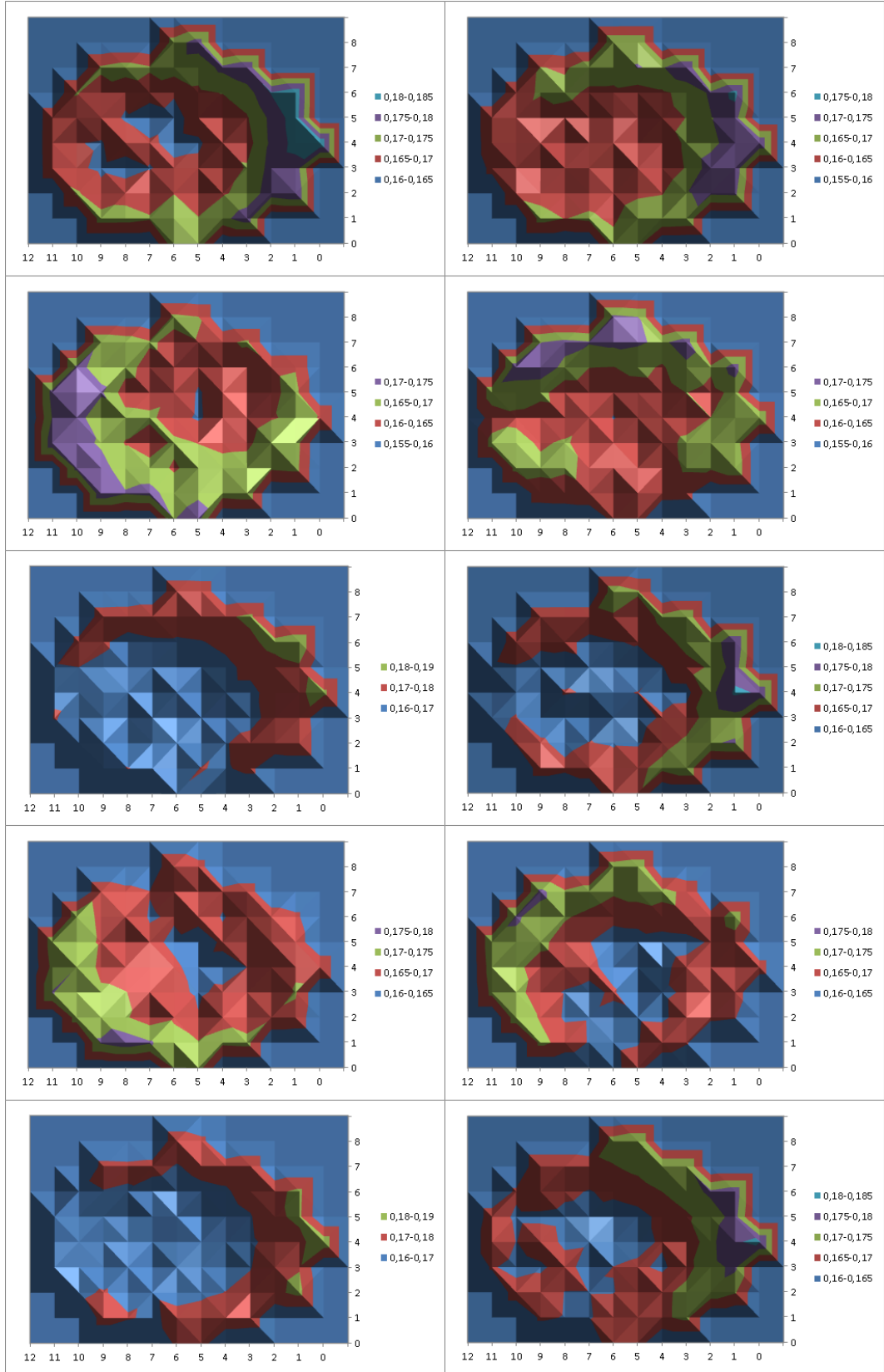


Figure A.32.: M170Y 370 μm smiling wafermaps



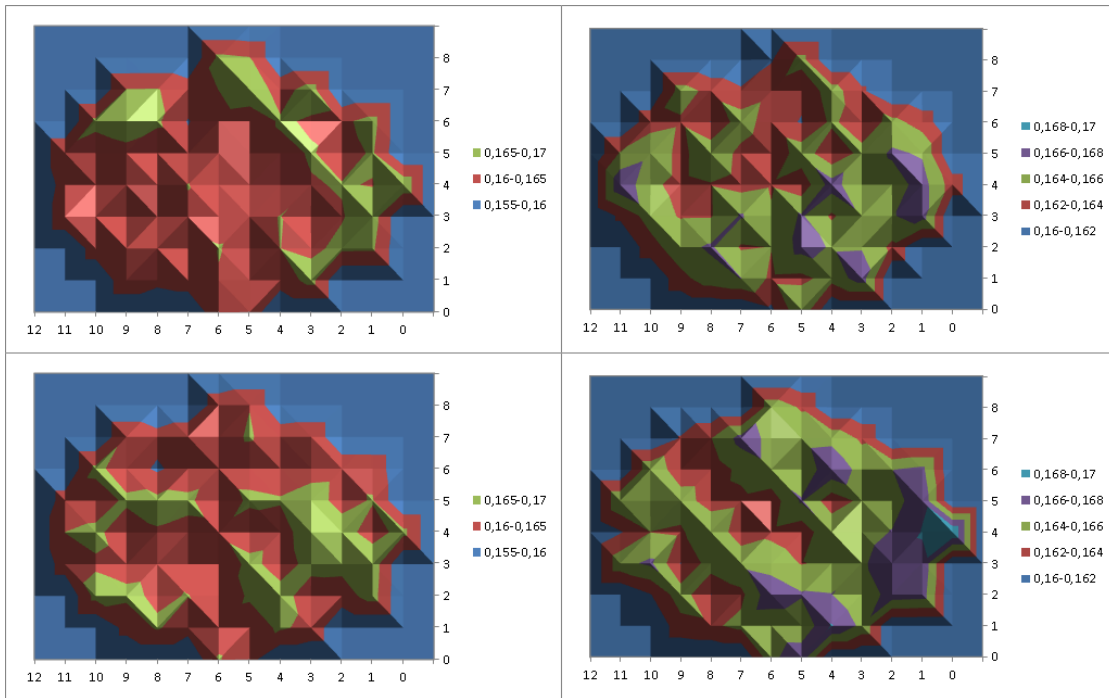


Figure A.34.: M170Y 80 μm smiling wafermaps

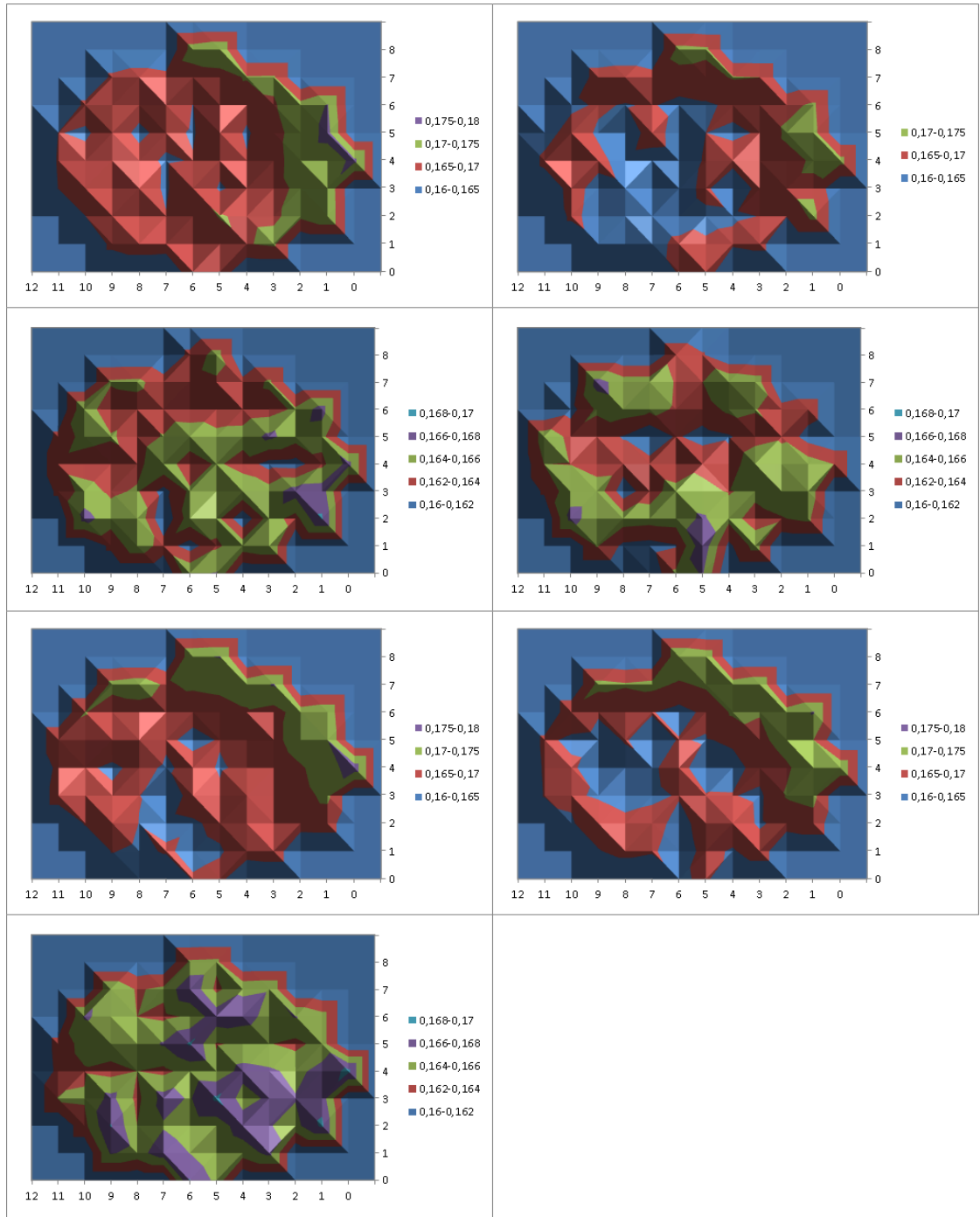


Figure A.35.: M170Y 90 μ m smiling wafermaps

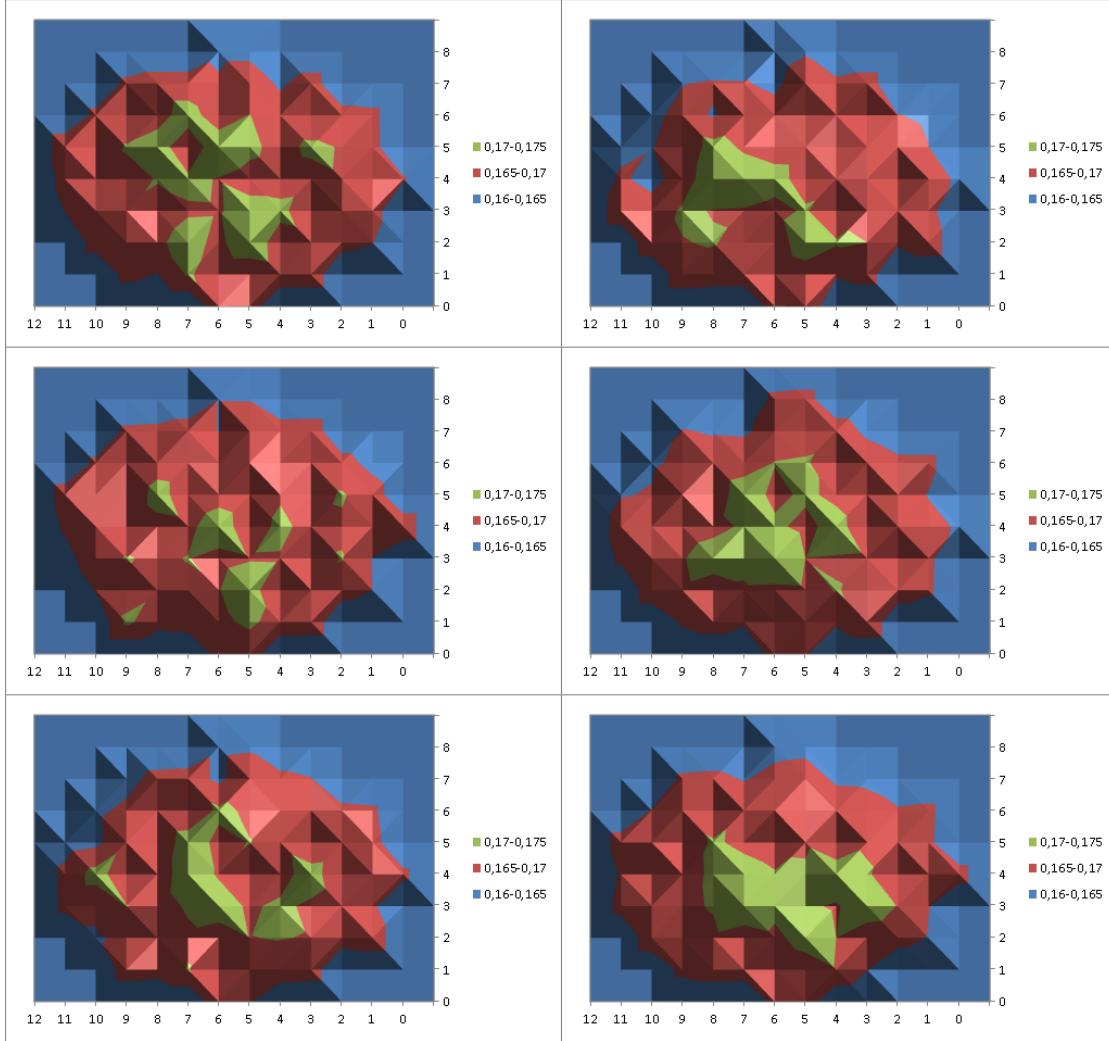


Figure A.36.: M170Y 275 μm crying wafermaps (repetition)

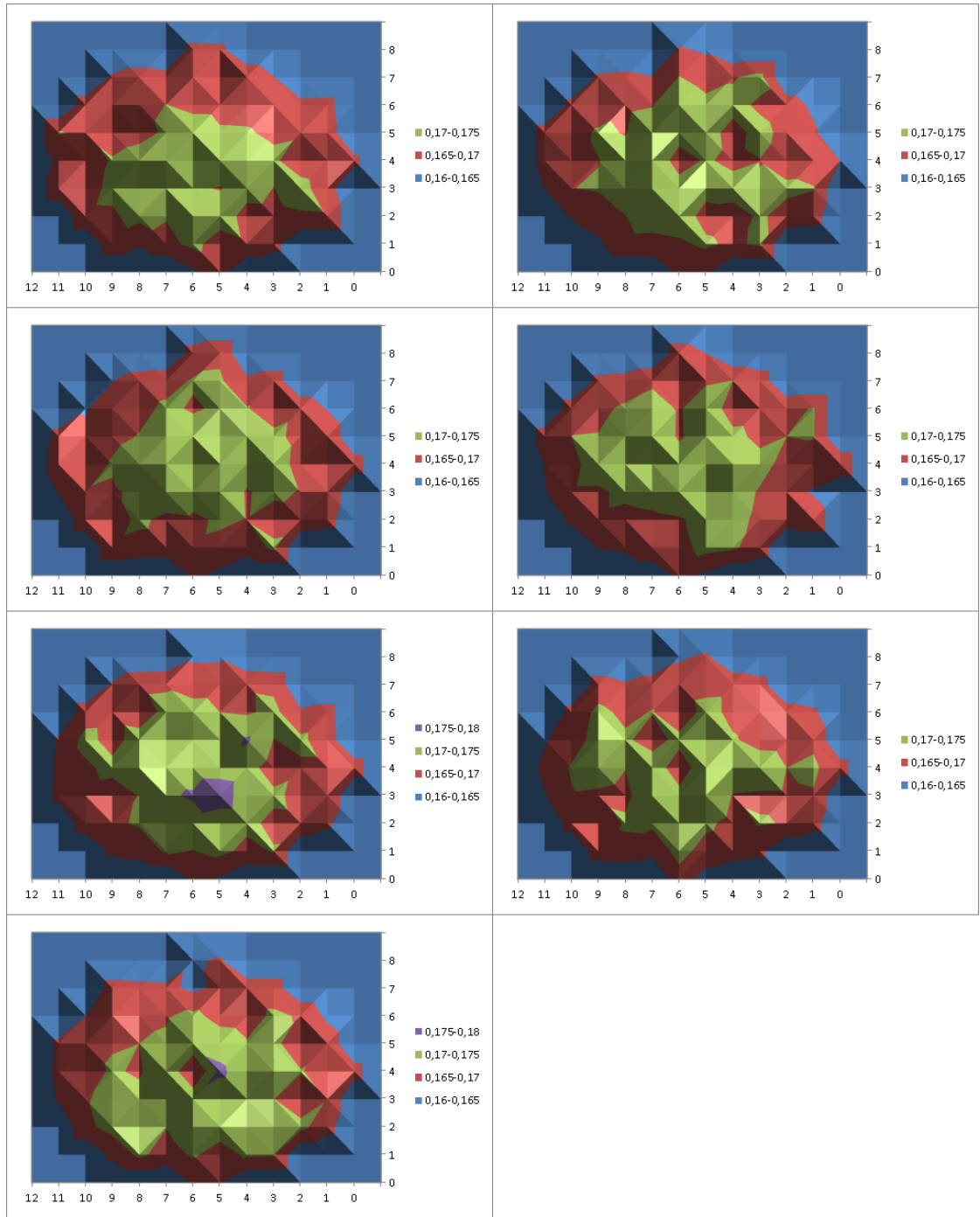


Figure A.37.: M170Y 385 μm crying wafermaps (repetition)

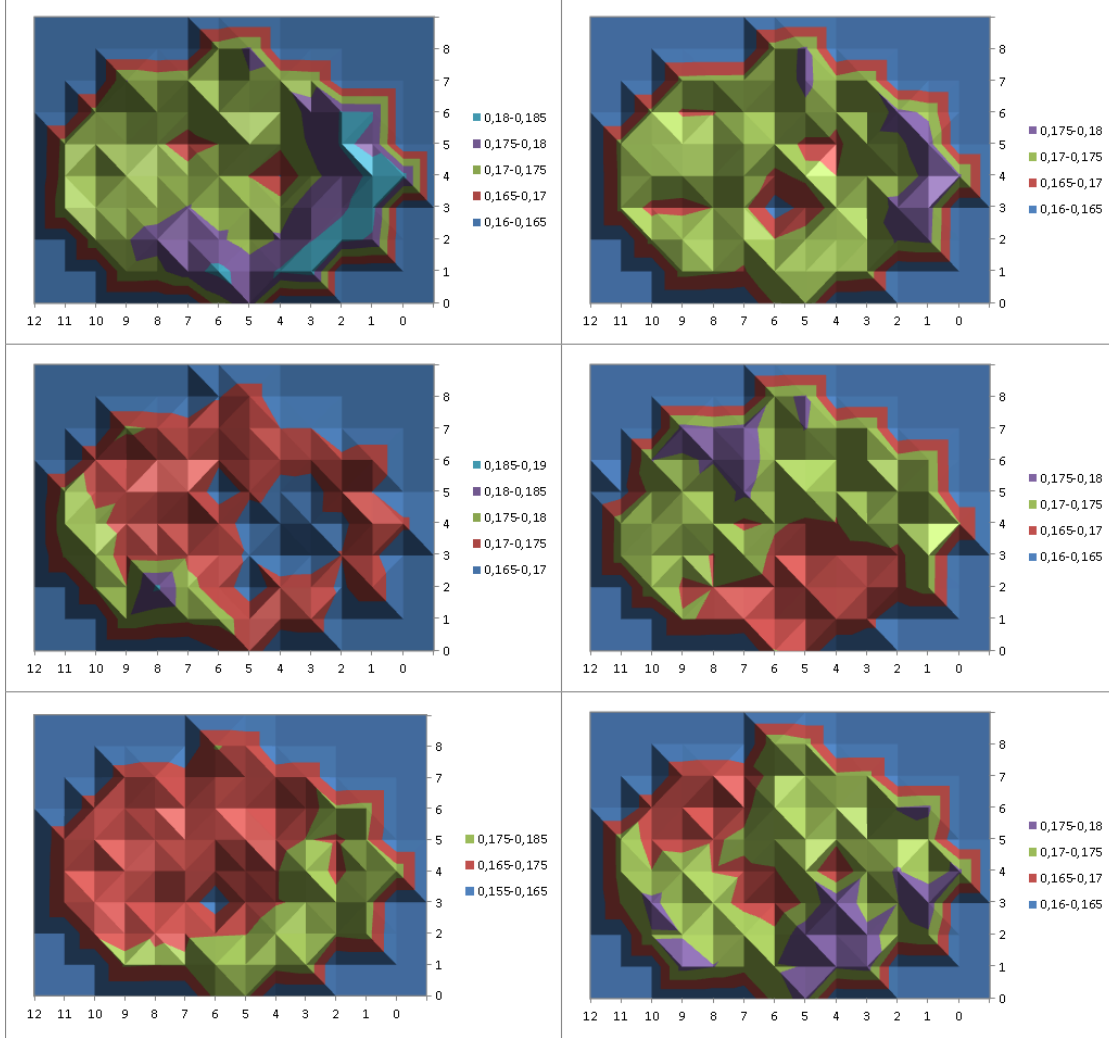


Figure A.38.: M170Y 255 μm smiling wafermaps (repetition)

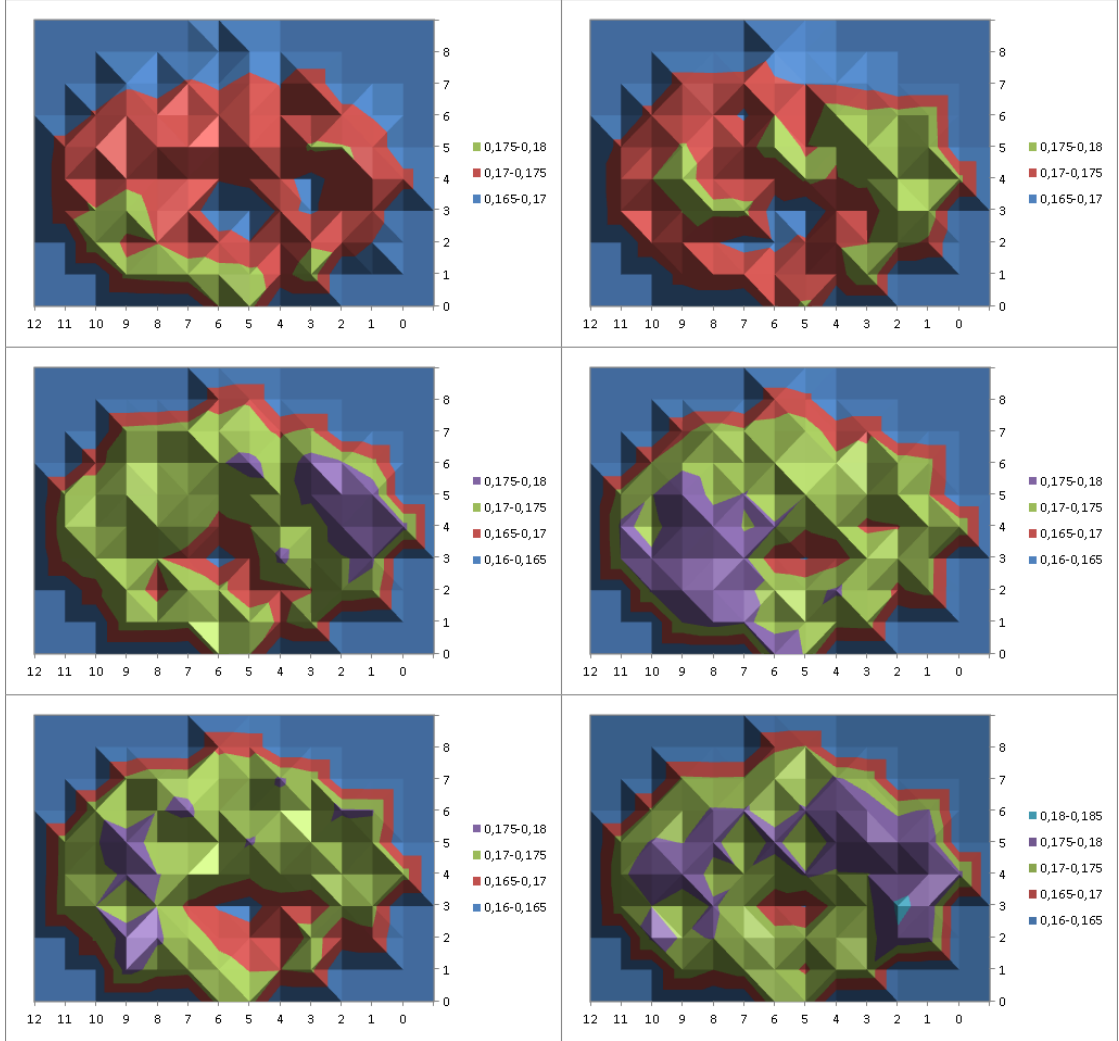


Figure A.39.: M170Y 370 μm smiling wafermaps (repetition)